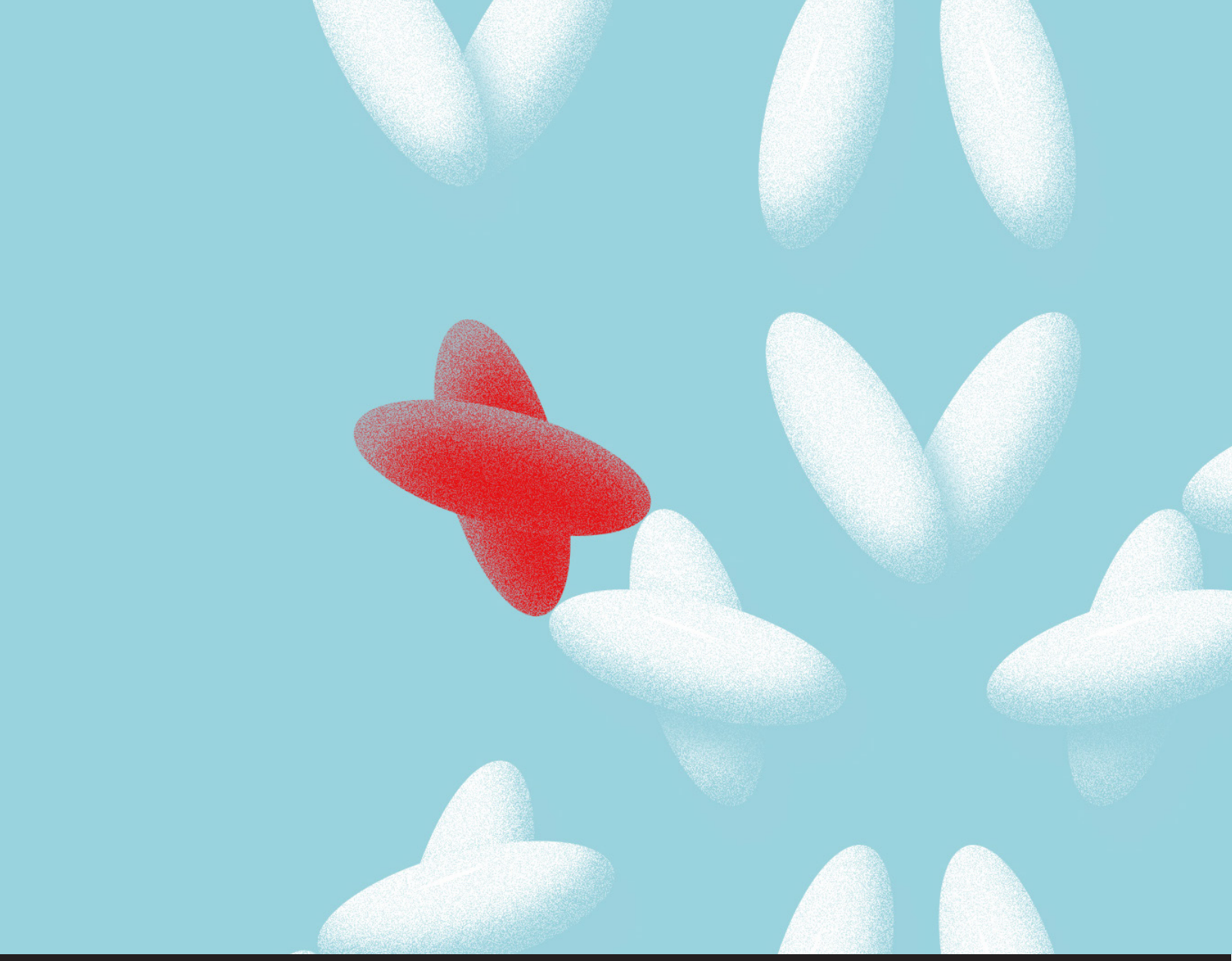

Advances in Downstream Processing of Complex Antibodies

ARTICLE COLLECTION

Sponsored by:

WILEY

CURRENT PROTOCOLS
A Wiley Brand

ThermoFisher SCIENTIFIC

Thermo Fisher SCIENTIFIC

The way forward in antibody therapeutics purification

Let's simplify antibody purification together

We have developed an innovative portfolio of affinity chromatography resins to support you in the downstream process of next-generation antibody therapeutics. These resins are specifically designed for the purification of monoclonal antibodies (mAbs) and engineered antibody modalities such as Fab fragments, bi-specific antibodies and Fc-fusion proteins.

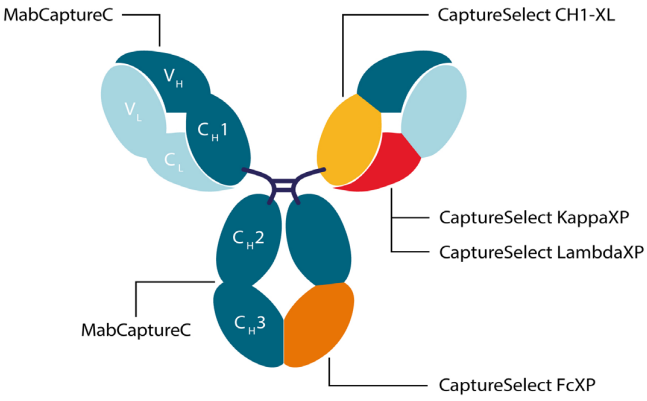

Figure 1. Binding sites of all subdomain specific affinity resins.

Features and benefits:

- Antibody-subdomain specific resins allowing purification of engineered antibodies and fragments
- High-capacity resins, addressing process demand and high-tither feedstocks
- Mild elution conditions for successful purification of pH-sensitive modalities
- A high-capacity and high productivity Protein A resin, based on an in-house manufactured Protein A ligand

Affinity Matrix	Purifies
MabCaptureC™	Conventional mAbs
CaptureSelect™ CH1-XL	Fab fragments
CaptureSelect™ FcXP	Engineered mAbs and Fc-fusion proteins
CaptureSelect™ LambdaXP and KappaXP	Bi-specific antibodies with either a Kappa or Lambda light chain

Discover more at **thermofisher.com/antibody-therapeutics**

thermo scientific

Contents

4
Introduction

6
Evaluation of Strategies to Control Fab Light Chain Dimer During Mammalian Expression and Purification: A Universal One-Step Process for Purification of Correctly Assembled Fab

BY JENNIFER SPOONER, JENNY KEEN, KALPANA NAYYAR, NEIL BIRKETT, NICHOLAS BOND, DAVID BANNISTER, NATALIE TIGUE, DANIEL HIGAZI, BENJAMIN KEMP, TRISTAN VAUGHAN, ALISTAIR KIPPEN, ANDREW BUCHANAN

Biotechnology and Bioengineering

12
Microbial Transglutaminase and c-myc-Tag: A Strong Couple for the Functionalization of Antibody-Like Protein Scaffolds from Discovery Platforms

BY PATRICK DENNLER, LAURA K. BAILEY, PHILIPP R. SPYCHER, ROGER SCHIBLI, ELIANE FISCHER

ChemBioChem

19
The Quest for Affinity Chromatography Ligands: Are the Molecular Libraries the Right Source?

BY GÉRALD PERRET, PATRICK SANTAMBIEN, EGISTO BOSCHETTI

Journal of Separation Science

33
Cation Exchange Chromatography Performed in Overloaded Mode is Effective in Removing Viruses During the Manufacturing of Monoclonal Antibodies

BY YUMIKO MASUDA, MASASHI TSUDA, CHIE HASHIKAWA-MUTO, YUSUKE TAKAHASHI, KOICHI NONAKA, KAORI WAKAMATSU

Biotechnology Progress

41
Efficient Removal of Aggregates from Monoclonal Antibodies by Hydrophobic Interaction Chromatography In Flow-Through Mode

BY APPLICATION NOTE

Thermo Fisher Scientific Application Note

Introduction

Therapeutic antibodies have become one of the most rapidly growing classes of drugs, revolutionizing modern medicine. Since 1986, over 100 monoclonal antibodies (mAbs) have been designated as drugs by the FDA, treating a plethora of complex conditions in a more targeted and personalized fashion. Optimized manufacturing and purification processes are critical to ensure the quality, safety, and efficacy of mAb products, as well as to ensure the widescale use of mAb therapeutics in patients.

Approximately 60-80% of the total cost of mAb production is attributed to downstream processing, the phase where the target product is purified, concentrated and stabilized, and critical impurities are removed. As emerging mAbs and next-generation antibodies continue to grow in complexity, traditional capture chromatography approaches (i.e., protein A) may no longer work sufficiently, creating a need for novel purification solutions. This underlies the importance of identifying and implementing the right purification tools to intensify the downstream process, improve overall yield, and reduce cost.

To overcome these challenges, bioprocessing scientists have been creating innovative solutions in both capture and polish steps of complex antibody purification. Novel affinity chromatography resins that target different regions of mAbs and mAb fragments have been developed in recent years to take the place of a traditional protein-A capture step. These resins have unique selectivity, such that a broad range of antibody modalities can be captured, harness the power of affinity chromatography in process intensification, reducing chromatography steps, saving time and cost of goods, are utlimately suitable for cGMP manufacturing. Aside from affinity chromatography solutions, unique solutions are also being developed for the polishing step to help remove additional impurities and contaminants. Together, the goal of these solutions is to simplify the downstream processing of newly-developed complex mAbs and mAb fragments, increasing the overall yield and purity of the final product.

In this article collection, we highlight publications that showcase advancements in the downstream processing of complex antibodies. First, Spooner et al. (2015) present the development of methods to remove light chain (LC) dimer impurities during Fab expression. Additionally, they demonstrate that a novel C_H1 affinity resin, consisting of camelid antibody fragments, expressed in yeast, that bind the C_H-1 and λ LC, enables an efficient one-step purification, which generates correctly assembled Fabs. Together, these findings show the utility of anti-C_H1 affinity capture as a scalable, efficient route for Fab production.

Next, Dennler et al. (2015) study functionalization of antibody-like protein scaffolds, presenting a conjugation strategy that targets the c-myc-tag for the site-specific modification of antibody-like proteins. They attached eight different functionalities to a c-myc-tagged antibody fragment (ESC11-Fab) and used the bioconjugates for various downstream applications. Their results demonstrate the versatility of their enzymatic conjugation platform for transforming c-myc-tagged proteins into different probes.

Following these articles, Perret et al. (2015) review the most common affinity chromatography ligand libraries. Additionally, they discuss strategies for selecting an appropriate ligand for a particular application, and the power and promise of biological libraries to generate ligands to novel therapeutic targets. Next, Masuda et al. (2019) investigate the use of cation exchange chromatography in overloaded mode for the removal of viruses during the polishing step of mAb purification. They evaluated the viral clearance ability in overloaded mode using murine leukemia virus (MLV) and found that high-load conditions led to the removal of MLV from mAb solutions. The overload mode was found to remove other types of viruses as well. Taken together, these findings indicated that viral removal via the overload mode was comparable to the bind-elute mode, suggesting that this method is a viable option to reduce production cost.

Finally, the collection is rounded out by an Application Note from ThermoFisher (2018). The authors illustrate a solution for the removal of aggregates from mAbs by hydrophobic interaction chromatography in flow-through mode. Analysis of the final product showed efficient clearance of dimers and aggregates. Together, this work demonstrated a more simple and cost-effective polish step utilizing the POROS Benzyl Ultra resin in flow-through mode as an alternative to the generic mixed-mode bind/elute step commonly employed. Additionally, the study highlighted the utility of optimizing the POROS Benzyl Ultra Resin for removing aggregates from complex mAbs while maintaining ≥99% purity.

Through the applications presented in this article collection, we hope to educate downstream processing scientists on novel solutions that can be used to enhance purification of complex mAbs. For more information regarding these solutions , we encourage you to visit the ThermoFisher Scientific Bioprocess Resins page and explore the possibilities presented there for your research.

Emily E. Frieben, Ph.D.
Associate Editor, *Wiley Interdisciplinary Reviews*

References

Spooner, J., Keen, J., Nayyar, K., Birkett, N., Bond, N., Bannister, D., Tigue, N., Higazi, D., Kemp, B., Vaughan, T., Kippen, A. and Buchanan, A. (2015), Evaluation of strategies to control Fab light chain dimer during mammalian expression and purification: A universal one-step process for purification of correctly assembled Fab. *Biotechnol. Bioeng.*, 112: 1472-1477. https://doi.org/10.1002/bit.25550

Dennler, P., Bailey, L.K., Spycher, P.R., Schibli, R. and Fischer, E. (2015), Microbial transglutaminase and c-myc-tag: A strong couple for the functionalization of antibody-like protein scaffolds from discovery platforms. *ChemBioChem*, 16: 861-867. https://doi.org/10.1002/cbic.201500009

Perret, G., Santambien, P. and Boschetti, E. (2015), The quest for affinity chromatography ligands: are the molecular libraries the right source?. *J. Sep. Science*, 38: 2559-2572. https://doi.org/10.1002/jssc.201500285

Masuda, Y., Tsuda, M., Hashikawa-Muto, C., Takahashi, Y., Nonaka, K., Wakamatsu, K. (2019), Cation exchange chromatography performed in overloaded mode is effective in removing viruses during the manufacturing of monoclonal antibodies. *Biotechnol. Progress.* 35:e2858. https://doi.org/10.1002/btpr.2858

Efficient removal of aggregates from monoclonal antibodies by hydrophobic interaction chromatography in flow-through mode. (2018), [Application Note]. ThermoFisher Scientific. 1-9.

COMMUNICATION TO THE EDITOR

BIOTECHNOLOGY and BIOENGINEERING

Evaluation of Strategies to Control Fab Light Chain Dimer During Mammalian Expression and Purification: A Universal One-Step Process for Purification of Correctly Assembled Fab

Jennifer Spooner, Jenny Keen, Kalpana Nayyar, Neil Birkett, Nicholas Bond, David Bannister, Natalie Tigue, Daniel Higazi, Benjamin Kemp, Tristan Vaughan, Alistair Kippen, Andrew Buchanan

MedImmune, Granta Park, Cambridge, United Kingdom; telephone: +44 1223 471471; fax: +44 1223 471472; e-mail: buchanana@medimmune.com

ABSTRACT: Fabs are an important class of antibody fragment as both research reagents and therapeutic agents. There are a plethora of methods described for their recombinant expression and purification. However, these do not address the issue of excessive light chain production that forms light chain dimers nor do they describe a universal purification strategy. Light chain dimer impurities and the absence of a universal Fab purification strategy present persistent challenges for biotechnology applications using Fabs, particularly around the need for bespoke purification strategies. This study describes methods to address light chain dimer formation during Fab expression and identifies a novel C_H1 affinity resin as a simple and efficient one-step purification for correctly assembled Fab.

Biotechnol. Bioeng. 2015;112: 1472–1477.

KEYWORDS: fab; antibody fragment; purification; expression; light chain dimer

Introduction

Fabs (antigen-binding fragments) are an important class of antibody derivative, which are used as research reagents, diagnostics, and therapeutics. They are classically generated by digesting immunoglobulin with papain followed by Protein A affinity chromatography to separate the two Fab fragments from Fc and undigested antibody (Ghose et al., 2005). This method requires optimisation for each antibody, is relatively inefficient and produces a ragged hinge that can result in immunogenicity (Brezski and Jordan, 2010). Following advances in expression systems, strain engineering, and production processes Fabs can now be recombinantly expressed in a range of mammalian (CHO, HEK), microbial (*S. cerevisiae*, *P. pastoriis*, *E. coli*), and cell free systems (Spadiut et al., 2014, Stafford et al., 2014). A common observation with IgG and Fab expression and assembly is that the light chain (LC) is over expressed, typically leading to the formation of LC dimers in mammalian and microbial systems (Ho et al., 2013; Lin et al., 2012; Makino et al., 2011; O'Callaghan et al., 2010; Skerra and Plückthun, 1991). Depending on the purification approach used, LC dimer impurities can be difficult to remove, resulting in lower product recoveries. In addition there is no universal strategy for native Fab purification equivalent to protein A for IgG (El Khoury and Lowe, 2013; Ljunglöf et al., 2013). The routine use of Fab heavy chain (HC) affinity tags (Skerra, 1994) does not address the LC dimer when native Fab is required e.g., when the tag interferes with downstream research or therapeutic use. In this paper we report strategies to reduce the proportion of LC dimer formed during Fab mammalian expression and demonstrate the benefit of a new anti- C_H1 affinity resin to enable a one-step purification to generate correctly assembled Fab.

A panel of seven sequence diverse human Fabs were transiently expressed in CHO cells. The unpurified cell free supernatants were analysed for Fab and LC dimer content using capillary gel electrophoresis. Analysis of the non-reduced supernatants reveals the presence of both intact Fab and LC dimer that ranged from 16–58% of the Fab titre (Fig. 1A). The proportion of LC dimer did not correlate with the level of Fab expression. It has been demonstrated for transient CHO IgG production that increasing the ratio of HC to LC genes reduces the proportion of LC dimer formation (Schlatter et al., 2005). We investigated the impact of altering the HC:LC gene ratio on transient Fab production for Fab 6, a Fab with a high proportion of light chain dimer. Using a two vector system increasing the ratio of HC:LC from 1:1 to 4:1 significantly reduced the proportion of LC dimer from 68% to 22% without significantly reducing the Fab titre (Fig. 1B). However, the persistence of low levels of LC dimer indicates that either the LC gene may be transcribed and translated faster or the mRNA is more stable than

Correspondence to: A. Buchanan

Received 6 November 2014; Revision received 6 January 2015; Accepted 13 January 2015
Accepted manuscript online 24 January 2015;
Article first published online 12 March 2015 in Wiley Online Library (http://onlinelibrary.wiley.com/doi/10.1002/bit.25550/abstract).
DOI 10.1002/bit.25550

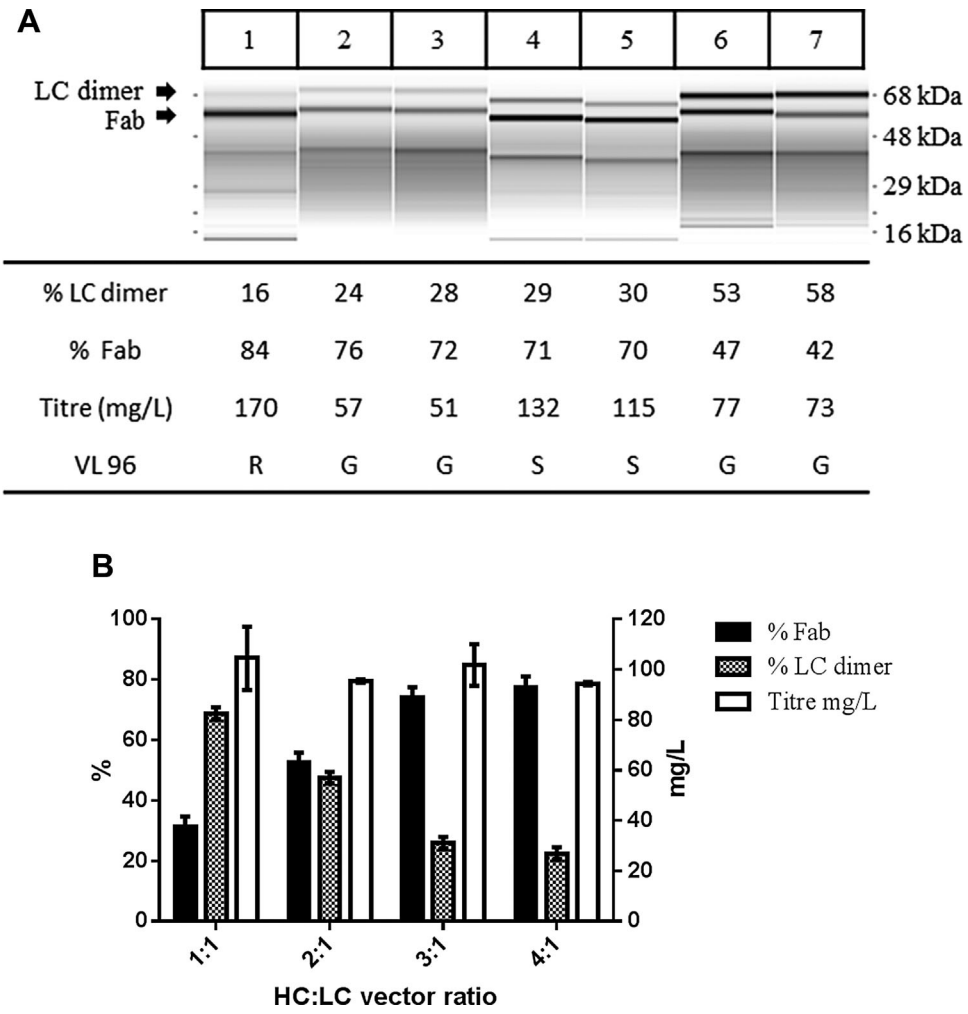

Figure 1. (A) Light chain dimer profile from supernatants of a panel of lambda and kappa Fabs expressed in CHO. The proportion of LC dimer and intact Fab expression was assessed by capillary gel electrophoresis. Titre is the quantification of intact Fab. VL96 is the amino acid at that kabat position. (B) Impact of modulating the HC:LC DNA vector ratio on the proportion of intact Fab, LC dimer and titre for Fab 6. Data is mean and SEM for three replicates.

the HC as described for IgG's (O'Callaghan et al., 2010), or the LC protein itself may be more stable than its HC counterpart.

The role of charged residues in variable domains have been demonstrated to reduced scFv and IgG aggregation (Dudgeon et al., 2012; Buchanan et al., 2012). It has previously been proposed that charged amino acids in V_L–V_L interface residues reduce LC dimer formation, particularly those at Kabat position 96 in LC CDR3 (Kim et al., 2014; Stevens et al., 1980). Our data supports this hypothesis as only Fab 1 among the panel tested encoded a positively charged residue, R96, at this position and this Fab produced the smallest proportion of LC dimer (Fig. 1A). Additional mutagenesis studies would be required to confirm the significance of such charged residues on LC dimerization. As the impact of mutations will be unique to each antibody's sequence and charge environment this will likely not be an efficient method to be generally applicable.

In addition to altering the HC:LC ratio we explored whether altering the Fab λ constant domain could enhance Fab assembly. The heavy-light interchain disulphide is the weakest disulphide bond in an antibody and the IgG1λ bond is weaker than the IgG1κ due the additional C terminal Ser 106 after Cys 105 in the λ chain (Liu et al., 2011). Deletion of λ Ser 106 is reported to increase mammalian transient IgG1 expression potentially by improving the stability of the heavy-light interchain disulphide bond interaction during assembly in the ER (Shen et al., 2013). To investigate if this mechanism translates to improved intact Fab expression with reduced LC dimer formation we constructed λ delta 106 S (λΔS) vectors for Fabs 3, 6, and 7. Following expression at a HC:LC ratio of 1:1 an incremental reduction in LC dimer was observed for two of the Fabs, but with no impact on the third (Table I). Combining λΔS with increased HC:LC ratio did not result in any additional reduction in LC dimer compared to the altered vector ratio alone (data not shown). The λΔS strategy had a modest impact on reducing LC dimer but is not applicable to all Fabs with a λ LC.

In addition to the protein engineering described above we investigated utilising a purification strategy in an attempt to efficiently remove LC dimer. Currently, there is no universal Fab

Table I. The impact of λ LC delta 106 S (ΔS) mutation on the LC dimer profile of three Fabs expressed in CHO. The proportion of LC dimer and intact Fab expression was assessed by capillary gel electrophoresis. Titre is the quantification of intact Fab.

	Fab 3	Fab 3 LCΔS	Fab 6	Fab 6 LCΔS	Fab 7	Fab 7 LCΔS
% LC dimer	27	16	73	60	65	62
% Fab	73	84	27	40	35	38
Titre (mg/L)	67	75	72	99	33	32

purification process that is not detrimentally affected by LC dimer. We tested the ability of a novel anti-C_H1 resin, CaptureSelect Ig-C_H1, to purify correctly assembled Fab and remove LC dimer and compared it to the anti-λ resin, LambdaFabSelect. These resins consist of camelid antibody fragments that specifically bind the C_H-1 and λ LC respectively. Two Fabs, Fab 6 and Fab 3 with 70% and 30% LC dimer respectively in the culture supernatant, were transiently expressed at a HC:LC ratio of 1:1 and the resins used as a one-step purification. The proportion of purified, correctly assembled Fab product and LC dimer were quantified by capillary gel electrophoresis (Fig. 2A). The identity and sequence of Fab and LC dimer was confirmed by liquid chromatography coupled to mass spectrometry (LC–MS) (Fig. 2B). The anti-λ resin was only effective in purifying intact Fab when the level of LC dimer in the supernatant was low. In the case of Fab 6, 30% of the anti-λ purified product remained as LC dimer and would require additional purification steps to remove this impurity. In contrast, the anti-C_H1 resin was much more effective at purifying the intact Fab and removing the LC dimer as a generic one-step process for both Fabs.

The observation that the remaining LC dimer, post purification, was reduced to LC monomer indicated that the LC dimer is stabilised by a covalent linkage (Fig. 2A). Reduced and non-reduced peptide mapping was conducted to identify the position of disulphide bonds formed in the LC dimer (Fig. 3). This analysis confirmed that the LC was correctly folded with the canonical variable and constant cysteine bridges present. The LCs were covalently linked via their C terminal λ Cys 105. These Fab LC dimers are distinct from the LC oligomers described as Bence Jones proteins linked via V_L–V_L interactions (Peterson et al., 2010).

The studies described here demonstrate that LC dimer formation is a feature of Fab expression as previously described for IgG expression. During Fab production we have demonstrated the excess LC results in formation of LC dimer that is linked via C terminal Cys 105. This is a distinct linkage from that recently described for IgGs with extra light chains (Lu et al., 2013). Increasing the proportion of HC vector DNA can reduce but not eliminate the production of LC dimer. Whereas, deleting the λ LC terminal Ser 106 only leads to a modest improvement of the expression profile and not for all Fabs. The LC dimer has created challenges for the development of a generic Fab purification platform as the LC dimer behaves chromatographically as a Fab and can overwhelm the capacity of an ion-exchange chromatography step. The implementation of an anti-C_H1 affinity resin provides a universal, robust, and scalable one-step process for the purification of correctly assembled Fab. This overcomes the persistent excess LC production and LC dimer formation and should be applicable to other expression platforms. The combination of transient expression and anti-C_H1 affinity capture provides a scalable and efficient route for rapid Fab production to enable biotechnology applications.

Methods

Fab Expression and Titre Determination

Separate HC and LC expression plasmids were used for transient transfection. The vectors were modified to contain the EBV origin of replication (*OriP*). The Fab HC vector contained only constant region 1 (C_H1) and Hinge regions, C_H2 and C_H3 were removed. HC and LC DNA was added to 150 mM NaCl and 25-kDa linear PEI (Polysciences Europe, Germany 23966), according to manufacturer's recommendations. To vary the ratio of HC:LC the total amount of DNA was constant and the proportion of each plasmid was varied. The DNA–PEI complex was then added to 100 mL of Chinese Hamster Ovary wild type (CHO wt) cells derived from a CHOK1 cell line (ECACC No: 85051005) adapted for suspension culture (Daramola O et al., 2014). After seven days the cells were harvested by centrifugation and the supernatants filtered. Titre was determined using anti-CH1 biosensors and the Octet 384QK from Pall. The samples were diluted 1:5 in binding buffer to reduce matrix effects and analysed according to the manufactures instructions. A homologous standard curve was run alongside the samples to calculate titre from supernatant samples. Anti-C_H1 biosensors were hydrated for at least 30 min before the analysis was performed.

Purification

50 mL of cell culture supernatant containing the Fab protein was loaded directly onto a chromatography column packed with 5 mL CaptureSelect IgG-C_H1 (Life Technologies, Carlsbad, CA) or 5 mL LambdaFabSelect (GE Healthcare, Little Chalfont, UK) at a flow rate of 5 mL/min using an Äkta Purifier (GE Healthcare). The columns were equilibrated and washed with Phosphate Buffered Saline (PBS) pH 7.2 and eluted with 20 mM sodium citrate, 150 mM sodium chloride, pH 3.5 (CaptureSelect IgG-CH1) or 100 mM sodium acetate, pH 3.5 (LambdaFabSelect) according to the resin manufacturer's instructions. Eluted Fab was adjusted to pH 5.5 and filtered (0.22 μm Steriflip, Millipore EMD, Bethesda, MD) prior to analysis. Protein concentration was determined by absorbance at 280 nm using a DU520 UV/vis spectrophotometer (Beckman Coulter, Brea, CA). Sample purity was determined using a TSKgel G3000SWxl column (Tosoh Bioscience, Tokyo, Japan) and a 1100 HPLC system (Agilent Technologies, Santa Clara, CA) running at 1.0 mL/min.

Capillary Gel Electrophoresis

Reduced and non-reduced capillary gel electrophoresis separations were performed using either an Agilent 2100 Bioanalyzer and Protein 230 assay kit or a LabChip GXII with a Protein Express LabChip (PerkinElmer, Waltham, MA) according to the manufacturer's protocol. The respective software was used for run control and data analysis.

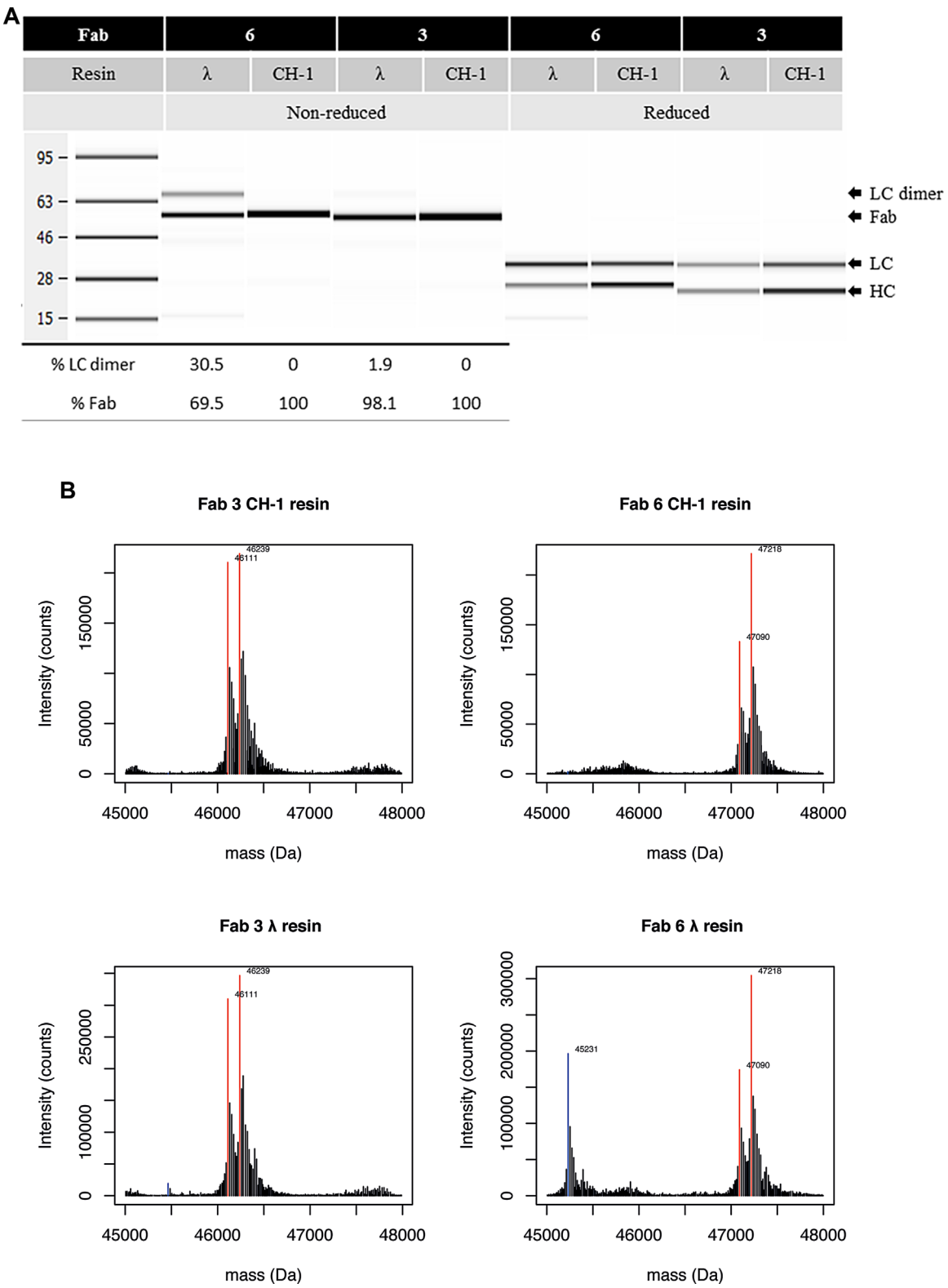

Figure 2. (A) Capillary gel electrophoresis analysis of purified Fab products following single step purification with either CH-1 or λ affinity resin. (B) Intact mass analysis of purification eluent of two Fabs purified using CH-1 resin or λ select resin. Ions corresponding with intact Fab +/− C-terminal lysine are coloured red, ions corresponding to light chain dimers are coloured blue.

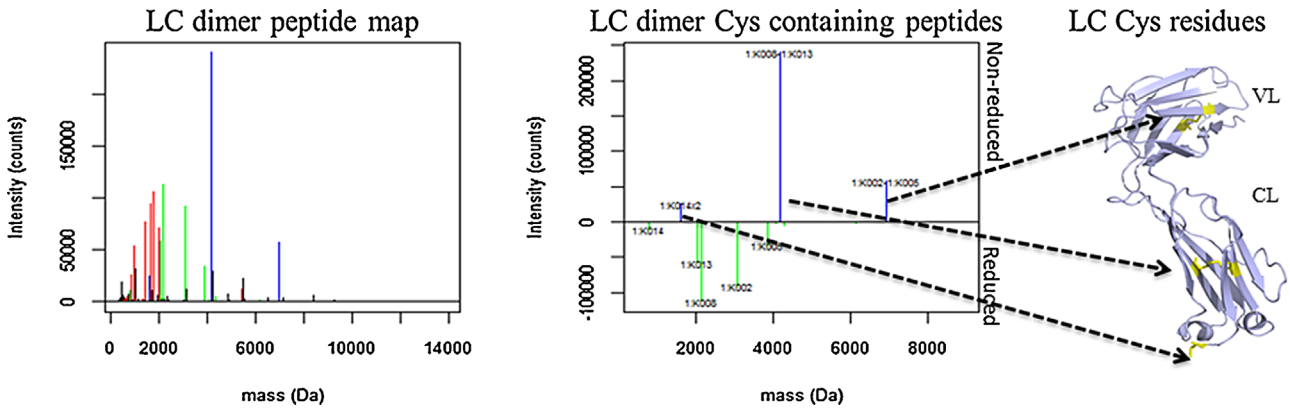

Figure 3. Disulphide linkage determination of LC dimer by reduced and non-reduced MS analysis. Three covalently linked cysteine containing peptides were detected exclusively by non-reduced peptide map analysis (blue) and their five constituent peptides detected independently following reduction (green). Noncysteine containing peptides were common to both analyses (red). The covalently linked Cys containing peptides are mapped to a model Fab LC variable (VL) and constant (CL) domains with Cys residues in yellow.

LC-MS

Reverse phase (RP) LC–MS analysis was performed using an Acquity UPLC coupled to a Synapt G1 quadrupole time of flight (QToF) mass spectrometer (Waters, Milford, MA). 2 μg of purified protein diluted in 10 mM Tris HCl pH 8 at 1 mg/mL was injected onto a 50 mm × 2.1 mm, 1.7 μm particle size BEH300 C4 analytical column held at 65°C (Waters, Milford). Protein was eluted at a constant flow rate of 0.15 mL/min using a 5 min binary gradient; solvent B was initially increased from 5 to 95% over 1 min, reduced to 20% over 2 min and returned to 5% over a further 2 min. The column was cleaned prior to the subsequent injection by oscillating between high (95%) and low (5%) solvent B for 5 min. Solvent A (water) and B (acetonitrile) were supplemented with 0.01% (v/v) trifluoroacetic acid and 0.1% (v/v) formic acid. Spectra were acquired between 500–4500 *Th*. Key instrument parameters included +ve ionisation mode, source voltage: 3.4 kV, sample cone voltage: 50 V, source temperature: 140°C, desolvation temperature: 400°C. BioPharmaLynx (Waters, Milford) was used to deconvolute the charge envelopes.

Disulphide Bond Mapping

For each sample, 50 μg of protein was prepared at 3 mg/mL in 100 mM sodium phosphate, 1 mM N-ethylmaleimide, pH 7.0 buffer and incubated for 20 min at room temperature. Dried samples were resuspended in 7 M Guanidine HCl, 100 mM NaCl, 10 mM sodium phosphate and incubated at 37$^{\Delta}$C for 30 min. Denatured protein was diluted to 0.3 mg/mL and digested with lysyl endopeptidase (Wako Pure Chemical Industries, Osaka, Japan) at an E:S ratio of 1:50 in 2 M Guanadine, 100 mM sodium phosphate, 0.1 mM EDTA, pH7.0 at 37$^{\Delta}$C. After 2 h a second, equal aliquot of lysyl endopeptidase was added. After a further 2 h the digest was split; for the reduced analysis the digest was incubated with 50 mM Dithiothreitol for 15 min at room temperature. Reduced and non-reduced samples were analysed by RP LC-MS using an Acquity UPLC coupled to a Synapt G2 QToF mass spectrometer (Waters, Milford). For each sample, 5 μg of lysyl endopeptidase digest was injected onto a 150 mm × 2.1 mm, 1.7 μm particle size BEH300 C18 analytical column held at 55°C (Waters, Milford). Peptides were eluted at a constant flow rate of 0.2 mL/min using a 75 min binary gradient; solvent B was increased from 0% to 35%. The column was cleaned prior to the subsequent injection by oscillating between high (95%) and low (5%) solvent B for 5 min. Solvent A (water) and B (acetonitrile) were supplemented with 0.02% (v/v) trifluoroacetic acid. Spectra were acquired between 50–2000 *Th* using a data independent mode of acquisition. Low and high energy spectra were processed using BioPharmaLynx (Waters, Milford).

The authors would like to thank the DNA Chemistry and Tissue Culture teams at MedImmune for their invaluable support of this work.

References

Brezski RJ, Jordan RE. 2010. Cleavage of IgGs by proteases associated with invasive diseases: An evasion tactic against host immunity? MAbs 2:212–220.

Buchanan A, Clementel V, Woods R, Harn N, Bowen MA, Mo W, Popovic B, Bishop SM, Dall'Acqua W, Minter R, Jermutus L, Bedian V. 2013. Engineering a therapeutic IgG molecule to address cysteinylation, aggregation and enhance thermal stability and expression. MAbs 5:255–262.

Dudgeon K, Rouet R, Kokmeijer I, Schofield P, Stolp J, Langley D, Stock D, Christ D. 2012. General strategy for the generation of human antibody variable domains with increased aggregation resistance. Proc Natl Acad Sci U S A. 109: 10879–10884.

El Khoury, Lowe G. 2013. A biomimetic protein G affinity adsorbent: An Ugi ligand for immunoglobulins and Fab fragments based on the third IgG-binding domain of protein G. J Mol Recognit 26:190–200.

Ghose S, Allen M, Hubbard B, Brooks C, Cramer SM. 2005. Antibody variable region interactions with protein A: Implications for the development of generic purification processes. Biotechnol Bioeng 92:665–673.

Ho SC, Koh EY, van Beers M, Mueller M, Wan C, Teo G, Song Z, Tong YW, Bardor M, Yang Y. 2013. Control of IgG LC:HC ratio in stably transfected CHO cells and study of the impact on expression, aggregation, glycosylation and conformational stability. J Biotechnol 165:157–166.

Kim DY, To R, Kandalaft H, Ding W, van Faassen H, Luo Y, Schrag JD, St-Amant N, Hefford M, Hirama T, Kelly JF, MacKenzie R, Tanha J. 2014. Antibody light chain variable domains and their biophysically improved versions for human immunotherapy. MAbs 6:219–235.

Lin S, Houston-Cummings NR, Prinz B, Moore R, Bobrowicz B, Davidson RC, Wildt S, Stadheim TA, Zha D. 2012. A novel fragment of antigen binding (Fab) surface display platform using glycoengineered Pichia pastoris. J Immunol Methods 375:159–165.

Liu H, Zhong S, Chumsae C, Radziejewski C, Hsieh CM. 2011. Effect of the light chain C-terminal serine residue on disulfide bond susceptibility of human immunoglobulin G1. Anal Biochem 408:277–283.

Ljunglof A, Lacki KM, Mueller J, Harinarayan C, van Reis R, Fahrner R, Van Alstine JM. 2007. Ion exchange chromatography of antibody fragments. Biotechnol Bioeng 96:515–524.

Lu C, Liu D, Liu H, Motchnik P. 2013. Characterization of monoclonal antibody size variants containing extra light chains. MAbs 5:102–113.

Makino T, Skretas G, Kang TH, Georgiou G. 2011. Comprehensive engineering of Escherichia coli for enhanced expression of IgG antibodies. Metab Eng 13: 241–251.

O'Callaghan PM, McLeod J, Pybus LP, Lovelady CS, Wilkinson SJ, Racher AJ, Porter A, James DC. 2010. Cell line-specific control of recombinant monoclonal antibody production by CHO cells. Biotechnol Bioeng 106:938–951.

Peterson FC, Baden EM, Owen BA, Volkman BF, Ramirez-Alvarado M. 2010. A single mutation promotes amyloidogenicity through a highly promiscuous dimer interface. Structure 18:563–570.

Schlatter S, Stansfield SH, Dinnis DM, Racher AJ, Birch JR, James DC. 2005. On the optimal ratio of heavy to light chain genes for efficient recombinant antibody production by CHO cells. Biotechnol Prog 21:122–133.

Shen Y, Zeng L, Zhu A, Blanc T, Patel D, Pennello A, Bari A, Ng S, Persaud K, Kang YK, Balderes P, Surguladze D, Hindi S, Zhou Q, Ludwig DL, Snavely M. 2013. Removal of a C-terminal serine residue proximal to the inter-chain disulfide bond of a human IgG1 lambda light chain mediates enhanced antibody stability and antibody dependent cell-mediated cytotoxicity. MAbs 5: 418–431.

Skerra A. 1994. A general vector, pASK84, for cloning, bacterial production and single-step purification of antibody Fab fragments. Gene 141:79–84.

Skerra A, Pluckthun A. 1991. Secretion and in vivo folding of the Fab fragment of the antibody McPC603 in Escherichia coli: Influence of disulphides and cis-prolines. Protein Eng 4:971–979.

Spadiut O, Capone S, Krainer F, Glieder A, Herwig C. 2014. Microbials for the production of monoclonal antibodies and antibody fragments. Trends Biotechnol 32:54–60.

Stafford RL, Matsumoto ML, Yin G, Cai Q, Fung JJ, Stephenson H, Gill A, You M, Lin SH, Wang WD, Masikat MR, Li X, Penta K, Steiner AR, Baliga R, Murray CJ, Thanos CD, Hallam TJ, Sato AK. 2014. In vitro fab display: A cell-free system for IgG discovery. Protein Eng Des Sel. 27:97–109.

DOI: 10.1002/cbic.201500009

Microbial Transglutaminase and c-myc-Tag: A Strong Couple for the Functionalization of Antibody-Like Protein Scaffolds from Discovery Platforms

Patrick Dennler,[a] Laura K. Bailey,[a] Philipp R. Spycher,[a] Roger Schibli,[a, b] and Eliane Fischer*[a]

Antibody-like proteins selected from discovery platforms are preferentially functionalized by site-specific modification as this approach preserves the binding abilities and allows a side-by-side comparison of multiple conjugates. Here we present an enzymatic bioconjugation platform that targets the c-myc-tag peptide sequence (EQKLISEEDL) as a handle for the site-specific modification of antibody-like proteins. Microbial transglutaminase (MTGase) was exploited to form a stable isopeptide bond between the glutamine on the c-myc-tag and various primary-amine-functionalized substrates. We attached eight different functionalities to a c-myc-tagged antibody fragment and used these bioconjugates for downstream applications such as protein multimerization, immobilization on surfaces, fluorescence microscopy, fluorescence-activated cell sorting, and in vivo nuclear imaging. The results demonstrate the versatility of our conjugation strategy for transforming a c-myc-tagged protein into any desired probe.

Introduction

Display libraries are a virtually inexhaustible source of affinity reagents for research and drug development.[1] The biomolecules selected from such discovery platforms include antibody fragments, but also alternative antibody-like protein scaffolds, for example affibodies, nanobodies, or DARPins.[2] These small proteins are invaluable tools in early drug development because they are easy to produce and are thus perfectly suited for screening drug candidates.

Transformation of lead candidates into functional entities for downstream applications often requires site-specific bioconjugation. This is particularly important for the functionalization of small proteins because random modification is more likely to affect their binding properties. Furthermore, site-specific bioconjugation enables the direct comparison of different antibody-like proteins as highly specific molecular probes in a range of applications. For example, biotinylation is a widely used approach for protein detection, multimerization, surface immobilization for biosensor technologies, or pretargeting strategies in vivo[3] and takes advantage of the exceptionally high binding affinity between biotin and (strept)avidin ($K_d \sim 10^{-15}$ M).[4] Also, antibody-like proteins are frequently functionalized with fluorescent dyes or radiolabels for molecular imaging in vitro and in vivo. Radiometals are particularly interesting for positron emission tomography (PET) or single-photon emission computed tomography (SPECT) imaging, but the protein must generally be functionalized with a chelator prior to radiolabeling. Alternatively, an antibody-like protein can also be indirectly functionalized by first introducing a chemical functionality that is then treated with a second entity, for example, a protein or a drug.

The methods to attach chemically reactive amino acids, for example, cysteines, noncanonical amino acids, or genetically encoded tags to the C or N terminus of proteins are current technologies for generating site-specifically modified bioconjugates.[5] The addition of a terminal cysteine is the most basic approach, but the resulting maleimide–thiol bond is prone to in vivo instability.[6] While the incorporation of non-natural amino acids requires the re-establishment of protein expression conditions, tagging of proteins is simple and straightforward. Formylglycine-generating enzymes (FGE) convert the cysteine of a terminal CXPXR-tag to formylglycine, thereby creating a bioorthogonal functionality that can be used for site-specific protein modification.[7] However, the conjugation yield is limited due to hydration of the formylglycine to diol-formylglycine.[8] Another innovative approach exploits the transpeptidic activity of sortase A to join a LPXTG-tag to a polyglycine-linked substrate.[9] However, the necessity for a polyglycine motif restricts the commercial availability of substrates because they usually have to be tailor made.

Transglutaminases are a family of enzymes (EC 2.3.2.13) that catalyze the covalent formation of an isopeptide bond between the γ-carbonyl amide group of glutamines and the primary amine of lysines.[10] Unlike other enzymes that are used

[a] P. Dennler,[+] Dr. L. K. Bailey,[+] Dr. P. R. Spycher, Prof. R. Schibli, Dr. E. Fischer
Center for Radiopharmaceutical Sciences ETH-PSI-USZ
Paul Scherrer Institute
OIPA10A, 5232 Villigen PSI, (Switzerland)
E-mail: Eliane.fischer@psi.ch

[b] Prof. R. Schibli
Institute of Pharmaceutical Sciences, ETH Zürich
Vladimir-Prelog-Weg 4, 8093 Zürich (Switzerland)

[+] These authors contributed equally to this work.

Supporting information for this article is available on the WWW under http://dx.doi.org/10.1002/cbic.201500009.

for site-specific bioconjugation,[5b] MTGase does not require a consensus sequence and targets various glutamines in a protein backbone. However, these residues are rare as they must be located in a flexible or disordered region of the polypeptide.[11] For this reason, MTGase can be used as a valuable tool for site-specific protein modification by targeting either endogenous glutamine residues that fulfill the aforementioned requirements or terminal glutamine-containing tags.[12]

We established a versatile, MTGase-based bioconjugation platform that exploits the C-terminal c-myc-tag (EQKLISEEDL, Figure 1 A and B) on proteins as the glutamine donor for the enzymatic attachment of various functionalities (Figure 1 C). The c-myc-tag is widely used for the sensitive detection of recombinant proteins with a high-affinity anti-c-myc antibody and thus is already integrated in a broad variety of pro- and eukaryotic expression vectors. Therefore, proteins and in particular antibody-like scaffolds that derive from phage-display libraries are often c-myc-tagged.[13] Additionally, MTGase recognizes only one glutamine, located in the CH2 domain, as acyl-donor within the sequence of a native IgG. Consequently, our conjugation strategy can be exploited to site-specifically functionalize c-myc-tagged antibody fragments that lack the CH2 domain such as Fab fragments or scFvs.

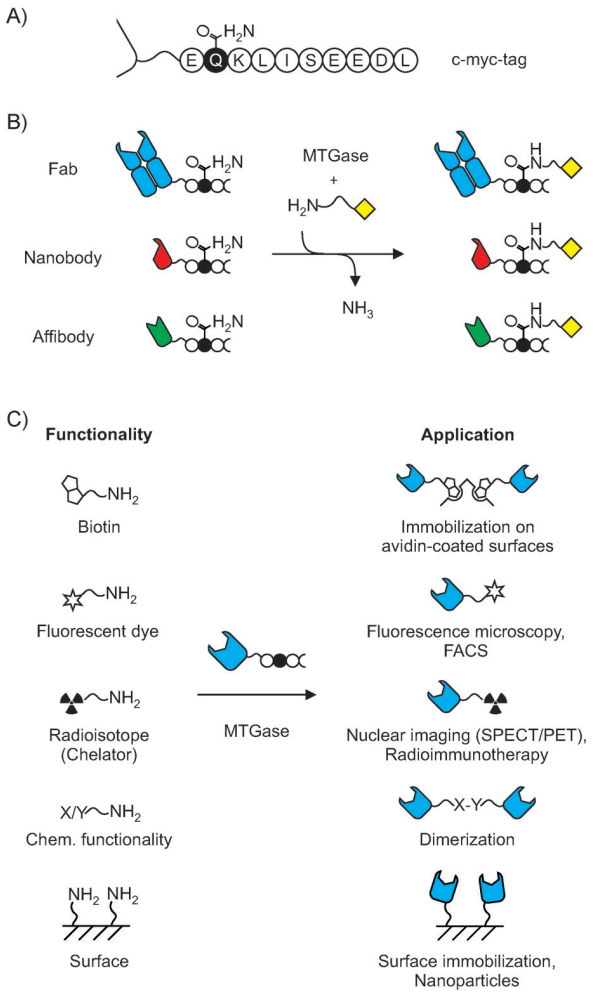

Figure 1. A) Amino acid sequence of the c-myc-tag. B) Various c-myc-tagged antibody-like protein scaffolds from discovery platforms can be site-specifically modified with a broad variety of primary-amine-functionalized substrates (yellow diamond) by MTGase. C) The different functionalities (left) that have been used in this study to modify a c-myc tagged targeting protein and a selection of possible downstream applications (right).

Results and Discussion

To demonstrate the applicability of our enzymatic bioconjugation platform, we functionalized a c-myc-tagged Fab fragment and two c-myc-tagged antibody-like scaffolds, that is, a nanobody and an affibody, with amine-derivatized biotin (Figure S1) and monitored the reaction by mass spectrometry. We observed an increase in mass of 311 Da for all three proteins; this corresponds to the attachment of exactly one biotin per protein (Figure 2). Conversely, no biotinylation was observed after incubation of the corresponding untagged nanobody with MTGase and amine-derivatized biotin (Figure S2), thus indicating that MTGase selectively targets the glutamine of the c-myc-tag even on different protein scaffolds. The identification of the biotinylated c-myc-tag by peptide mapping (Table S1) ultimately proved the site-specificity of our enzyme bioconjugation platform.

Encouraged by the finding that virtually every c-myc-tagged protein can be functionalized by using our MTGase-based technology, we chose the Fab fragment, derived from the anti-fibroblast activation protein (α-FAP) antibody ESC11,[14] as a model protein to demonstrate the versatility of the conjugation platform. We aimed to modify the c-myc-tagged Fab-fragment, designated ESC11-Fab, with a variety of different functionalities that are useful for a range of downstream applications (Figure 1 C).

Eight different functionalities were attached to ESC11-Fab by incubation with MTGase and the corresponding amine-derivatized substrate (Figure S1). Mass spectrometry analysis revealed that all the chemical entities could be attached to ESC11-Fab (Figure 2 B). Although the reaction yield with biotin, both fluorescent dyes, and the azide linker was quantitative (>95%), we observed a lower yield with the dibenzylcyclooctyne (DBCO) functionality (~50%). Among the three different chelating systems that were tested, NH_2-PEG_4-DOTA gave the highest conjugation yield (~80%) compared to ~75 and 65% for NH_2-PEG_4-DOTA-GA and NH_2-PEG_4-NODA-GA, respectively (Figure S3) and was therefore selected for further studies. It has been shown that acidic residues on the acyl acceptor are not favorable for MTGase-mediated conjugation.[15] Based on the conjugation result of the DBCO linker and our experience, we hypothesized that the same is true for bulky cyclic structures. We subsequently used the generated conjugates for a panel of different in vitro and in vivo applications.

The biotinylated ESC11-Fab, for example, was incubated with streptavidin to show that the interaction between biotin and streptavidin is retained after the enzymatic modification process. As expected, streptavidin formed a tetrameric complex when incubated with four molar equivalents of biotinylated ESC11-Fab (Figure S4). We then tested the ability of ESC11-Fab to bind to its antigen once it was immobilized on a strepta-

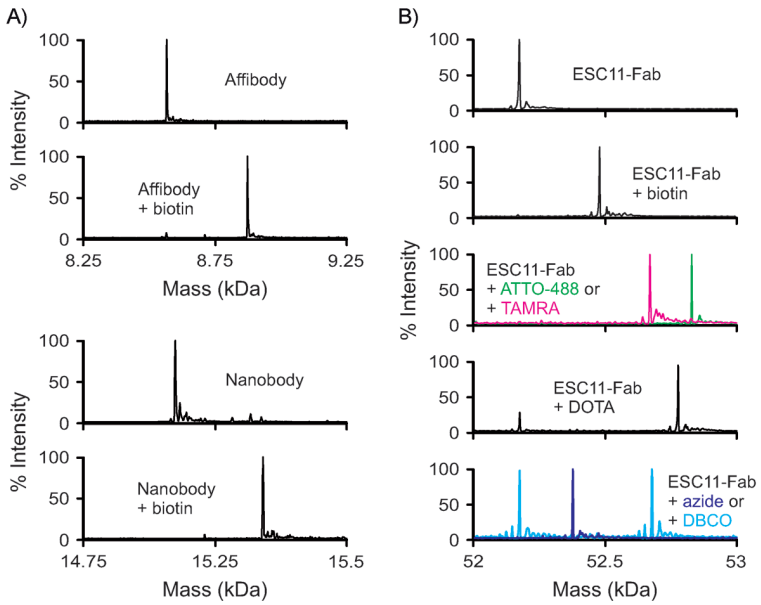

Figure 2. Monitoring of MTGase-catalyzed protein conjugation by mass spectrometry. A) MaxEnt1 deconvoluted mass spectra of an affibody and a nanobody before and after incubation with MTGase and *N*-(biotinyl)cadaverine (designated "biotin"). The mass shift corresponds to the attachment of exactly one biotin (311 Da). B) MaxEnt1 deconvoluted mass spectra showing the successful conjugation of different functionalities to ESC11-Fab. The two individual spectra of ESC11-Fab-ATTO-488 and ESC11-Fab-TAMRA as well as ESC11-Fab-azide and ESC11-Fab-DBCO are merged into one spectrum.

vidin-coated surface by adding recombinant FAP (Figure S5 A). Highly quenched fluorescein-labeled gelatin revealed the specific capturing of enzymatically active FAP by the biotinylated immobilized ESC11-Fab (Figure S5 B). Finally, we demonstrated that the biotinylated ESC11-Fab could be specifically immobilized on an avidin-coated patterned surface (Figures 3 A and S6). This site-specific in vitro biotinylation approach enables us to immobilize proteins in an oriented manner that can contribute to an increased sensitivity of biosensors.[16] It also overcomes common problems of the classical BirA-mediated biotinylation in *Escherichia coli*, such as decreased protein-expression levels, because it does not rely on variable cellular processes.[17]

ESC11-Fab equipped with (ATTO-488)cadaverine was used for FACS analysis of HT1080FAP cells. FAP^+ cells could be specifically stained, whereas FAP^- cells did not show any fluorescent signal (Figure 3 B). We further functionalized ESC11-Fabs with another dye, *N*-(TAMRA)cadaverine, and could directly stain a series of FAP^+ cell lines, including activated fibroblasts, melanoma, and liposarcoma cells, with the two bioconjugates (Figure 3 C, Figure S7). While this direct staining helps to streamline and shorten immunofluorescence experiments, we envisage our conjugation strategy also being applied in assays in which it is not possible to use a secondary antibody and direct fluorescence labeling of the protein is required, for example, fluorescence anisotropy, analytical ultracentrifugation, or even optical in vivo imaging.

In order to transform the ESC11-Fab-DOTA into a radiotracer suitable for SPECT-CT imaging, we labeled it with $^{111}InCl_3$ to give ^{111}In-ESC11-Fab-DOTA which has specific activity of ~0.9 MBq per μg protein (Figure S8). We then injected ~18 MBq into liposarcoma tumor-bearing mice and successfully visualized the subcutaneous tumors by SPECT-CT imaging (Figure 3 D). These radioactive conjugates can also be used for biodistribution studies; moreover, therapeutic probes could easily be generated by using a suitable radionuclide.

Next, we attempted to generate homodimeric ESC11-Fab complexes by incubating ESC11-Fabs that have been conjugated with either an azide or DBCO functionality. Five hours after incubation at RT or 37 °C, we could detect by SDS-PAGE a band of approximately 100 kDa, which corresponds to the molecular weight of the desired bivalent product (Figure 3 E). The rather low reaction yield might be due to steric clashing of the two ESC11-Fabs. We have previously demonstrated the potential of transglutaminase-mediated coupling of a bioorthogonal entity to monoclonal antibodies.[18] In this case, a DBCO-derivative of the toxin monomethyl auristatin E (MMAE) could be efficiently attached to the site-specifically modified antibody by strain-promoted alkyne–azide cycloaddition. In a thorough study on using copper-free click chemistry to generate protein–protein fusions, it was demonstrated that the coupling yield depends both on the proteins and on the localization of the azide and DBCO functionality.[19] From these observations, we speculate that further optimization of the small-molecule linkers could potentially help to increase the yield of the dimerization with c-myc-tagged Fabs by reducing steric hindrance.

As a last example, we tried to directly immobilize the ESC11-Fab onto a surface. We used supported lipid bilayers (SLBs) as a model because they are compatible with a number of characterization tools, for example, quartz crystal microbalance with dissipation monitoring (QCM-D). In combination with patterning technologies, SLBs represent a potent option in the field of biosensor design.[20] To create SLBs that display amine donors for MTGase, we mixed maleimide-functionalized (PE-MCC) phospholipids and phosphocholine lipids (POPC) to generate liposomes that, when exposed to a solid support, formed a SLB. A peptide containing a cysteine (reactive towards the maleimide) and lysine (amine donor for MTGase; Figure S1) was coupled to the SLB in a second step that enabled us to covalently attach the ESC11-Fab to the SLB by using MTGase (Figure S9). The ESC11-Fab could then be efficiently anchored on the membrane, as indicated by a fast decrease in the resonant frequency of the quartz crystal, which corresponds to an increase in mass on the surface (Figure 3 F). The ability to de-

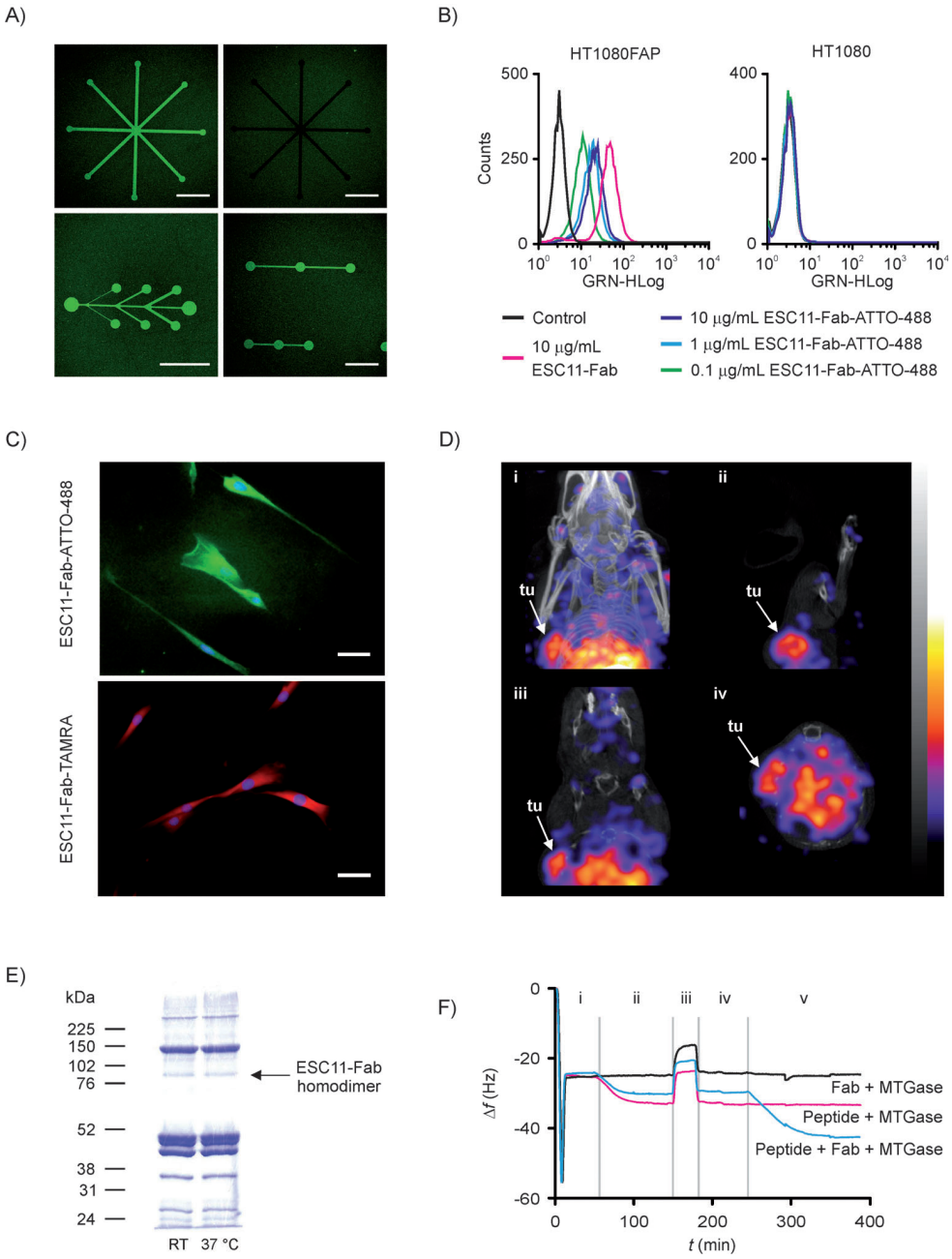

Figure 3. Downstream applications with different ESC11-Fab conjugates. A) Specific immobilization of biotinylated ESC11-Fab (Alexa Fluor 488-labeled) on different avidin-coated micropatterns and a negative control (top right, non-biotinylated Alexa Fluor 488-labeled ESC11-Fab). Scale bars: 50 μm. B) FACS analysis of FAP^+ (HT1080FAP) and FAP^- (HT1080) cells with different concentrations of ESC11-Fab-ATTO-488, and ESC11-Fab as a positive control. C) Immunofluorescence microscopy of FAP-expressing activated fibroblasts with ESC11-Fab-ATTO-488 (green), ESC11-Fab-TAMRA (red) and Hoechst 33342 (blue, for visualizing the cell nucleus). Scale bars: 50 μm. D) In vivo SPECT-CT imaging of liposarcoma (SW-872) tumor-bearing mouse with ^{111}In-ESC11-Fab-DOTA. Tumor cells (tu) were injected s.c. on the left shoulder. i) maximum intensity projection (MIP), ii) sagittal, iii) coronal, and iv) transverse views. E) Coomassie-stained SDS-PAGE gels after incubation of ESC11-Fab-PEG_3-azide and ESC11-Fab-PEG_4-DBCO. The clicked homodimer can be seen at ~100 kDa. F) QCM-D sensogram of direct MTGase-mediated ESC11-Fab immobilization on a SLB (blue). Additionally, unspecific adsorption (black) and MTGase self-immobilization (magenta) were tested. The different phases of the immobilization experiment were i) formation of the SLB, ii) cysteine–maleimide coupling of Lys-containing peptide to the SLB, iii) quenching of unreacted maleimides, iv) buffer exchange, v) MTGase-mediated immobilization of ESC11-Fab on SLB. A decrease in frequency corresponds to an increase in mass and, hence, conjugation of protein to the SLB surface.

termine the ratio between the PE-MCC and POPC enabled us to control the incorporation rate of amine functionalities and, as a consequence, the density of immobilized and oriented proteins on an SLB. Moreover, it is conceivable to directly functionalize liposomes with a targeting protein and use them as a drug-delivery system.

Conclusions

In conclusion, we have established a versatile enzyme conjugation platform that allows the site-specific functionalization of any c-myc-tagged antibody-like protein. Furthermore, we have demonstrated that the same protein can be easily transformed into different probes. Ultimately, these different conjugates could be used for in vitro or in vivo applications such as immunofluorescence assays, FACS, nuclear imaging, surface immobilization, and multimerization. Although we have only used a selection of functionalities for our studies, there are, nevertheless, numerous additional possibilities that are conceivable. Toxic agents, for example, could be used to transform a given protein into a therapeutic agent. As long as a primary amine functionality can be incorporated into a molecule, it is a potential substrate for MTGase. Consequently, there are virtually no limits to which extent our enzymatic bioconjugation platform could be expanded.

Experimental Section

General: All restriction enzymes were purchased from Fermentas (Thermo Fischer) and used according to manufacturer's instructions. Microbial transglutaminase (MTGase), *N*-(biotinyl)cadaverine, (ATTO-488)cadaverine, and *N*-(tetramethylrhodaminyl)cadaverine (TAMRA) were purchased from Zedira (Darmstadt, Germany), DBCO-PEG_4-amine and 11-azido-3,6,9-trioxaundecan-1-amine (azido-PEG_3-amine) were from Jena Bioscience GmbH (Jena, Germany) and 2,2′,2″-(10-(17-amino-2-oxo-6,9,12,15-tetraoxa-3-azaheptadecyl)-1,4,7,10-tetraazacyclododecane-1,4,7-triyl)triacetic acid (NH_2-PEG_4-DOTA) was from CheMatech (Dijon, France). The myc-tagged nanobody and affibody were kindly donated by collaborative partners.

Plasmid construction for ESC11-Fab: Primers specific for the 5′-end of ESC11 VL (5′-AGTGC ACTTG AAACG ACACT CACGC AGTCT CCAGG CA) and the 3′-end of ESC11 VH (5′-CTACC TCAGC GAAAA CTATA GACCC CGGTT CCCTG TTCCA GTGGC AG) were used to amplify the Fab VL-CL-VH sequence by using the pCES1 ESC11-Fab DNA[14] as a template. The taq-amplified PCR product (REDTaq DNA polymerase, Sigma) was cloned into the pCR2.1-TOPO vector (Invitrogen) and transformed into *E. coli* TOP10F′, after which blue/white screening was performed. Positive clones were verified by sequencing (Microsynth AG). SfiI sites were introduced at the 5′- and 3′-ends of the Fab in a two-step PCR reaction. In the first step, HUVK5 and hujh3 primers[21] were used to introduce the 5′-SfiI site. The PCR product was purified (illustra GFX PCR DNA and Gel Band Purification Kit, GE Healthcare) and used as a template for the second PCR step. Here, HUVK5 and c-3′fivh primers[21] were used to introduce the 3′-SfiI site, after which the PCR product was cloned into a pCR2.1-TOPO vector as before. A SfiI digest was performed to remove the ESC11-Fab insert, after which it was ligated into SfiI-digested pC3C vector (a kind gift from Prof. Christoph Rader, NIH, USA) that had been engineered to include a myc/His_6 tag. Clones were verified by sequencing.

Expression and purification of ESC11-Fab: pC3C ESC11-Fab was transformed into *E. coli* Top10F′. Stationary overnight cultures were diluted 1:10 into fresh 2TY medium, grown until an OD_{600} ~0.5 was reached, and induced with isopropyl β-D-1-thiogalactopyranoside (IPTG, 1 mM; Sigma). The protein was expressed for 20 h at 37 °C and 250 rpm, after which the cells were pelleted. The medium containing the ESC11-Fab was removed, filtered and applied directly onto CaptureSelect LC-Kappa agarose (2 mL, Life Technologies) by using a peristaltic pump at a flow rate of 1.5 mL min^{-1}. The resin was washed extensively with phosphate-buffered saline (PBS) before fractions (0.5 mL) of ESC11-Fab were eluted with glycine (0.1 M, pH 2.7) directly into neutralization buffer (Tris·HCl, 1 M, pH 8) to achieve a final pH of ~7.4. Fractions were analyzed by SDS-PAGE, and those containing ESC11-Fab were pooled and concentrated on a Vivaspin 6 column (10 kDa MWCO; LuBio Science) prior to purification by size-exclusion chromatography (SEC) on a Superdex S75 10/300 GL column (GE Healthcare) with a 0.5 mL min^{-1} flow rate. Fractions were analyzed by SDS-PAGE, and those containing only ESC11-Fab were pooled and concentrated as before. LC-ESI-MS analysis was performed to establish the purity of the protein.

Enzymatic functionalization of recombinant proteins: Recombinant proteins were functionalized as previously described.[18,22] Briefly, protein (6.6 μM) in PBS was incubated with the corresponding amine-functionalized chemical entity (80 molar equiv) and MTGase (6 U mL^{-1}) for 16 h at 37 °C. Unless stated otherwise, excess substrate and MTGase were removed by SEC on a Superdex 75 10/300 GL column with a 0.5 mL min^{-1} flow rate.

Chemical functionalization of ESC11-Fab with fluorescent dye: Alexa Fluor 488 NHS ester (10 molar equiv, Life Technologies, 10 mg mL^{-1} stock in DMSO) was added to ESC11-Fab (biotinylated and nonbiotinylated, ~4.5 mg mL^{-1} in $NaHCO_3$ buffer 100 mM, pH 8.3), and the mixture was incubated for 1 h at RT with vigorous shaking before being purified on a NAP-5 column (GE Healthcare). The degree of labeling was determined on a P-class NanoPhotometer (Implen GmbH, Munich, Germany) with the default settings for Alexa Fluor 488 (on average 2 dyes per ESC11-Fab).

LC-ESI-MS analysis of proteins: LC-MS analysis was performed on a Waters LCT Premier mass spectrometer. Samples were chromatographed on an Uptisphere 5BP1#15QS C18, 150×2 mm column (Interchim, Montluçon, France) heated to 40 °C by using a linear gradient from 20 to 80% solvent A over 20 min plus 5% solvent C (solvent A: acetonitrile + 0.1% formic acid, solvent B: water + 0.1% formic acid, solvent C: propan-2-ol) at a flow rate of 0.5 mL min^{-1}. The eluent was ionized by using an electrospray source. Data were collected with MassLynxV4.1, and deconvolution was performed by using MaxEnt1.

Peptide mapping: The protocol for tryptic digestion was adapted from a previously published paper.[23] Briefly, dithiothreitol (DTT; 0.96 μL, 1 M) was added to a solution of protein (6.6 nmol) in ammonium bicarbonate (50 μL, 50 mM, pH 8.0) containing 0.1% Rapidgest SF (Waters), and the mixture was incubated for 30 min at 55 °C. After the sample had been cooled to room temperature, iodoacetamide (IAM; 1.92 μL, 1 M) was added, and the samples were incubated for 40 min in the dark at RT. Sequencing-grade modified trypsin (1:20, *w/w*, Promega) was added, and the protein was digested for 16 h at 37 °C. Prior to LC-ESI-MS measurement, the samples were diluted 1:1 (*v/v*) with 1% formic acid in 10% CH_3CN. An auxiliary pump was used to spray a solution of leucine enkephalin (50 pmol mL^{-1}) in CH_3CN/H_2O (50:50) containing 0.1% formic acid for mass accuracy (lockmass channel). The system was calibrated by using a sodium formate infusion (0.05 M NaOH + 0.5% formic acid). The peptide mixture was then separated on a AerisPEPTIDE 3.6 μm XB-C18, 150×2.1 mm column (Phenomenex) heated to 80 °C by using the following gradient: 0–5 min, 3% solvent A; 5–60 min, 3–45% solvent A; 60–65 min, 45–90% solvent A, 65–

70 min, 90–3% solvent A. Data were collected and analyzed with MassLynxV4.1.88

Native gel of streptavidin–ESC11-Fab complex: Different molar ratios of streptavidin (Thermo)/biotinylated ESC11-Fab (1:1, 1:2, 1:3, 1:4, 1:5, 1:8) were incubated for 1.5 h at RT, an aliquot of the reaction mixture was then loaded onto a native gel (7.5% polyacrylamide, pH 8.8, 160 V, 50 min), and the gel was stained with Coomassie Brilliant Blue.

ESC11-Fab immobilization on a streptavidin-coated surface and functionality test: Biotinylated ESC11-Fab (100 μL, 10 μg mL^{-1}) in reaction/wash buffer (25 mM Tris·HCl, 150 mM NaCl, pH 7.2, 0.1% BSA, 0.05% Tween20) was added to a streptavidin-coated 96-well plate (Reacti-Bind Streptavidin-coated plate, Pierce, Thermo Scientific), which was incubated for 2 h at RT and 220 rpm. The wells were washed with wash buffer (3×200 μL) before incubation with fibroblast activation protein (FAP, 100 μL, 5 μg mL^{-1}, Sigma) for 1 h at RT and 220 rpm. The wells were washed wash buffer (3×200 μL) and then incubated with DQ Gelatin (100 μL, 0.1 mg mL^{-1} in PBS, Life Technologies) at 37 °C for 88 h. The fluorescent intensity was measured on a Multilabel Plate Reader (VICTOR X3, PerkinElmer) by using a preset protocol for fluorescein (λ_{ex} = 485 nm, λ_{em} = 535 nm, 0.1 s, bottom). The raw data were processed by using GraphPad Prism 6.0.

ESC11-Fab immobilization on avidin-coated micropatterns: Micropatterns were created as previously described.[24] Briefly, the clean patterned glass slides were incubated with nitrodopamine-mPEG (100 μg mL^{-1}, SuSoS, Dübendorf, Switzerland) in high-salt MOPS buffer (100 mM 3-(*N*-morpholino)propanesulfonic acid, pH 6, 600 mM NaCl, 600 mM K_2SO_4 readjusted to pH 6) for 4 h at 80 °C. After incubation, the samples were rinsed with ultrapure water before being washed in HEPES buffer (10 mM (4-(2-hydroxyethyl)-1-piperazineethanesulfonic acid, 150 mM NaCl, pH 7.4) for 24 h at RT with gentle agitation to remove unbound PEG polymer. The glass slides were rinsed with ultrapure water, dried with nitrogen, and mounted in a tailor-made microscopy cell, where they were incubated with avidin (40 μg mL^{-1}, Sigma–Aldrich) in Tris-buffered saline (TBS, 10 mM tris(hydroxymethyl)aminomethane, 150 mM NaCl, pH 7.4) for 1 h at RT, then washed with TBS (10 mL), incubated with biotinylated or nonbiotinylated Alexa Fluor 488-conjugated ESC11-Fab (30 μg mL^{-1}), and finally washed with TBS (10 mL). Images of the patterns were captured on a Leica SP5 confocal microscope, and raw data were processed with ImageJ (NIH, USA).

Cell lines: All cell lines were kindly donated by Prof. Christoph Renner (University Hospital Zürich). Rheumatoid arthritis synovial fibroblasts (RASFs), melanoma cell line SK-Mel-187, fibrosarcoma cell line HT1080 (FAP$^-$), and HT1080FAP (FAP$^+$) were maintained in RPMI 1640 (Bioconcept). The liposarcoma cell line SW-872 was maintained in DMEM high glucose. Media were supplemented with 10% fetal calf serum (FCS), glutamine (2 mmol L^{-1}), penicillin (100 units mL^{-1}), streptomycin (100 μg mL^{-1}), and fungizone (0.25 μg mL^{-1} BioConcept). In addition, 3% normal human serum (NHS, Millipore) and 1% nonessential amino acids (NEAA, Bioconcept) were added to the medium for RASFs and SW-872, respectively. The cells were maintained at 37 °C under 5% CO_2.

Fluorescence-activated cell sorting (FACS): Cells were harvested with Accutase (Millipore), washed with 1% BSA-supplemented PBS (PBS/BSA) and incubated with ESC11-Fab or ESC11-Fab-ATTO-488 (10, 1, or 0.1 μg mL^{-1}) for 2 h at RT. Cells were washed on ice with PBS/BSA (3×200 μL), and those treated with ESC11-Fab only were incubated with a goat anti-human IgG-FITC (1:200 dilution in PBS/BSA, Santa Cruz Biotechnology) for 30 min at 4 °C in the dark, then washed as before. All cells were resuspended in PBS/BSA (200 μL) and directly submitted to flow cytometry (Guava easyCyte Flow Cytometer, Merck Millipore). Data were analyzed with FlowJo software (TreeStar Inc.).

Fluorescence microscopy: Cells were seeded in Nunc 8-well Lab-Tek II Chamber Slides (Thermo Scientific) at a density of 5000 cells per well and allowed to attach overnight at 37 °C under 5% CO_2. The cells were washed with PBS (3×400 μL), fixed with pre-warmed (37 °C) 4% paraformaldehyde (400 μL) for 15 min at 37 °C, washed with PBS (3×400 μL), incubated with 1 drop of ImageitFX (Invitrogen) for 30 min at RT, washed with PBS (3×400 μL), and incubated with either ESC11-Fab-ATTO-488 or ESC11-Fab-TAMRA (250 μL, 10 μg mL^{-1} in PBS/BSA) for 2 h at RT. The cells were then washed with ice-cold PBS (3×400 μL), incubated with Hoechst 33342 (250 μL 1 mM) for 10 min at RT, and washed with deionized water (3×400 μL). The medium chamber was dismounted, the slides were drained and dried with a tissue, and the cells were covered with one drop of Prolong Gold (Invitrogen). The coverslip was sealed with nail polish, and the slides were stored in the dark at 4 °C. Images were captured on a Zeiss Axiovert 200M microscope, and raw data were processed with ImageJ (NIH, USA).

Radiolabeling: NH_2-PEG_4-DOTA was enzymatically conjugated to ESC11-Fab, as described above. After 16 h of incubation at 37 °C, MTGase activity was blocked by the addition of MTGase-blocker (500 μM, Zedira, Darmstadt, Germany). The reaction mixture was buffer-exchanged into NH_4OAc (0.5 M, pH 5.5) by using a Vivaspin 6 column (10 kDa MWCO), radiolabeled with $^{111}InCl_3$ (1 MBq per μg ESC11-Fab-DOTA) for 1 h at 37 °C, after which it was purified by SEC on a Superdex 75 10/300 GL column, 0.5 mL min^{-1} flow rate, and the major peak fractions were pooled.

Biodistribution and SPECT/CT imaging: Animal studies were conducted in compliance with Swiss laws on animal protection. All experiments were approved by the animal welfare commission of the cantons BS-BL-AG, Switzerland, and permitted by the local government (Departement Gesundheit und Soziales, Veterinärdienst des Kantons Aargau, Switzerland; permission number 75528). All efforts were made to minimize suffering. Housing and animal husbandry were conducted according to local law on animal protection.

Female 5-week-old CB17/Icr-Prkdc scid/Crl mice (Charles River, Sulzfeld, Germany) were inoculated subcutaneously (left shoulder) with 5×10^6 liposarcoma cells SW-872 each, and tumors were allowed to grow for 4 weeks before the mice were randomly divided into two groups (n = 4) and injected with ~18 MBq ^{111}In-ESC11-Fab-DOTA (~20 μg protein). SPECT/CT (NanoSPECT/CT, Bioscan Europe, Paris, France) imaging was performed 1 and 24 h p.i. The scans were acquired by using Nucline software (version 1.02, Bioscan, Inc.), and the data sets were analyzed with the InVivoScope post-processing software (version 2.0, Bioscan, Inc.).

Dimerization: The reaction conditions to generate homo-bifunctional Fab fragments by using copper-free click chemistry were adapted from a previously published procedure.[19] Briefly, ESC11-Fab-PEG_3-azide (20 μM) was treated with ESC11-Fab-PEG_4-DBCO (40 μM) at RT or 37 °C. An aliquot of the reaction mixture was analyzed by SDS-PAGE (10% polyacrylamide) after 5 h of incubation.

Supported lipid bilayers

Production of liposomes: Lipids 1-palmitoyl-2-oleoyl-*sn*-glycero-3-phosphocholine (POPC) and 1,2-dioleoyl-*sn*-glycero-3-phosphoethanolamine-*N*-[4-(*p*-maleimidomethyl)cyclohexane-carboxamide] PE-MCC (Avanti Polar Lipids) were mixed in the ratio of 90:10 (mol%). The solvent was evaporated under a gentle stream of argon for 1 h

to obtain a dried lipid film, which was rehydrated with TBS (50 mM tris(hydroxymethyl)aminomethane, 150 mM NaCl, pH 7.2) so that a final lipid concentration of 2 mg mL^{-1} was reached. The liposome suspension was then extruded 31 times through two polycarbonate filters (Avestin, Ottawa, Canada) with a pore size of 100 nm by using a LiposoFast extruder (Avestin, Canada).

Quartz crystal microbalance with dissipation monitoring (QCM-D): A Q-Sense E4 quartz crystal microbalance with dissipation monitoring (QCM-D; Q-Sense AB, Sweden) was used to investigate supported lipid-bilayer functionalization. SiO_2-coated 4.95 MHz QCM-D crystals (Q-Sense AB, Sweden) were sonicated for 20 min in toluene, then for 20 min in isopropanol. The crystals were washed with Milli-Q water and blow-dried with nitrogen followed by exposure to UV/ozone for 30 min (UV/Ozone Procleaner, Bioforce Nanosciences, USA). All buffers were degassed prior to use, and measurements were performed at 25 °C. A multichannel dispenser equipped with 0.51 mm tygon tubing (IPC Ismatec SA, Switzerland) was used to inject all the solutions. The measurement cell was rinsed with TBS (pH 7.2 or 7.6) between all steps for 20 min at a flow rate of 50 μL min^{-1}. The cleaned crystals were mounted into the cells, and the baseline was equilibrated with TBS (pH 7.2). Afterwards, a liposome solution (100 μg mL^{-1}) was injected at a flow rate of 376 μL min^{-1} for 30 s, then at 10 μL min^{-1} for 50 min. The lipid bilayer was exposed to the lysine-containing peptide (168 μM in TBS, pH 7.2, Ac-FKGGERCG-NH_2, Genscript, Piscataway, NJ, USA) for 50 min (10 μL min^{-1}). Unreacted maleimides were quenched with β-mercaptoethanol (5 mM; Sigma–Aldrich) for 5 min. The buffer was then changed to TBS (pH 7.6) for the enzymatic immobilization of the ESC11-Fab. The peptide-modified SLB was exposed to a mix of MTGase (0.2 U mL^{-}) and to ESC11-Fab (50 μg mL^{-1}) at a flow rate of 376 μL min^{-1} for 30 s and then at 10 μL min^{-1} for 50 min. The stock mixture of ESC11-Fab and MTGase was kept on ice to avoid deamination of the reactive glutamine. The represented graphs are measured at the fifth overtone ($f_5 \approx 25$ MHz).

Acknowledgements

This work was funded by the Swiss National Science Foundation (Grant Nr. 132611). The authors would like to thank Susan Cohrs for technical assistance with cell culture and for performing in vivo SPECT-CT imaging.

Keywords: c-myc-tag · enzymes · microbial transglutaminase · protein modifications · site-specific modification

[1] C. E. Chan, A. P. Lim, P. A. MacAry, B. J. Hanson, *Int. Immunol.* **2014**, *26*, 649 – 657.
[2] U. H. Weidle, J. Auer, U. Brinkmann, G. Georges, G. Tiefenthaler, *Cancer Genomics Proteomics* **2013**, *10*, 155 – 168.
[3] a) B. M. Hutchins, S. A. Kazane, K. Staflin, J. S. Forsyth, B. Felding-Habermann, P. G. Schultz, V. V. Smider, *J. Mol. Biol.* **2011**, *406*, 595 – 603; b) G. Papalia, D. Myszka, *Anal. Biochem.* **2010**, *403*, 30 – 35; c) E. Frampas, C. Rousseau, C. Bodet-Milin, J. Barbet, J. F. Chatal, F. Kraeber-Bodere, *Front. Oncol.* **2013**, *3*, 159.
[4] P. C. Weber, D. H. Ohlendorf, J. J. Wendoloski, F. R. Salemme, *Science* **1989**, *243*, 85 – 88.
[5] a) C. H. Kim, J. Y. Axup, P. G. Schultz, *Curr. Opin. Chem. Biol.* **2013**, *17*, 412 – 419; b) M. Rashidian, J. Dozier, M. Distefano, *Bioconjugate Chem.* **2013**, *24*, 1277 – 1294.
[6] S. C. Alley, D. R. Benjamin, S. C. Jeffrey, N. M. Okeley, D. L. Meyer, R. J. Sanderson, P. D. Senter, *Bioconjugate Chem.* **2008**, *19*, 759 – 765.
[7] I. S. Carrico, B. L. Carlson, C. R. Bertozzi, *Nat. Chem. Biol.* **2007**, *3*, 321 – 322.
[8] D. Rabuka, J. S. Rush, G. W. deHart, P. Wu, C. R. Bertozzi, *Nat. Protoc.* **2012**, *7*, 1052 – 1067.
[9] a) H. Mao, S. A. Hart, A. Schink, B. A. Pollok, *J. Am. Chem. Soc.* **2004**, *126*, 2670 – 2671; b) R. Policarpo, H. Kang, X. Liao, A. Rabideau, M. Simon, B. Pentelute, *Angew. Chem. Int. Ed.* **2014**, *53*, 9203 – 9208; *Angew. Chem.* **2014**, *126*, 9357 – 9362.
[10] K. Mehta, R. L. Eckert, *Transglutaminases: Family of Enzymes with Diverse Functions*, Karger, Basel, **2005**.
[11] a) A. Fontana, B. Spolaore, A. Mero, F. M. Veronese, *Adv. Drug Delivery Rev.* **2008**, *60*, 13 – 28; b) B. Spolaore, S. Raboni, A. Ramos Molina, A. Satwekar, N. Damiano, A. Fontana, *Biochemistry* **2012**, *51*, 8679 – 8689.
[12] a) P. Strop, S.-H. Liu, M. Dorywalska, K. Delaria, R. Dushin, T.-T. Tran, W.-H. Ho, S. Farias, M. Casas, Y. Abdiche, D. Zhou, R. Chandrasekaran, C. Samain, C. Loo, A. Rossi, M. Rickert, S. Krimm, T. Wong, S. Chin, J. Yu, et al., *Chem. Biol.* **2013**, *20*, 161 – 167; b) T. Tanaka, N. Kamiya, T. Nagamune, *Bioconjugate Chem.* **2004**, *15*, 491 – 497; c) K. Moriyama, K. Sung, M. Goto, N. Kamiya, *J. Biosci. Bioeng.* **2011**, *111*, 650 – 653.
[13] M. Weber, E. Bujak, A. Putelli, A. Villa, M. Matasci, L. Gualandi, T. Hemmerle, S. Wulhfard, D. Neri, *PLoS One* **2014**, *9*, e100000.
[14] E. Fischer, K. Chaitanya, T. Wuest, A. Wadle, A. M. Scott, M. van den Broek, R. Schibli, S. Bauer, C. Renner, *Clin. Cancer Res.* **2012**, *18*, 6208 – 6218.
[15] M. T. Gundersen, J. W. Keillor, J. N. Pelletier, *Appl. Microbiol. Biotechnol.* **2014**, *98*, 219 – 230.
[16] A. Trilling, M. Harmsen, V. Ruigrok, H. Zuilhof, J. Beekwilder, *Biosens. Bioelectron.* **2013**, *40*, 219 – 226.
[17] Y. Li, R. Sousa, *Protein Expression Purif.* **2012**, *82*, 162 – 167.
[18] P. Dennler, A. Chiotellis, E. Fischer, D. Bregeon, C. Belmant, L. Gauthier, F. Lhospice, F. Romagne, R. Schibli, *Bioconjugate Chem.* **2014**, *25*, 569 – 578.
[19] J. E. Hudak, R. M. Barfield, G. W. de Hart, P. Grob, E. Nogales, C. R. Bertozzi, D. Rabuka, *Angew. Chem. Int. Ed.* **2012**, *51*, 4161 – 4165; *Angew. Chem.* **2012**, *124*, 4237 – 4241.
[20] E. Reimhult, M. K. Baumann, S. Kaufmann, K. Kumar, P. R. Spycher, *Biotechnol. Genet. Eng. Rev.* **2010**, *27*, 185 – 216.
[21] T. Hofer, W. Tangkeangsirisin, M. G. Kennedy, R. G. Mage, S. J. Raiker, K. Venkatesh, H. Lee, R. J. Giger, C. Rader, *J. Immunol. Methods* **2007**, *318*, 75 – 87.
[22] P. Dennler, R. Schibli, E. Fischer in *Antibody–Drug Conjugates, Vol. 1045* (Ed.: L. Ducry), Humana, Totowa, **2013**, pp. 205 – 215.
[23] H. Xie, A. Chakraborty, J. Ahn, Y. Q. Yu, D. P. Dakshinamoorthy, M. Gilar, W. Chen, S. J. Skilton, J. R. Mazzeo, *mAbs* **2010**, *2*, 379 – 394.
[24] P. R. Spycher, H. Hall, V. Vogel, E. Reimhult, *Biomater. Sci.* **2015**, *3*, 94 – 102.

Received: January 7, 2015
Published online on February 16, 2015

J. Sep. Sci. 2015, *38*, 2559–2572

Gérald Perret[1]
Patrick Santambien[1]
Egisto Boschetti[2]

[1]LFB Biotech, Les Ulis, France
[2]Bioconsultant, JAM Conseil, Neuilly, France

Received March 27, 2015
Revised April 26, 2015
Accepted May 10, 2015

Review Article

The quest for affinity chromatography ligands: are the molecular libraries the right source?†

Affinity chromatography separations of proteins call for highly specific ligands. Antibodies are the most obvious approach; however, except for specific situations, technical and economic reasons are arguments against this choice especially for preparative purposes. With this in mind, the rationale is to select the most appropriate ligands from collections of pre-established molecules. To reach the objective of having a large structural coverage, combinatorial libraries have been proposed. These are classified according to their nature and origin. This review presents and discusses the most common affinity ligand libraries along with the most appropriate screening methods for the identification of the right affinity chromatography selective structure according to the type of library; a side-by-side comparison is also presented.

Keywords: Affinity chromatography / Aptamers / Ligands / Peptides / Protein purification
DOI 10.1002/jssc.201500285

1 Introduction

With the advent of biotechnological and therapeutic applications, protein separation from recombinant technologies or from natural extracts becomes a crucial unavoidable preparative operation. This is mainly turned to practice using various chromatographic unitary operations, the most important being affinity chromatography [1]. Affinity chromatography can be used on very wide scope since it extends from the separation of groups of proteins (e.g. glycoproteins) to single gene products. The specificity of the method is played at the level of the selectivity of the affinity ligand grafted on the solid separation support. When a very specific interaction is desired, antibodies against the target protein are naturally used, the affinity chromatography approach being called immunoaffinity chromatography [2].

Affinity chromatography is a selective protein capture method involving a classical solid-state support on which a molecule called a 'ligand', able to specifically interact with the target protein, is covalently grafted. Here the notion of ligand is very distinct from what is intended in drug discovery domain: while in drug discovery/evaluation the ligand is the target (it can be a receptor), in affinity separation it is a small or large molecule capable to interact selectively with a protein to be isolated from complex biological mixtures.

From the 1970s, affinity chromatography represented an immense promise even if in current practice a number of concerns limited its development; the main one being the design or the selection of specific ligands interacting exclusively with the target proteins. Only few ligands of narrow specificity are commercially available, so the obvious solution was the preparation of antibodies. Considering the practical limitations of antibodies as discussed later in this document, scientists tried to select potential affinity ligands from random collections of molecules such as reactive dyes [3] with some level of success; however the more rational solution is to make and screen rational combinatorial molecules that are called libraries. The first combinatorial chemical libraries were not invented for affinity chromatography purposes, but rather for pharmaceutical applications with the objective of novel drug discovery [4,5], then, with the advent of novel technological developments, the concept of combinatorial libraries demonstrated its validity also for affinity chromatography purposes. In this domain several types of libraries were progressively proposed such as novel chemical libraries adapted for chromatographic applications [6], combinatorial peptides [7], polypeptides obtained by randomized expression in microorganisms [8] and randomized oligonucleotides [9]. All these solutions allowed pushing further and further the specificity of ligands for chromatography while enlarging the number of species present in each library [10]. At this stage to identify the right molecular structure specific for the target protein novel screening

Correspondence: Egisto Boschetti, Bioconsultant, JAM Conseil, Neuilly, 11, rue cote a belier, 78290 Croissy sur Seine, France
E-mail: egisto.boschetti@gmail.com

Abbreviations: EPO, erythropoietin; **CHAPS**, 3-[3-chloramidopropyl)-dimethylammonio)propanesulfonate; **CHO**, Chinese hamster ovary cells; **HEPES**, hydroxyethyl -piperazine-ethanesulfonic acid; **LC**, Liquid chromatography; **SELEX**, systematic evolution of ligands by exponential enrichment

†This paper is included in the virtual special issue on Separation Science in South America available at the Journal of Separation Science website.

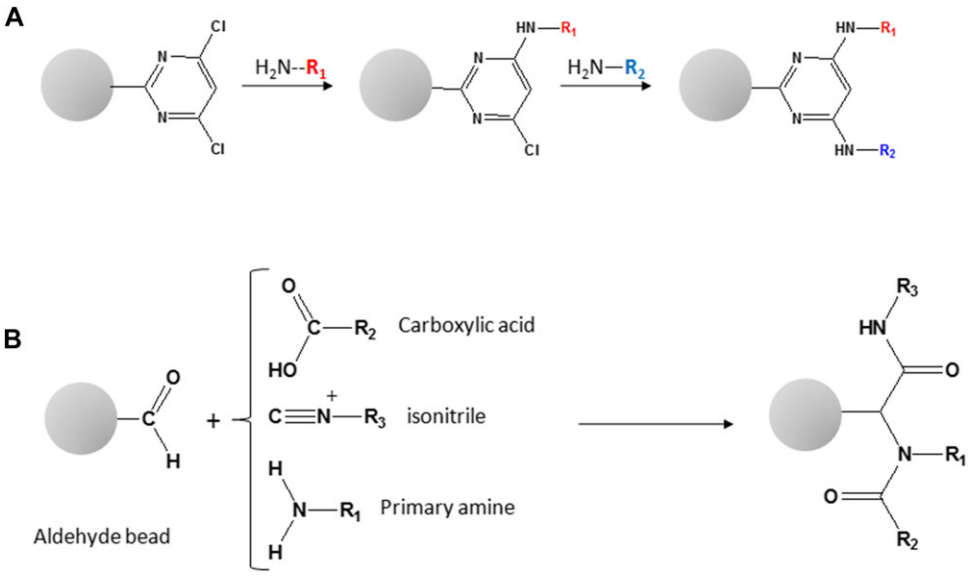

Figure 1. Chemical routes for the preparation of affinity combinatorial ligands.
Panel "A" represents the reaction sequence for the triazine-based ligands.
Panel "B" shows schematically the multicomponent UGI reaction. A very large diversity can be obtained if considering that about 95 000 primary amines are commercially available, more than 500 carboxylic acids are available as well as more than 1000 isonitriles can be made.

solutions had to be set up to find the one that is further produced in the amount required for the preparation of the affinity chromatography material. Little by little the definition of the ideal affinity chromatography ligand has been coined and perfected; at the same time the use of combinatorial ligand libraries as sources of specific bait for capturing given proteins was progressively imposed.

It is within this context that the present review stands. Most important affinity ligand libraries are presented as well as the mode of selection of the effective ligand for the chosen purpose.

2 Affinity ligand libraries

The first libraries of organic molecules have been designed in the early 90's in response to pharmaceutical needs [4]. By exploring the largest panel of molecules the probability to fish out an effective drug candidate for a given disease was considered relatively high. The binding mechanism of these molecules to cell receptors being similar to what is encountered in affinity chromatography, a library of molecules could also be considered as an assembly of potential ligands for protein isolation from where appropriate structures could be retrieved and grafted on chromatographic solid supports [11]. Basically once identified, the ligand is chemically attached and the resulting support conjugate is used to selectively adsorb a single protein from complex mixtures. The separated protein is then desorbed isolated and either characterized for well-known uses in research (e.g. molecular characterization) or used for diagnostic purposes or even as biodrug candidates for a targeted therapy.

In affinity chromatography the structure of a ligand needs to comply with well-known characteristics. First, it should be a relatively small molecule with the highest possible specificity to bind the target protein to be purified with the possibility to be covalently attached onto a polymeric support. Nevertheless the association constants should not be too high to allow the dissociation of the ligand-protein complex under relatively mild conditions preventing both the protein denaturation and the ligand degradation in order to enter successive and numerous separation cycles contributing thus to the overall process economy. An important consequence of this definition is a high stability over time even in the presence of quite stringent cleaning agents used in LC between cycles.

In practice when starting from large ligand libraries it is common to encounter situations where the ligand identified as specific for the targeted protein is of unknown structure. To resolve this question libraries are designed and screened with the capability to retrieve the full structure of the affinity ligand that has to be produced in large amount and then grafted on the chromatographic support [12].

The following sections describe the preparation of chemical libraries peptide-based structures, polypeptides and oligonucleotides with associated technical features.

2.1 Chemical ligand libraries

Many synthetic chemical ligand libraries have been described [see for example reviews 13–15], but those that have produced various and consistent affinity ligands for chromatographic applications are limited in number: the most known are triazine biomimetic structures [16], multicomponent UGI reaction libraries [17–20] and peptoids [21–23].

Triazine biomimetic structures are obtained by reacting trichloro-s-triazine, a well known tripolar reactive compound, with three different chemical substituents, the reactions being modulated by temperature changes. Chemical substituents are selected among available collections of primary amines and according to a preliminary selection dictated by molecular modeling [6]. Basically the first reaction is

to attach the trichloro-s-triazine on amino-derived chromatographic beads by one reactive point; this reaction performed at low temperature leaves the two other diversity points free for subsequent reactions. Then the second and the third diversity points are serially reacted with appropriate amino chemicals that are selected for their potential affinity for the target protein as described by Teng et al. [6] (see Fig. 1 A). The synthesis is relatively easy (a detailed recipe can be found in Roque et al. [24]); however, the substituents have to be rationally selected to react on the diversity points of triazine. This process has been approached by the group of Lowe [16, 25, 26] from molecular models and docking software that rendered possible the selection of the most probable chemical substituents to produce ligand structures with a relatively high probability of success. The principle virtually applies to any protein type since the ligand-protein affinity interaction is based on molecular docking conditioned by amino acid interactions (electrostatic, hydrophobic, hydrogen bonding). From a library of molecules only one is selected and used for the target protein separation (see Section 3 below). In practice the synthesis of such a combinatorial ligand library is conducted in parallel (as for instance in a 96-well plate) manually or robotically where each chemical member of the solid phase library is identified by the plate coordinates. The library could be very large if one considers the large number of primary amines commercially available (around 95 000); however, the use of molecular docking software largely reduces the number of pertinent aminated molecules; hence the library is generally composed of a limited number of diversomers (diverse ligands). As the reaction is a solid-phase synthesis, the ligands are already attached on the chromatographic support. The work that remains to be done is the systematic evaluation of each diversomer with respect to the affinity chromatography performance measured by its specificity, the number and the amount of protein impurities and the binding capacity of the solid phase. Using this approach many proteins have been purified from crude extracts as reported in a recent review [27]. One of the pioneering experimental works was from Li et al. [28] while attempting to design and make biomimetic ligands having high affinity properties for immunoglobulin G (IgG) as a possible replacement of Protein A. The triazine diversity center was substituted by phenylamine and *p*-aminophenol both coming from a rational investigation about the docking epitope where the interaction was supposed to occur. The reached affinity constant was between 10^5 and 10^6 M^{-1} and was considered acceptable for the separation of monoclonal antibodies and polyclonal IgG of murine and human origin. The replacement of phenylalanine by 4-amino-1-naphtol did not change significantly the affinity constant value, but improved the specificity as described with a binding capacity for IgG of few dozens of mg/mL of sorbent [29]. With human IgG it has been demonstrated that the capture efficiency was 94% and the purity obtained was close to 92% after an elution allowing a recovery of about 60%.

One of these triazine combinations designed as antibody binder became also commercially available involving *p*-aminophenol and *o*-aminophenol as triazine substituents. With a capture of antibodies in 25 mM sodium phosphate buffer pH 7.6 and elution obtained with 100 mM glycine-HCl, pH 2.5 the purity of monoclonal IgG was very effective with a binding capacity of 27 mg/mL [30].

Still for IgG purification a triazine-based ligand was designed to capture the antibodies by interacting with Fab fragment (a mimic of Protein L). In this case the first substituent was aminobutyric acid and the second was *p*-aminobenzamide; the ligand was attached to the solid support by means of a spacer arm of six carbons [31]. The separation of IgGs from goat and human blood sera at a purity of 91% was performed in a physiological phosphate buffered saline and the desorption obtained using 100 mM glycine-HCl buffer pH 2.0. Other examples of triazine-based ligands have been described among which Kallikrein, insulin and α1-antitrypsin [32].

Multicomponent UGI reaction libraries, another category of chemical ligands, are produced by a single reaction involving an aldehyde (this is part of the solid support), a carboxylated compound, a primary amine and an isonitrile structure (Fig. 1B). Considering the very large diversity of available carboxyl-containing structures as well as primary amines, aldehydes, and isonitriles, the number of diversomers theoretically obtainable can reach several hundreds of millions. To reduce the efforts of ligand screening, more focused libraries have been prepared after selecting the building blocks using docking model already adopted for the triazine-based ligand libraries as described above. By this way an erythropoietin (EPO) specific ligand has been selected from a limited library [18]. The chemical substituents had been selected to comply with informatics docking models based on the crystallographic structure of EPO cell-surface receptor. The most effective ligand was sorted out from a collection of only few variants and was able to selectively bind human rEPO from a CHO cell culture supernatant. The elution performed with 20 mM phosphate buffer, pH 7.4 containing 0.25% CHAPS, allowed purity of EPO estimated around 80% in a single run. In another example Qian et al. [19] selected a ligand resulting from the reaction of an aldehyde sorbent with 4-aminobenzamide, indole-3 acetic acid and isopropyl isocyanide. This ligand was supposed to mimic Protein G as a proteinaceous ligand for IgG. It was very effective in purifying IgG from various mammals with a capturing efficiency up to 100% and purity of about 65% that is comparable to genuine Protein G affinity chromatography. Interestingly antibodies could be recovered using a neutral buffer added with some amount of ethylene glycol. When replacing indole-3 acetic acid by hydroxyphenyl benzoic acid some changes have been observed in terms of affinity constant and ability to increase the purity and the specificity for antibodies of IgG class [20]. Actually separations processes for IgG and Fab fragments from crude mammalian and yeast cell cultures showed a capture yield close to 99% and a purity of 93%.

Another category of chemical ligands are peptoids. They are linear integrating primary amines where the diversity is played on the side chains of the selected building blocks. Primary amines can be used under combinatorial mode or

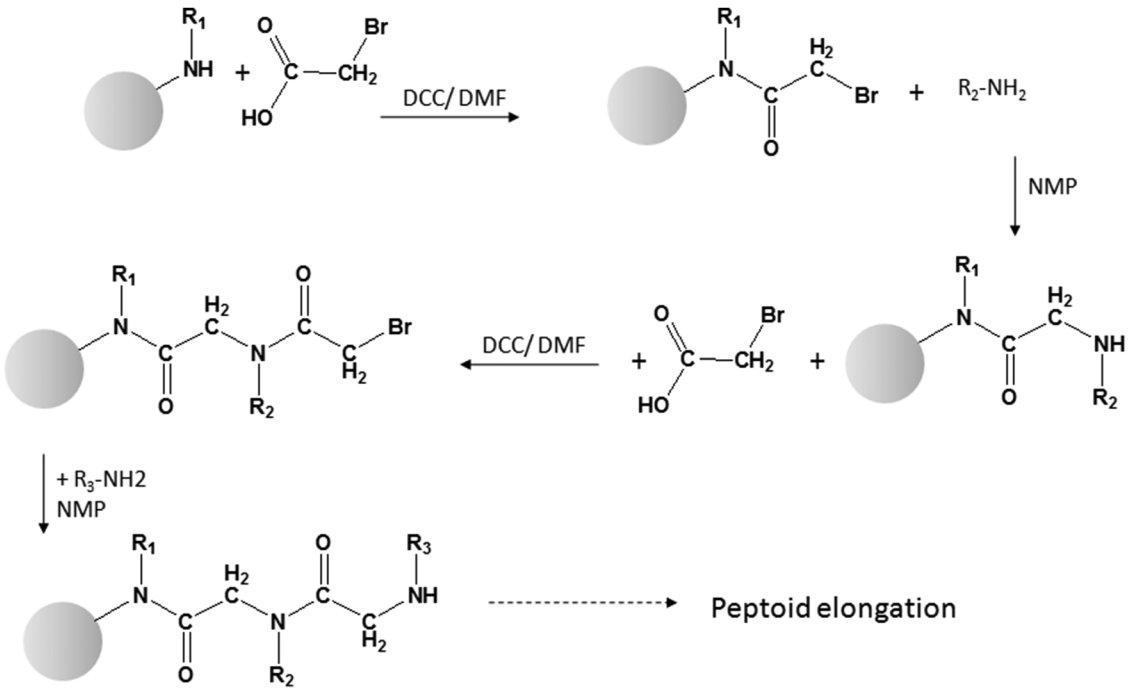

Figure 2. Schematic representation of reaction sequence for the preparation of peptoids (N-glycine substituted oligomers). Primary amines are added sequentially alternated by the introduction of bromacetic acid. The first reaction is performed under anhydrous conditions and in the presence of a condensation agent; the amine coupling is made directly by reaction with the mobile bromine in alkaline conditions. DCC = dicyclohexyl carbodiimide; NMP = *N*-methyl pyridine.

not and thus generating diversomers in very large number. For example starting from only ten different amines it is possible to obtain one million of diverse ligands if the length of the ligand chain is composed of a sequence of six building blocks assembled under a combinatorial rule (10^6). Considering that the commercially available primary-amine-containing molecules are at least dozens of thousands the number of possible affinity ligands theoretically obtainable, even short, is huge. When searching for one affinity ligand with very selective properties for the protein to isolate, the probability to find a good candidate is increased by enlarging the size of the library, therefore it is always useful to deal with large diversity ligands. The synthesis process is relatively easy since it starts from a solid phase chromatographic support carrying a secondary amino terminal group that is reacted under anhydrous conditions with bromacetic acid in the presence of a condensation agent such as a carbodiimide [22]. The resulting compound is then reacted again with a bromacetic acid and so on (Fig. 2). The synthesis yields stable N-substituted glycine oligomers of a very large diversity. Using this approach a number of affinity selective ligands have been obtained; this is the case for amyloid beta 42 protein where a very effective ligand has been retrieved from a library of 38416 unique peptoids made with six building blocks [23].

2.2 Combinatorial peptide ligand libraries

Most commonly synthetic peptide libraries are obtained by reacting sequentially single amino acids to elongate the chain.

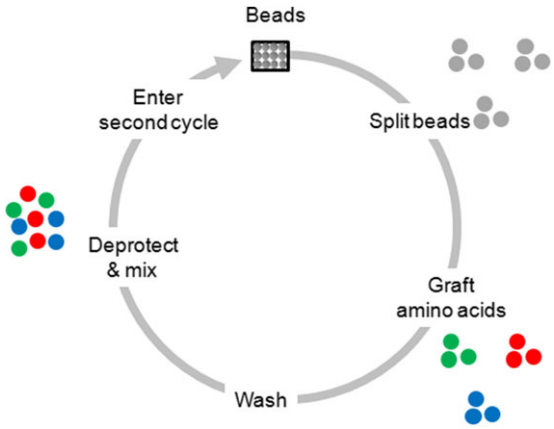

Figure 3. Schematic representation of the preparation of a combinatorial peptide library (one cycle). The cycle of synthesis involves a series of parallel couplings (beads split) determined by the number of amino acid used; this is followed by wash, a deprotection of grafted amino acids and a novel bead blend to get a homogeneous mixture. Then a novel split equal to the number of involved amino acids is made to enter a novel cycle of coupling. The number of cycles drives the length of the peptide. The number of diverse peptides is obtained by the combination of the amino acids and the number of cycles.

The synthesis is operated on solid phase supports and is easily organized to obtain combinations of structures. A quite simple combinatorial synthesis method has been described by Furka et al. [33] and largely developed by Lam et al. [34]. The technical approach is illustrated in Fig. 3. The number of ligands that can be obtained depends on the length of

the peptide and the number of amino acids used. With natural amino acids the libraries are limited to few dozen of millions; however, unnatural amino acids can also be used with a significant extension of the number of diversomers. The larger the size of the library the more difficult the screening step, thus the most convenient way is to limit the number of well selected building blocks to create limited libraries easier to sort out. The length of these peptide libraries is rarely extended beyond eight or ten amino acids since a sequence folding may occur and synthesis difficulties are then encountered. These libraries are presently also used as mixed-mode mixed-bed affinity ligands in proteomics applications to reduce the dynamic range of protein extracts [35, 36].

They have extensively been used for the identification of specific ligands for affinity chromatography. The most representative examples are the purification of fibrinogen [37] and immunoglobulins G [38, 39]. In the first case the target protein was purified at high purity using the sequence FLLVPL directly starting from human crude plasma. The target protein was captured with 20 mM HEPES buffer pH 6.8 and desorbed using 2.5% acetic acid after a wash with 0.1 M sodium chloride. In the second case IgGs were purified from various crude sources using the peptide HWRGWV with a final purity and recovery that reached respectively up to more than 95% and around 85% depending on the starting material.

Peptides for affinity chromatography have also been obtained by ribosome display as described by Menegatti et al. [40], for the purification of IgGs from a variety of mammalian species with an affinity for their Fc region. The sorted out ligand was a cyclic peptide *Link*-M-WFRHY-K and was used as chromatographic sorbent with physiological phosphate buffered saline and captured IgG recovered using 0.2 M acetate buffer pH 4 at a purity of 93 ± 3% and recovery of 96 ± 2%, respectively.

2.3 Libraries of large polypeptides

Immunopurification involving monoclonal antibodies as ligands for chromatography is not discussed in this review; however, a word is necessary to say that libraries of naïve antibodies have been reported as sources of macroligands [41, 42]. Although these libraries followed by phases of maturations can be successfully used for the development of antibodies for therapeutic applications [43], they have only weak probabilities of being used for large-scale affinity chromatography because of their high price and the disadvantage inherent to their large mass. Furthermore they are multimeric proteins stabilized by reversible disulfide bonds and are glycosylated, hence they are of limited stability for chromatography uses. It is because of these limitations that the interest was redirected towards other solutions better complying with attributes related to affinity chromatography constraints. Investigations performed around the construction strategies of combinatorial proteinaceous libraries allowed to propose few dozens of protein scaffolds comprising variable peptide inserts for target protein recognition. For more information on these structures mostly studied for future medical and diagnostic applications, the readers should refer to Binz et al. [44] and Groenwall et al. [45].

In this section it is out of question to make an exhaustive review of all possible polypeptide library proposals of the last few years; rather several representative examples are given among the most known and successfully applied systems.

An interesting story is the one that started with the discovery of single-chain antibodies in Camel and Llama [46]. They are composed of a single chain comprising two constant domains and a single variable domain (VHH) called 'nanobodies' with a mass of 15 kDa, the smallest available intact antigen binding fragments. To create a library of VHH domains, the antigen binding fragments repertoire from an immunized camelid is cloned into a phage display vector followed by the selection of the right polypeptide ligand for a given protein to purify. The highly specific selected polypeptide can then be easily produced in recombinant yeasts and chemically immobilized on current chromatographic sorbents. This process of making affinity ligands has been successfully applied to a number of protein purification processes such as IgA and IgG. In the first case [47] recombinant IgA1 were produced by CHO cells *in vitro* and the expressed antibodies were purified on an immobilized camelid anti-human alpha-chain IgA. The protein was recovered at high purity degree in a single chromatographic step saving thus working time compared to current separation procedures based on Jacalin affinity chromatography [48] followed by hydrophobic interaction chromatography. IgG purification was also achieved using specific VHH nanobody expressed in *E. coli* and then immobilized on a solid support [49]. The affinity sorbent could bind IgG of different species under physiological conditions and the antibody was recovered by an elution at pH 5, a mild condition preserving the biological properties of the separated molecules. The sorbent showed good stability over repeated cycles.

Affibodies are polypeptides originated from the Z domain of Protein A, a well-known ligand for immunoglobulins G. They consist in three alpha helices without disulfide bridges with a total molecular mass of 6 kDa. Out of 58 amino acids 13 are randomized from where the constructs acquire their affinity properties for proteins [50]. Thanks to their conformation affibodies are very stable in extreme conditions of pH as well as to temperatures up to 90°C. As per other polypeptide libraries they can be obtained by phage display from where the appropriate affibody for the intended application is sorted out. Large and stable libraries can be obtained with potential ligands for many proteins as demonstrated by a number of published reports describing the purification of various proteins among them epidermal growth factor receptor [51], interleukin-2 receptor [52], human blood transthyretin [53], amyloid beta peptides [54] and human IgA [55] to mention a few. In the latter case it was observed a similar specific capture efficiency for the two classes of IgA as well for secretory IgA with no cross reactivity for IgG or IgM.

Table 1. Summary characteristics of combinatorial polypeptide ligand libraries

Generic name	Molecular mass	Scaffold	Origin
Antibodies[a]	150 kDa as native	Immunoglobulins G	Mammal blood serum
Nanobodies	15 kDa	Single-chain antibodies	Camel, Llama blood serum
Affibodies	6 kDa	Z domain of protein A	*Staphylococcus aureus*
DARPins	Very large size	Ankyrin	Membrane cytoskeleton
Nanofitins	7 kDa	Sac7d protein family	*Sulfulobus acidocaldarius*
Affimers	13 kDa	Stefin	Mammalian cells

a) Antibodies are mentioned as reference, but are not discussed in this review.

Ankyrin, a large polypeptide encoded by ANK3 gene with a molecular mass larger than antibodies, has also been used to create libraries of numerous structures. It comprises three structural domains: (i) an amino-terminal domain with ankyrin repeats, (ii) a central region with a highly conserved spectrin binding domain, and (iii) a carboxy-terminal regulatory domain. The human genome encodes and expresses more than a thousand ankyrin domains from where the first level of diversity generates. Contrary to antibodies, these structures, called Designed Ankyrin Repeat Proteins (DARPins), do not require affinity maturation which is a significant technical advantage [56]. In spite of these properties these polypeptides mostly used to speed-up the development of bio-drugs are poorly adapted as chromatographic ligands due essentially to their large size.

Another category of potential ligand library for affinity chromatography are engineered proteins from thermophiles (mainly *Sulfulobus acidocaldarius)* originated from Sac7d family that are natural DNA-binders to protect the genome from fusion [57]. They are small single chain proteins (7 kDa that is twenty times smaller than regular antibodies) with no disulfide bonds, stable at relatively high temperature and under extreme pH conditions. Randomized and selected using current ribosome display methodology [58] they can then be produced at acceptable cost in recombinant *E. coli*. After proper purification their attributes can make them effective ligands for bioaffinity chromatography.

An additional interesting group of proteinaceous ligands comes from engineered Stefin A. Stefin A is a single chain protease inhibitor against members of cathepsin family of proteases. To enhance its affinity ligand properties, residues responsible for binding cathepsins have been abolished and a randomized oligonucleotide has been introduced in the open reading frame corresponding to loop 2 [59]. With these changes, polypeptide libraries can be produced and screened for their specificity towards a given protein target. The resulting affinity ligands known under the name of Affimers are very stable at quite high temperatures and have good attributes for applications in affinity chromatography. They can be produced by recombinant technology from where they need to be extracted and purified.

Table 1 summarizes key information on polypeptide libraries.

All the above polypeptide ligands issued from combinatorial libraries have a great specificity for the target protein to be purified but exihibit a common issue which is their expression by recombinant technology. Expression implies a mass fermentation production, separation and isolation before the chemical immobilization on solid substrates. Thus the main weakness of this process is related to the presence of cell culture impurities that can contaminate the proteinaceous affinity ligand.

2.4 DNA-RNA aptamer libraries

A very promising affinity ligand library is the one based on oligonucleotides known under the term “Aptamers”. They are single stranded RNA and DNA nucleic acids composed of a limited number of bases able to form intrachain base-pairs with complementary sequences; therefore they compose three-dimensional structures that are at the basis of the molecular recognition of a given target. The latter could be any type of molecule including peptides, proteins, microorganisms and even salts. Aptamers can be of very high specificity with affinity constants covering large zones and are thus particularly indicated for the selection of affinity ligands for protein purification. They are applied in various domains of molecular recognition [60, 61] thanks to their advantages over other ligands such as their high degree of specificity and their tunable dissociation constants. Libraries of oligonucleotide aptamers are produced from large naive combinatorial oligonucleotide libraries and screened by means of a well-established technology called SELEX (systematic evolution of ligands by exponential enrichment) discussed in the following section [62, 63]. As a result of their high specificity they are frequently compared to antibodies, with several other advantages: smaller molecular size, oriented immobilization, stability of extreme conditions, reversible denaturation, stable in the presence of proteases and amendable to further chemical modifications. In spite of all these interesting properties only a limited number of affinity chromatography applications are published to date. The limitation seems related to the chemical problems for the covalent grafting to solid supports. This difficulty has successfully been resolved by the modification of one of the extremities of the aptamer allowing it to be coupled to appropriate sorbents [64]. Nevertheless aptamer affinity chromatography has been reported for example in the separation of proteins such as thrombin [65], *Thermus*

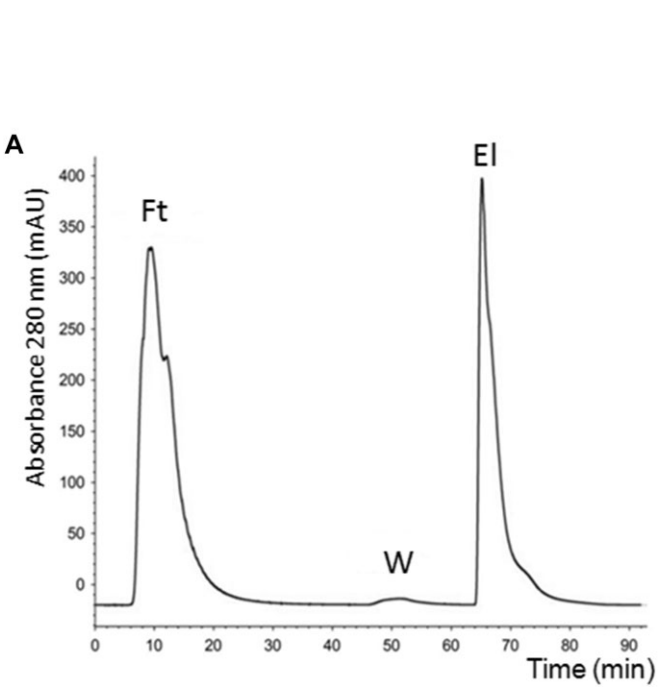

Figure 4. Purification of human blood Factor IX in a single step using a DNA aptamer issued from SELEX screening.
Panel A represents the chromatographic profile obtained with a specific aptamer grafted on agarose beads. Sample: intermediate fraction from human plasma. Capture buffer: 50 mM Tris-HCl, 150 mM sodium chloride, 2 mM calcium chloride, 1 mM magnesium chloride, pH 7.4. Washing solution: capturing buffer containing 0.5M sodium chloride. Elution solution: 200 mM EDTA, pH 8. FT = flowthrough; W = washing; El = elution.
Panel B shows the analytical SDS-PAGE of fractions. Left lane (M*r*) is a protein ladder. Silver staining. (Figure provided by LFB, France; results obtained using a proprietary aptamer grafting technology [64]).

aquaticus recombinant DNA polymerase [66], immunoglobulin G [67], His-Tag fusion proteins [68] and lysozyme [69]. Upon the application of stringent selection rules of aptamer ligands it is interesting to underline the possibility to purify a target protein to homogeneity in a single step as per the example illustrated in Fig. 4.

3 Sorting out specific affinity ligands from libraries

Various selection methods have been devised for ligand identification from complex libraries. The developed procedures differ substantially from each other depending on the type and nature of the library. Most common methods with related references for technical details are described below. As a preliminary remark it is important to underline that certain conditions have to be predefined such as the composition of the buffer where the specific interaction between the ligand and the protein should occur (affinity adsorption or protein capture). This can be determined using the purified target protein; however, the process is more effective when crude extracts comprising the target protein are used. Another important point is to define the conditions of desorption that must comply with the biological stability of the target protein. Four main methods of specific ligand selection are currently used: (i) bead sorting applied to short peptide libraries beads all mixed together, (ii) solid-phase ligand selection applied to most of chemical library molecules prepared as small parallel single batches, (iii) *in vivo* cycling-amplification processes applied to large polypeptides and (iv) *in vitro* cycling amplification approaches such as ribosome display adapted for proteinaceous ligands and others adapted for nucleic acid aptamers.

3.1 Ligand selection applied to peptide beaded libraries

Small peptides are generally synthesized on solid phases. Various methods are described but the one that is simple and capable to give very large libraries starting from virtually all amino acids is the so-called "split-&-recombine" method [33, 34] yielding a configuration of one-ligand-one-bead. Libraries can be as large as the number of beads available, typically from 10^4 to 10^7. Most generally peptides that are individually anchored on beads are selected directly without the need of dissociating them from their substrate.

In practice the peptide ligand library is mixed with a protein extract under pre-defined conditions (see Fig. 5A). Then the solid phase is separated by filtration or centrifugation and the excess of proteins washed away. The peptide library beads are then incubated with an antibody against the target protein and revealed by immunostaining. Highlighted beads are finally taken off and individually submitted to peptide sequencing. Unfortunately this rational process shows a number of false positives due to (i) the adsorption of the target protein to various peptide structures by different affinity constants, (ii) the non-specific adsorption of antibodies on peptide beads and (iii) the co-adsorption of other proteins on the same beads where the target protein interacts. This is the reason why various variants have been devised to reduce most of false negatives.

A direct method was first described consisting of the use of a target protein previously labeled with a detectable

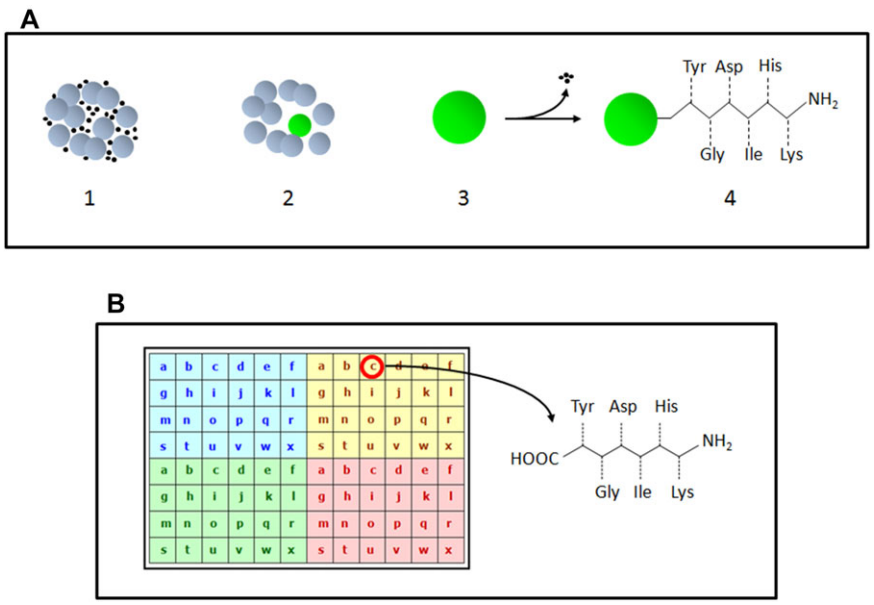

Figure 5. Schematic representation of on-bead ligand selection techniques.
"A" represents the case when each beads carries a different peptide and all the beads are mixed together (library obtained by "split & recombine" method).
1: The bead library is incubated with the biological sample comprising the target protein (small black dots) in the selected buffer. A wash follows to eliminate the excess of proteins.
2: Beads having captured the target protein are detected using a labeled antibody. The revealed beads are then isolated manually or mechanically.
3. Isolated positive beads are submitted to stringent eluting agents to desorb the labeled antibody and the captured proteins.
4: Each positive depleted bead is sequenced to obtain the peptide sequence.
"B" represents the case when the beads are segregated in different locations (e.g. wells of 96-well plated) identified by their coordinates. Parallel incubations are performed with the sample containing the target protein under different buffer conditions (plate quadrants of different color). Beads that are able to capture the target proteins are then submitted to peptide sequencing.

enzyme or a fluorescent molecule [34]. Further optimizations of the approach have been described later on [70, 71]. Other variants used to reduce the level of false positives and involving two colors have been described by Lam et al. [72] and by Buettner et al. [73] with the use of two orthogonal staining methods. These approaches significantly reduced the number of false positives but are considered still questionable. Therefore more elaborated techniques have been devised to improve the selection process. With the reduction of the number of positive beads the sequencing workload was also largely reduced. This was with the technologies developed by Lehman et al. [74] and Lathrop et al. [75] known respectively under the terms of *image subtraction* and *bead blot*. Recently it has been found that diminishing the density of peptides on the beads it is also possible to decrease very significantly the number of false positive, but this approach is at the price of the use of very sensitive peptide sequencing analysis due to the low amount of peptide per bead [76]. This review would not be complete without mentioning the possibility of encoding the beads for easy ligand identification without long and tedious sequencing operations. Several approaches have been described for pre-encoding the beads during or before the preparation of the library to associate each bead to a peptide sequence. The most convincing are those involving mass-tag encoding strategies [77], or colloidal bar coding with grafted fluorescent particles [78] or libraries encoded with DNA sequences [79], or even by surface-enhanced Raman spectroscopic dots adsorbed on each bead [80]. All these labeling procedures are made during the construction of the ligand library.

3.2 Ligand screening and identification from chemical libraries

A large number of chemical libraries can be source of affinity ligands, but the selection methods of the appropriate structure for a given protein are similar. Here the library is considered as made by solid phase (the most popular) and constructed by individual discrete reactions as for instance in well-plates comprising 95, 384 or more wells. This is the case of solid-phase ligand libraries based on triazine scaffold, limited solid phase ligand libraries derived from UGI reactions and peptoids.

In practice each synthesized affinity solid phase in individual wells are contacted with the target protein and incubated under predefined conditions of pH, ionic strength, composition of the buffer, and temperature (Fig. 5B). Then the excess of protein is eliminated by washing and the potential adsorbed protein eluted by dissociation agents that can be of increasing stringency. At this stage various analyses can be performed but the most direct one is the determination of the amount of adsorbed and desorbed target protein. Protein adsorption can be qualitatively assessed also by fluorescence emission when the target protein is labeled with for instance fluorescein isothiocyanate [24]. Similar procedure is usable as described by El Khoury et al. [18] for the solid-phase screening of sorbents obtained by multicomponent UGI reaction. When dealing with a crude sample containing the target protein a direct estimation cannot be possible, thus the analysis of protein components (adsorbed and eluted) can be performed using modern methods of

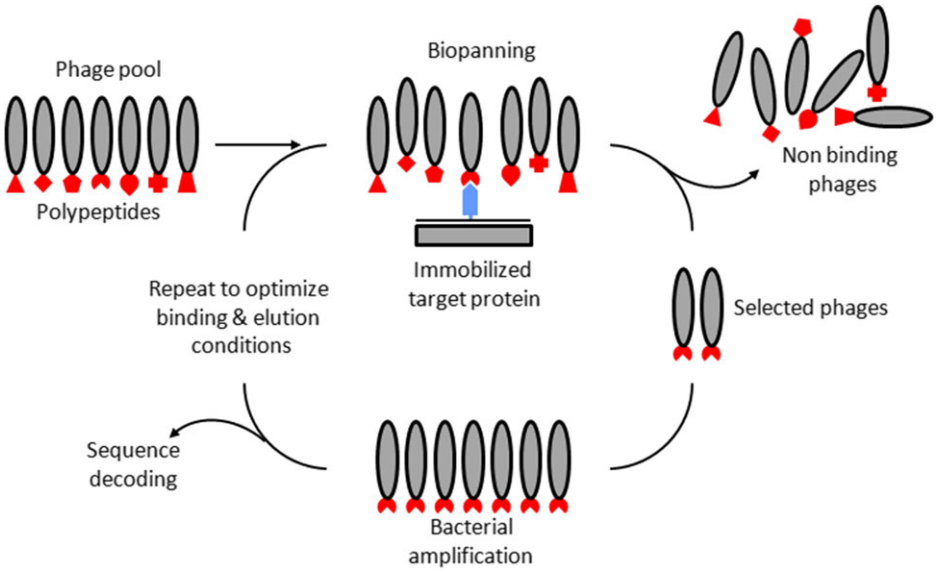

Figure 6. Scheme of phage display selection/ amplification cycle. Cloned phage genome with DNA encoding for millions of sequences is incubated with a solid phase carrying the target protein. Non-adsorbed phages are eliminated by washing and the captured species (specific for the target protein and also some others non-specifically adsorbed phages) are eluted, collected and amplified again in bacteria (e.g. *E. coli*). The amplified collection of phages is submitted again to the immobilized target protein to complete a second cycle of selection. Several cycles are necessary to reach a satisfactory level of purity. The affinity polypeptide ligand expressed on the surface of the phages is cut and then sequenced.

MS (identification and quantification). The synthesis can be performed in well-plates to recognize the structure of the affinity ligand by the topographical positioning on the plate and all the analysis of samples operated automatically as described previously [81].

These methods can also be adopted for the detection and identification of peptide ligands when they are synthesized as individual small homogeneous batches.

3.3 Ligand selection by *in vivo* cycling-amplification

Polypeptides are large molecules that are generally obtained by in vivo biosynthesis. In spite of various initial scaffolds as described in Section 2, the selection and amplification of the appropriate polypeptide ligand is generally operated using so-called phage display technique [82]. DNA encoding a large number of polypeptide variants is cloned in filamentous phage genome within the gene encoding for a phage coat protein. The expression of the fusion polypeptides is thus presented on the phage surface permitting the capture of the best structures on the immobilized target to enter a cycle of ligand selection and enrichment (Fig. 6). Actually affinity phages that are bound on the grafted target protein are recovered by elution and used to reinfect bacteria and grown to enter another cycle of selection where an enrichment of much less species occurs. By cycling the process several times and subject it to conditions of adsorption and elution from the target protein, it is possible to reach a situation of a specific polypeptide ligand selection [42]. Variants and optimized conditions to small targeted libraries are reviewed in a recent publication by Pande at al. [83].

3.4 Ligand selection by *in vitro* cycling-amplification

More than one method is devised for the *in vitro* cycling-amplification to detect and identify ligands. Most known are SELEX adapted for oligonucleotide ligands and Ribosome Display for proteins and peptides.

In the first case the library of oligonucleotide aptamers consists of a quite large number of sequences generally comprising 10^{15} diversomers, hence increasing the probability to find the ideal affinity ligand for a given protein. Each sequence is constituted of two main parts, a central random region responsible for the affinity for a given target and two peripheral regions with fixed sequences used for the amplification process. The selection of the right structure is schematically illustrated in Fig. 7. Basically once the nucleic acid library is constructed, it is exposed to the target protein grafted on a solid support. All non-interacting oligonucleotide structures are eliminated while those captured by the solid phase are desorbed and isolated. The latter are then submitted to a negative screening with other proteins that have similar properties to the target proteins and that represent a risk of non-specific binding. In this case only non-interacting species are collected and then amplified by PCR methodology. This cycle can be repeated several times so that to reach a high level of aptamer specificity. At the same time the screening process can be performed by fine tuning the conditions of protein adsorption and elution. The separated oligonucleotides are then amplified by PCR technique to enter another selection cycle. PCR amplification process is used when dealing with DNA aptamers while RT-PCR followed by *in vitro* transcription is used in the case of RNA aptamers. Several selection cycles are necessary to reach the required specificity. Conditions of complex formation and dissociation are fixed in advance to optimize the behavior of affinity chromatography exploitation. For a recent review see Djordjevic et al. [84].

Ribosome Display method for polypeptide ligand selection and amplification is an *in vitro*, cell-free evolution method based on the formation of protein-ribosome-mRNA complexes [85]. The latter are obtained by halting the translation at random or by deleting the stop codon preventing proteins to leave the ribosomes. In this technology, no cell transformation is necessary thus very large libraries can directly go

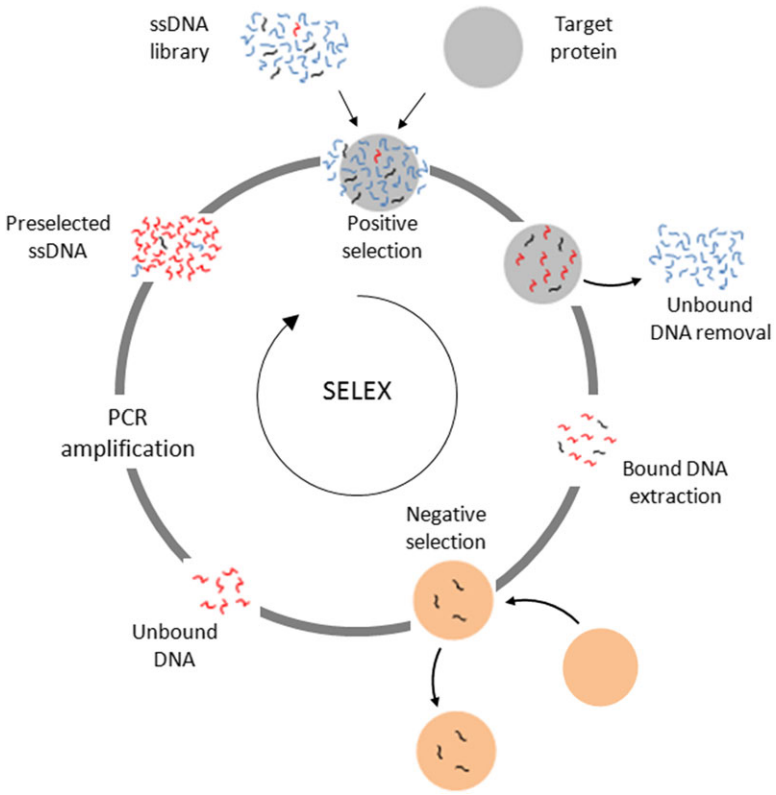

Figure 7. Scheme of oligonucleotide aptamer screening by SELEX cycling/ amplification. A ssDNA library is exposed to the immobilized target protein. Non-captured oligonucleotides are eliminated by simple washing and the others are desorbed from the beads. Once extracted these DNA molecules are submitted to a negative selection to remove all species that can recognize proteins similar to the target. Survival sequences of DNA are then amplified by PCR method and submitted to another selection cycle. By that way several options can be explored for capturing and eluting conditions appropriate for affinity chromatography applications.

into selection and *in vitro* amplification. A random oligonucleotide template is first synthesized. It is then put in presence of an amino acid mixture and S30 extract and incubated for 2–3 h at 30°C. Although both prokaryotic and eukaryotic *in vitro* polypeptide synthesis can be used, *E. coli*-based ribosome display is frequently preferred [86]. The transcription/ translation products are incubated with the target protein previously immobilized on a chromatographic support where the affinity material is adsorbed leaving all other products traveling through the column and eliminated. After washing, the adsorbed polysomes are disrupted with EDTA and mRNA is thus released. The latter is converted in cDNA and amplified to be ready for another cycle or to the separation of other non-specific mRNA molecules. Selected target-specific polypeptide ligand in then sequenced.

4 Ligand library comparison

Libraries of ligands for affinity chromatography are so diverse in composition, molecular structure and mode of production that a direct comparison is quite a hard task. Here the comparison is approached by first defining the theoretical attributes of these structures. Clearly for affinity ligands the specificity is probably the most important characteristic; however, this is not enough because beyond the specificity, the ligand needs to be stable under extreme conditions to which the affinity chromatography support is submitted cycle after cycles as for instance cleaning and sanitization. It must also be able to be grafted on the solid support by means of a strong covalent bond. To reach relatively high binding capacity for the affinity sorbent, the ligand should be as small as possible to confer a "molar advantage" and finally it is preferably made by chemical synthesis. From the ligand libraries described above a tentative comparison is illustrated on Table 2. This table does not consider the questions related to the screening difficulties that are also discriminating while selecting a ligand. Nevertheless the screening of the right ligand for a given application although laborious, remains a task that is most of the time affordable in comparison to the long-term exploitation of the selected ligand.

What can be extracted from the comparative properties of ligand from the considered libraries is the best balance between analyzed parameters since no ideal situation is generally reached, the latter depending also on the context of the purification. There are situations where the affinity ligand is used in the initial phase of protein purification (e.g. capture step); hence the question of the presence of few impurities is marginal. On the contrary the absolute absence of protein impurities is necessary at the final stage of the purification processes (e.g. polishing). From what is illustrated on Table 2 one can conclude that the best results are reached with libraries of polypeptides or with nucleic acid aptamers. However, there are other considerations that have to be taken into account. An important one is the molecular mass of the ligand. If it is postulated that one molecule of ligand interacts and captures one molecule of the target protein, a limited amount of a small ligand is enough to raise high binding capacities. This is not

Table 2. Main properties of affinity ligand families

Type of ligand	Molecular mass	Specificity	Graftability	Preparation	Purification	Stability
Chemical	Small	Acceptable	NA	On-bead syhthesis	Not required	High
Peptide	Small-medium	Acceptable-high	NA	On-bead synthesis	Not required	High
Polypeptide	Large	Very high	Various ways[a]	Recomb. expression	Intense workload	High to average
Oligonucleotide	Large	Very high	By design	Chemical synthesis	Polishing	High

a) Current chemical grafting methods do not provide an oriented immobilization for polypeptides.

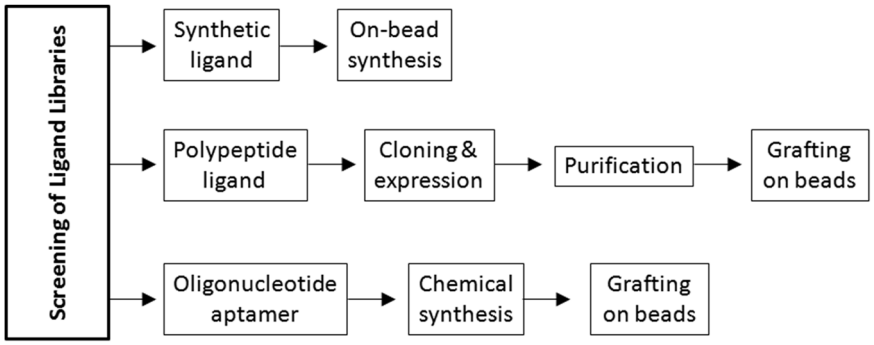

Figure 8. Block diagram summarizing the steps that are to be performed after the screening phase to prepare the affinity chromatography sorbent as a function of the type of ligand.

the case with large ligands as for instance antibodies that in the best cases deliver binding capacity close to 1–2 mg of the target protein per mL of sorbent. At the center of the game are small peptides that are produced synthetically and screened *in vitro*. Demonstration has been made that they are stable and usable for the purification of proteins up to quite high levels; nevertheless the specificity is logically lower than the one measured with peptides of larger mass. Yet with a good control of the screening method as discussed above, small peptides constitute a workable option. When examining all the ligand attributes, nucleic acid aptamers appear as the best compromise for preparative chromatography applications.

To complete this analysis there is another implication to consider: the production of the selected ligand before the covalent grafting on the chromatographic support. A simple schematic summary is represented in Fig. 8. This block diagram allows easily comparing the tasks related to the production of the affinity ligand. It appears that the easiest way is to proceed with synthetic chemical ligands that are directly prepared on beads. Nevertheless, as mentioned in the previous sections, the probability to reach specificity as high as the one obtained with polypeptides or nucleotide aptamers is low. As a reminder the ligand once produced has to be covalently attached on a solid support. This operation is not avoided of risks concerning the reduction of specificity especially for polypeptides that are folded molecules and are immobilized randomly (non-oriented manner). This is perfectly illustrated by a polypeptidic ligand selected by phage display for the purification of immunoglobulins A [87]. The ligand had all the attributes for a perfect affinity; however, once grafted the specificity was partially lost as attested by the presence of protein impurities present in separated IgA. This situation was resolved by creating additional mutations and additional screening to reduce the probability of hydrophobic associations at the origin of non-specific interactions with foreign proteins.

Depending on method of production the ligand can carry foreign structures that are detrimental to a proper purity of the target protein: potential contaminations represent a real issue when dealing with biopharmaceuticals. To overcome this question stringent purification processes must be applied to the purification especially of polypeptide ligands resulting from *in vivo* or *in vitro* expression. This is not the case for nucleic acid aptamers that are produced by synthetic processes and are submitted just to a cleaning step.

5 Concluding remarks and perspectives

The need of very pure proteins isolated from crude biological extracts, recombinant or not, is expected to grow in the future mainly due to multiplied therapeutic applications in view to correct metabolic disorders. Under the pressure of the purification cost, more specific and rapid purification processes will have to be built. They will probably involve affinity chromatography separations carrying more and more selective ligands. To try resolving the crucial question of the identification of appropriate ligands, the combinatorial libraries will increasingly provide valuable solutions to most or even all purification problems. From these large collections of molecules it will be easily possible to identify the best ligand candidate based on criteria previously described and devise thus the affinity chromatography system. This approach directly allows obtaining one solid phase instead of making numerous chromatography trials. However, with one library with thousands or millions of diverse structures only one affinity

column is made for a given protein to purify which appears a huge effort and time lost. This is not with considering that the library can be further used for the identification of many other affinity ligands each of them usable to purify other targeted proteins by affinity chromatography. The question that remains open is thus why do we use many large libraries if one would be enough? Each ligand source has specific merits and drawbacks that require to be put in perspective and in accordance with the technical and economical expectations. With this is mind it is expected that new companies will be created around the expertise in affinity ligand libraries providing not only collections of molecules but also services for the identification of the right ligand for the targeted protein, helping and supporting thus the companies that are involved in the production of pure biologicals with affinity chromatography separation solutions. This trend that is already a reality will presumably grow and improve.

The panel of affinity ligand from libraries is already very large, but the general attribute is that small chemical ligands might not be as specific as biologically produced ligands; however, they are less costly and probably more stable over time. Nevertheless, there are ligands from relatively 'young' libraries that have not been extensively evaluated to establish a ranking of value. For instance, recent work made with nucleic acid aptamers appeared very promising in term of high specificity, exceptional stability allowing repeated preparative applications. Their average molecular mass renders them attractive also because in certain cases it seems possible to reach high binding capacity values with incomparable purification factors obtained in a single step.

The authors have declared no conflict of interest.

6 References

[1] Urh, M., Simpson, D., Zhao, K., *Methods Enzymol.* 2009, *463*, 417–438.

[2] Moser, A. C., Hage, D. S., *Bioanalysis* 2010, *2*, 769–790.

[3] Boyer, P. M., Hsu, J. T., *Adv. Biochem. Eng. Biotechnol.* 1993, *49*, 1–44.

[4] Gordon, E. M., Barrett, R. W., Dower, W. J., Fodor, S. P. A., Gallop, M. A., *J. Med. Chem.* 1994, *37*, 1392–1401.

[5] Ecker, D. J., Crooke, S. T., *Biotechnology* 1995, *13*, 351–360.

[6] Teng, S. F., Sproule, K., Hussain, A., Lowe, C. R., *J. Mol. Recognit.* 1999, *12*, 67–75.

[7] Lebl, M., Krchnák, V., Sepetov, N. F., Seligmann, B., Strop, P., Felder, S., Lam, K. S., *Biopolymers* 1995, *37*, 177–198.

[8] Jones, C., Patel, A., Griffin, S., Martin, J., Young, P., O'Donnell, K., Silverman, C., Porter, T., Chaiken, I., *J. Chromatogr. A.* 1995, *707*, 3–22.

[9] Jayasena, S. D., *Clin. Chem.* 1999, *45*, 1628–1650.

[10] Saraswat, L. D., Zhang, H., Hardy, L. W., Jones, S. S., Bhikhabhai, R., Brink, C., Bergenstrahle, A., Haglund, R., Gallion, S. L., *Biotechnol. Prog.* 2005, *21*, 300–308.

[11] Lam, K. S., Lebl, M., Krchnak, V., *Chem. Rev.* 1997, *97*, 411–448.

[12] Wang, Y., Li, T., *Biotechnol. Prog.* 2002, *18*, 524–529.

[13] Nestler, H. P., Liu, R., *Comb. Chem. High Throughput Screen.* 1998, *1*, 113–126.

[14] Webb, T. R., *Curr. Opin. Drug Discov. Devel.* 2005, *8*, 303–308.

[15] Marasco, D., Perretta, G., Sabatella, M., Ruvo, M., *Curr. Protein Pept. Sci.* 2008, *9*, 447–467.

[16] Lowe, C. R., Burton, S. J., Burton, N. P., Alderton, W. K., Pitts, J. M., Thomas, J. A., *Trends Biotechnol.* 1992, *10*, 442–448.

[17] Domling, A., Ugi, I. *Angew Chem. Int. Ed. Engl.* 2000, *39*, 3168–3210.

[18] El Khoury, G., Wang, Y., Wang, D., Jacob, S. I., Lowe, C. R., *Biotechnol. Bioeng.* 2013, *110*, 3063–3069.

[19] Qian, J., El Khoury, G., Issa, H., Al-Qaoud, K., Shihab, P., Lowe, C. R., *J. Chromatogr. B.* 2012, *898*, 15–23.

[20] El Khoury, G., Lowe, C. R., *J. Mol. Recogn.* 2013, *26*, 190–200.

[21] Ford, B. K., Hamza, M., Rabenstein, D. L., *Biochemistry* 2013, *52*, 3773–3780.

[22] Kodadek, T., Bachhawat-Sikder, K., *Mol. Biosyst.* 2006, *2*, 25–35.

[23] Luo, Y., Vali, S., Sun, S., Chen, X., Liang, X., Drozhzhina, T., Popugaeva, E., Roque, A. C., Lowe, C. R., In *Affinity Chromatography; Methods and Protocols*. Second Edition, Zachariou, M. (Ed.), Humana Press, Totowa, NJ 07512, USA, 2008, pp 103–105.

[24] Lowe, C. R., *Curr. Opin. Chem. Biol.* 2001, *5*, 248–256.

[25] Roque, A. C., Lowe, C. R., *Biotechnol. Adv.* 2006, *24*, 17–26.

[26] Corredano, E., Baumann, H., *Methods Biochem. Anal.* 2011, *54*, 259–267.

[27] Li, R., Dowd, V., Stewart, D. J., Burton, S. J., Lowe, C. R., *Nat. Biotechnol.* 1998, *16*, 190–195.

[28] Teng, S. F., Sproule, K., Husain, A., Lowe, C. R., *J. Chromatogr. B.* 2000, *740*, 1–15.

[29] Newcombe, A. R., Cresswell, C., Davies, S., Watson, K., Harris, G., O'Donovan, K., Francis, R., *J. Chromatogr. B.* 2005, *814*, 209–215.

[30] Roque, A. C., Taipa, M. A., Lowe, C. R., *J. Chromatogr. A.* 2005, *1064*, 157–167.

[31] Roque, A. C., Gupta, G., Lowe, C. R., *Methods Mol. Biol.* 2005, *310*, 43–62.

[32] Bezprozvanny, I., *ACS Chem. Neurosci.* 2013, *4*, 952−962.

[33] Furka, A., Sebesryen, F., Asgedom, M., Dibo, G., *J. Pept. Prot. Res.* 1991, *37*, 487–493.

[34] Lam, K. S., Salmon, S. E., Hersh, E. M., Hruby, V. J., Kazmierski, W. M., Knapp, R. J., *Nature*. 1991, *354*, 82–84.

[35] Righetti, P. G., Candiano, G., Citterio, A., Boschetti, E., *Anal. Chem.* 2015, *87*, 293–305.

[36] Boschetti, E., Righetti, P. G., *Low-Abundance Protein Discovery: State of the Art and Protocols*, Elsevier, Waltham, MA 02451, USA, 2013.

[37] Kaufman, D. B., Hentsch, M. E., Baumbach, G. A., Buettner, J. A., Dadd, C. A., Huang, P. Y., Hammond, D. J., Carbonell, R. G., *Biotechnol. Bioeng.* 2002, *77*, 278–289.

[38] Naik, A. D., Menegatti, S., Gurgel, P. V., Carbonell, R. G., *J. Chromatogr. A.* 2011, *1218*, 1691–1700.

[39] Menegatti, S., Naik, A. D., Gurgel, P. V., Carbonell, R. G., *J. Sep. Sci.* 2012, *35*, 3139–3148.

[40] Menegatti, S., Hussain, M., Naik, A. D., Carbonell, R. G., Rao, B. M., *Biotechnol. Bioeng.* 2013, *110*, 857–870.

[41] Gram, H., Marconi, L. A., Barbas, C. F. 3rd, Collet, T. A., Lerner, R. A., Kang, A. S., *Proc. Natl. Acad. Sci. USA.* 1992, *89*, 3576–3580.

[42] Hoogenboom, H. R., de Bruïne, A. P., Hufton, S. E., Hoet, R. M., Arends, J. W., Roovers, R. C., *Immunotechnology* 1998, *4*, 1–20.

[43] Shahsavarian, M. A., Le Minoux, D., Matti, K. M., Kaveri, S., Lacroix-Desmazes, S., Boquet, D., Friboulet, A., Avalle, B., Padiolleau-Lefèvre, S., *J. Immunol. Methods* 2014, *407*, 26–34.

[44] Binz, H. K., Amstutz, P., Pluecktthun, A., *Nature Biotech.* 2005, *23*, 1257–1268.

[45] Groenwall, C., Stahl, S., *J. Biotechnol.* 2009, *140*, 254–269.

[46] Hamers-Casterman, C., Atarhouch, T., Muyldermans, S., Robinson, G., Hamers, C., Songa, E. B., Bendahman, N., Hamers, R., *Nature*. 1993, *363*, 446–448.

[47] Reinhart, D., Weik, R., Kunert, R., *J. Immunol. Methods* 2012, *378*, 95–101.

[48] Loomes, L. M., Stewart, W. W., Mazengera, R. L., Senior, B. W., Kerr, M. A., *J. Immunol. Methods* 1991, *141*, 209–218.

[49] Tu, Z., Xu, Y., Fu, J., Huang, Z., Wang, Y., Liu, B., Tao, Y., *J. Chromatogr B.* 2015, 983–984, 26–31.

[50] Nord, K., Gunneriusson, E., Ringdahl, J., Ståhl, S., Uhlén, M., Nygren, P. A., *Nat. Biotechnol.* 1997, *15*, 772–777.

[51] Wallberg, H., Lofdahl, P. K., Tschapalda, K., Uhlén, M., Tolmachev, V., Nygren, P. K., Stahl, S., *Protein Expr. Purif.* 2011, *76*, 127–135.

[52] Gronwall, C., Snelders, E., Palm, A. J., Eriksson, F., Herne, N., Stahl, S., *Biotechnol. Appl. Biochem.* 2008, *50*, 97–112.

[53] Ramstrom, M., Zuberovic, A., Gronwall, C., Hanrieder, J., Bergquist, J., Hober, S., *Biotechnol. Appl. Biochem.* 2009, *52*, 159–166.

[54] Gronwall, C., Jonsson, A., Lindstrom, S., Gunneriusson, E., Stahl, S., Herne, N., *J. Biotechnol.* 2007, *128*, 162–183.

[55] Rönnmark, J., Grönlund, H., Uhlén, M., Nygren, P. A., *Eur. J. Biochem.* 2002, *269*, 2647–2655.

[56] Milovnik, P., Ferrari, D., Sarkar, C. A., Plückthun, A., *Protein Engineering, Design & Selection* 2009, *22*, 357–366.

[57] Yang, J. M., Wang, A. H., *J. Biomol. Struct. Dyn.* 2004, *21*, 513–526.

[58] Mouratou, B., Behar, G., Paillard-Laurance, L., Colinet, S., Pecorari, F., *Methods Mol. Biol.* 2012, *805*, 315–331.

[59] Stadler, L. K. J., Hoffmann, T., Tomlinson, D. C., Song, Q., Lee, T., Busby, M., Nyathi, Y., Gendra, E., Tiede, C., Flanagan, K., Cockell, S. J., Wipat, A., Harwood, C., Wagner, S. D., Knowles, M. A., Davis, J. J., Keegan, N., Ferrigno, P. K., *Protein Eng. Des. Sel.* 2011, *24*, 751–763.

[60] Huang, Y. C., Ge, B., Sen, D., Yu, H. Z., *J. Am. Chem. Soc.* 2008, *130*, 8023–8029.

[61] McNamara, J. O., Kolonias, D., Pastor, F., Mittsler, R. S., Chen, L., Giangrande, P. H., Sullenger, B., Gilboa, E., *J. Clin. Invest.* 2008, *118*, 376–386.

[62] Tuerk, C., Gold, L., *Science* 1990, *249*, 505–510.

[63] Ellington, A. D., Szostak, J. W., *Nature* 1990, *346*, 818–822.

[64] Patent Application WO2012090183.

[65] Connor, A. C., McGown, L. B., *J. Chromatogr. A.* 2006, *1111*, 115–119.

[66] Oktem, H. A., Bayramoglu, G., Ozalp, V. C., Arica M. Y., *Biotechnol. Prog.* 2007, *23*, 146–154.

[67] Miyakawa, S., Nomura, Y., Sakamoto, T., Yamaguchi, Y., Kato, K., Yamazaki. S., Nakamura, Y., *RNA*. 2008, *14*, 1–10.

[68] Kokpinar, O., Walter, J-G., Shoham, Y., Stahl, F., Scheper, T., *Biotechnol. Bioeng.* 2011, *108*, 2371–2379.

[69] Han, B., Zhao, C., Wang, J. Y. H., *J. Chromatogr.* 2012, *903*, 112–117.

[70] Sepetov, N. F., Krchnák, V., Stanková, M., Wade, S., Lam, K. S., Lebl, M., *Proc. Natl. Acad. Sci. USA.* 1995, *92*, 5426–5430.

[71] Marani, M. M., MartínezCeron, M. C., Giudicessi, S. L., de Oliveira, E., Côté, S., Erra-Balsells, R., Albericio, F., Cascone, O., Camperi, S. A., *J. Comb. Chem.* 2009, *11*, 146–150.

[72] Lam, K. S., Wade, S., Abdullatif, F., Lebl, M., *J. Immunol. Meth.* 1995, *180*, 219–223.

[73] Buettner, J. A., Dadd, C. A., Baumbach, G. A., Masecar, B. L., Hammond, D. J., *Int. J. Peptide Protein Res.* 1996, *47*, 70–83.

[74] Lehman, A., Gholami, S., Hahn, M., Lam, K. S., *J. Comb. Chem.* 2006, *8*, 562–570.

[75] Lathrop, J. T., Fijalkowska, I., Hammond, D., *Anal. Biochem.* 2007, *361*, 65–76.

[76] Chen, X., Tan, P. H., Zhang, Y., Pei, D., *J. Comb. Chem.* 2009, *11*, 604–611.

[77] Hwang, S. H., Lehman, A., Cong, X., Olmstead, M. M., Lam, K. S., Lebrilla, C. B., Kurth, M. J., *Org. Lett.* 2004, *6*, 3830–3832.

[78] Marcon, L., Battersby, B. J., Rühmann, A., Ford, K., Daley, M., Lawrie, G. A., Trau, M., *Mol. Biosyst.* 2010, *6*, 225–233.

[79] Mannocci, L., Leimbacher, M., Wichert, M., Scheuermann, J., Neri, D., *Chem. Commun.* 2011, *47*, 12747–12753.

[80] Kim, J. H., Kang, H., Kim, S., Jun, B. H., Kang, T., Chae, J., Jeong, S., Kim, J., Jeong D. H., Lee, Y. S., *Chem. Commun.* 2011, *47*, 2306–2308.

[81] Guerrier, L., Boschetti, E., *Nat. Protocols* 2007, *2*, 831–837.

[82] Georgiou, G., Stathopoulos, C., Daugherty, P. S., Nayak, A. R., Iverson, B. L., Curtiss, R., *Nat. Biotechnol.*, 1997, *15*, 29–34.

[83] Pande, J., Szewczyk, M. M., Grover, A. K., *Biotechnol. Adv.* 2010, *28*, 849–858.

[84] Djordjevic, M., *Biomol. Eng.* 2007, *24*, 179–189.

[85] Plückthun, A., *Meth. Mol. Biol.* 2012, *805*, 3–28.

[86] He, M., Taussig, M. J., *Brief Funct. Genomic Proteomic.* 2002, *1*, 204–212.

[87] Hatanaka, T., Ohzono, S., Park, M., Sakamoto, K., Tsukamoto, S., Sugita, R., Ishitobi, H., Mori, T., Ito, O., Sorajo, K., Sugimura, K., Ham, S., Ito, Y., *J. Biol. Chem.* 2012, *287*, 43126–43136.

Received: 15 February 2019 | Revised: 29 April 2019 | Accepted: 29 May 2019

DOI: 10.1002/btpr.2858

RESEARCH ARTICLE

BIOTECHNOLOGY PROGRESS

Cation exchange chromatography performed in overloaded mode is effective in removing viruses during the manufacturing of monoclonal antibodies

Yumiko Masuda[1,2] | Masashi Tsuda[1] | Chie Hashikawa-Muto[1] | Yusuke Takahashi[1] | Koichi Nonaka[1] | Kaori Wakamatsu[2]

[1]Biologics Technology Research Laboratories, Daiichi Sankyo Co., Ltd., Ohra-gun, Gunma, Japan

[2]Graduate School of Science and Technology, Gunma University, Kiryu-shi, Gunma, Japan

Correspondence
Yumiko Masuda, Biologics Technology Research Laboratories, Daiichi Sankyo Co., Ltd., 2716-1, Kurakake, Akaiwa, Chiyoda-machi, Ohra-gun, Gunma 370-0503, Japan.
Email: masuda.yumiko.a3@daiichisankyo.co.jp

Abstract

Viral safety is a critical concern with regard to monoclonal antibody (mAb) products produced in mammalian cells such as Chinese hamster ovary cells. Manufacturers are required to ensure the safety of such products by validating the clearance of viruses in downstream purification steps. Cation exchange (CEX) chromatography is widely used in bind/elute mode as a polishing step in mAb purification. However, bind/elute modes require a large volume of expensive resin. To reduce the production cost, the use of CEX chromatography in overloaded mode has recently been investigated. The viral clearance ability in overloaded mode was evaluated using murine leukemia virus (MLV). Even under high-load conditions such as 2,000 g mAb/L resin, MLV was removed from mAb solutions. This viral clearance ability was not significantly affected by resin type or mAb type. The overloaded mode can also remove other types of viruses such as pseudorabies virus and reovirus Type 3 from mAb solutions. Based on these results, this cost-effective overloaded mode is comparable to the bind-elute mode in terms of viral removal.

KEYWORDS

cation exchange chromatography, monoclonal antibody, overloaded mode, purification, viral clearance

1 | INTRODUCTION

The biologics market is steadily expanding worldwide. Among the biologics, monoclonal antibodies (mAbs) are currently the fastest-growing sector of the pharmaceutical industry.[1,2] Culture broth of Chinese hamster ovary (CHO) cells contains high-molecular-weight species (HMWS), host cell protein (HCP), host cell DNA, and other process-related impurities. These impurities should be removed to an acceptable level via appropriate purification steps.[3] Usually, the downstream processing of mAbs includes protein A chromatography as a capture step, followed by two or three polishing steps.[4,5] Typically, the polishing steps are selected from among anion exchange (AEX), cation exchange (CEX), hydrophobic interaction, and hydroxyapatite chromatographies.[6]

In addition, viral safety is a critical concern with regard to mAb products produced in mammalian cells such as CHO cells.[7] CHO cells express noninfectious retrovirus-like particles.[8] Manufacturers are required to minimize the potential for adventitious virus contamination.[9-11] Furthermore, manufacturers must show that adventitious viruses and retrovirus-like particles are removed or inactivated during purification steps.

CEX chromatography is widely used in bind/elute mode as the polishing step to remove HMWS, HCP, and leached protein A to acceptable levels.[4,6] CEX chromatography can remove viruses such as murine leukemia virus (MLV), which is usually used as a model virus for retroviruses, pseudorabies virus (PRV), and reovirus Type 3 (Reo 3).[12]

The operation of CEX chromatography in bind/elute mode requires a large volume of expensive resin to bind all mAb molecules and certain

impurities. To reduce the cost of CEX chromatography, an overloaded mode has been investigated.[13,14] Although CEX chromatography, when used in bind/elute mode, is operated under loading conditions within the dynamic binding capacity, for example, <100 g mAb/L resin,[15] overloaded mode enables loads as large as 1,000 g mAb/L resin, which exceeds the amount loaded at the breakthrough by a factor of 10.[14]

It has been reported that when CEX chromatography is performed in overloaded mode, it effectively removes HCP, DNA, HMWS, and leached protein A.[14] The authors mentioned that the removal of these impurities was a result of mAb monomers being displaced by impurities. However, the application of viral clearance in overloaded mode has not yet been reported. If overloaded mode can remove viruses with the same efficiency as the bind/elute mode, then the overloaded mode can take the place of the expensive bind/elute mode.

The present study investigated the MLV clearance ability of CEX chromatography in overloaded mode using a POROS XS strong CEX resin with a high binding capacity. Additionally, MLV clearance was evaluated with other commercially available high-performance CEX resins, specifically Eshmuno CPX and Capto S ImpAct. Furthermore, the influence of flow rate on MLV removal was evaluated. The clearance of other viruses such as murine minute virus (MMV), PRV, and Reo 3, which are commonly evaluated in CHO-derived products, were also evaluated in overloaded mode. To investigate the mechanism of viral clearance in overloaded mode, the elution profiles of MLV, MMV, PRV, and Reo 3 in bind/elute mode were analyzed.

2 | MATERIALS AND METHODS

2.1 | Materials

Two humanized monoclonal antibodies, mAb1 and mAb2 (IgG1), were used in this study. The load material for this study was prepared from CHO cell culture fluid. The cultured cells were removed, and mAbs were subsequently purified via a traditional method that included protein A chromatography and AEX chromatography. The AEX chromatography pool was titrated to a pH of 5.0, filtered with a 0.2 μm filter, and then stored at −80°C until CEX loading. The conductivity of prepared CEX load material was approximately 5 mS/cm. Chromatography runs of this preparation were performed on an AKTA Explore 100 system (GE Healthcare) at room temperature. Chromatography was monitored at 280 nm.

2.2 | Viral spiking studies and viral assays

Viral spiking studies and viral assays were performed at a BioReliance laboratory (Stirling, UK). Viral titers were determined using reliable quantitative infectivity assays (50% tissue culture infectious dose [$TCID_{50}$]) according to the standard operating procedure of BioReliance for each model virus and appropriate indicator cells: PG-4 cells (MLV), Vero cells (PRV), 324K cells (MMV), and L-929 cells (Reo 3). Viral titers were calculated according to the Spearman-Kärber formula, and 95% confidence limits were calculated by multiplying the standard error by a constant of 1.96. Prior to the viral spiking studies, a prestudy was performed to determine whether the process samples were toxic to the indicator cell lines or interfered with the virus infectivity of the indicator cells used for virus titration. The viral spiking studies were performed using a scaled-down model. In bind/elute mode, a MLV suspension was spiked to a CEX load of 5% [vol/vol]. For overloaded mode, the spike ratio of each virus was set to 1% [vol/vol]. The titer of the load material, load hold, eluted fractions, and product pools were determined by $TCID_{50}$. As for the product pools, a large volume titration was performed to increase the sensitivity of the assay. The log reduction value (LRV) was calculated using the viral titer and product volume.

2.3 | CEX chromatography method: Overloaded mode and bind/elute mode

To evaluate HMWS and HCP removal in overloaded mode, a POROS XS prepacked column (Repligen) with 0.5 cm I.D. × 5 cm bed height (column volume [CV] = 1 mL) was used. For the virus spiking studies, POROS XS, Eshmuno CPX, and Capto S ImpAct prepacked columns (Repligen) of the same size were used. The flow rate was set at 18–30 CV/h (residence time [RT] = 2–3.3 min). Typically, overloaded mode was operated under the binding conditions commonly used in bind/elute mode. In this study, for the overloaded mode, the conditions used were selected based on our previous studies (data not shown) on mAb purification and performance data provided by the manufacturer of each resin. The CEX columns were equilibrated with 50 mM acetate buffer, pH 5.0. Then, the CEX load materials were loaded onto the column up to 2,000 g mAb/L resin. After loading, the mAb remaining in the column was recovered with the equilibration buffer. A high-salt wash buffer containing 1 M sodium chloride was applied to strip all materials from the column.

For bind/elute mode, POROS XS, Eshmuno CPX, and Capto S ImpAct prepacked columns (Repligen) with 0.8 cm I.D. × 20 cm bed height (CV = 10 mL) were used at a flow rate of 15 CV/h (RT = 4 min). The CEX columns were equilibrated with 50 mM acetate buffer, pH 5.0. Then, the CEX load materials were loaded onto the column up to 85 g mAb/L resin, washed with equilibration buffer, and eluted with 50 mM acetate buffer containing 170 mM (mAb2) or 180 mM (mAb1) sodium chloride.

To analyze the viral elution profile in bind/elute mode, a POROS XS prepacked column (Repligen) with 0.8 cm I.D. × 20 cm bed height (CV = 10 mL) was used at a flow rate of 15 CV/h (RT = 4 min). The CEX columns were equilibrated with 50 mM acetate buffer, pH 5.0. Then, the CEX load materials were loaded onto the column up to 25 g mAb1/L resin, washed with equilibration buffer, and eluted by a stepwise gradient with five CV at each step. The stepwise gradient sodium chloride concentrations were set at 180, 200, 250, 300, 350, 400, 500, 600, and 1,000 mM in 50 mM acetate buffer for MLV, PRV, and Reo 3, and 90, 180, 200, 250, 300, 350, 400, 500, and 1,000 mM in 50 mM acetate buffer for MMV.

To evaluate the dynamic binding capacity of each resin, purified mAb1 was loaded at a flow rate of 15 CV/h (RT = 4 min) until the protein concentration in the effluent became equal to that of the load.

The dynamic binding capacity of each resin was calculated at 5% of the binding breakthrough.

2.4 | Assays

The mAb concentration was determined via high-performance liquid chromatography using a PA ID Sensor Cartridge (2.1 mm × 30 mm, Thermo Fisher Scientific). Via size-exclusion chromatography, HMWS, monomers of mAb, and low-molecular-weight species (LMWS) were separated using a TSKgel G3000SW$_{XL}$ column (5 μm, 7.8 mm × 300 mm, two columns in series, Tosoh) or ACQUITY UPLC Protein BEH SEC column (1.7 μm, 4.6 mm × 300 mm, Waters). A mobile phase containing 0.1 M phosphate buffer at pH 7.0 and 0.4 M sodium chloride was used. The HCP concentration was measured via enzyme-linked immunosorbent assay using a third-generation CHO HCP kit (Cygnus).

3 | RESULTS

3.1 | HMWS removal in overloaded mode

Figure 1 shows the changes in HMWS content in the effluent relative to that of the load with increasing load (up to 2,000 g mAb/L resin) of mAb1 and mAb2. The concentration of HMWS in the effluent was decreased to less than half of that in the load. The HMWS contents in the pool were decreased to 45% (mAb1) or 25% (mAb2) of that of the load, which is comparable to that obtained via the bind/elute mode (Table 1). In addition, the LMWS content was similar for both overloaded mode and bind/elute mode.

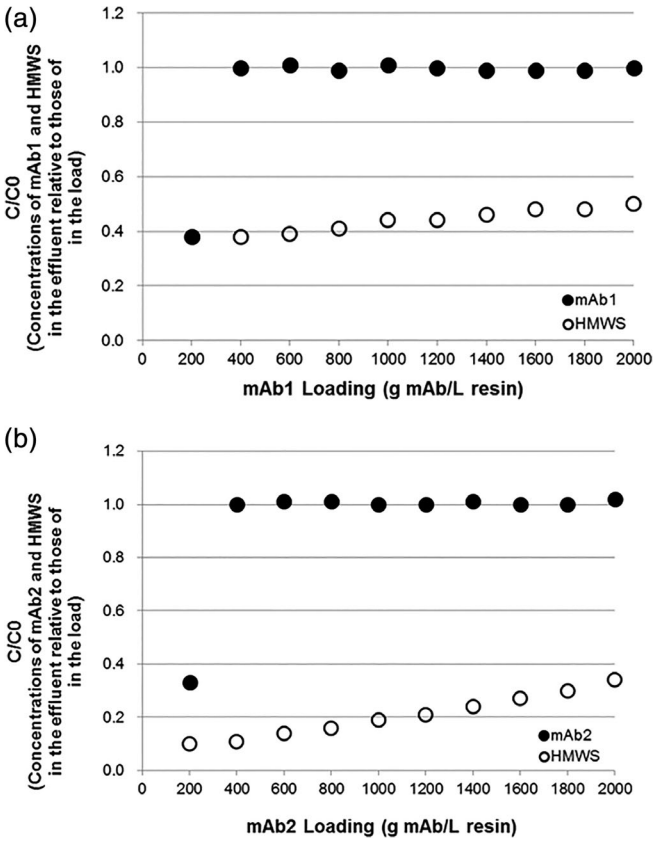

FIGURE 1 Removal of high-molecular-weight species (HMWS) from (a) mAb1 and (b) mAb2 in overloaded mode. The mAb solutions were loaded on a POROS XS column at a flow rate of 18 CV/h, and the concentrations of mAbs (filled circles) and HMWS (empty circles) in the effluent fractions were determined and expressed as ratios (C/C0) relative to the concentrations in the load

3.2 | HCP removal in overloaded mode

Table 1 shows the HCP removal in overloaded mode using up to 2,000 g mAb/L resin and POROS XS for mAb1 and mAb2. The HCP content in the load material was approximately 2×10^2 ng/mg mAb. The HCP was greatly removed to a degree close to or below the quantitation limit of the HCP assay, which was similar to the results obtained via the bind/elute mode.

3.3 | MLV removal in overloaded mode

It is reported that CEX chromatography with the strong cation exchanger Fractogel SO_3^- operated at pH 5.0 in bind/elute mode results in effective MLV clearance (>4 logs).[12]

In the present study, MLV removal in overloaded mode was investigated using the strong cation exchanger POROS XS. The mAb1 and mAb2 (up to 2,000 g mAb/L resin) were spiked with 1% (vol/vol) MLV and loaded onto a POROS XS column at pH 5.0 at a flow rate of 18 CV/h (as recommended by the manufacturer). Effluent fractions were collected at every 500 g mAb/L resin added. These fractions and their pool were assayed for MLV via determining their $TCID_{50}$. From the first fraction (at 500 g mAb/L resin) to the last fraction (at 2,000 g mAb/L resin), MLV was not detected (Figure 2). As a result, the MLV clearance in overloaded mode under 2,000 g mAb/L resin loading was calculated to be 6.09 logs for mAb1 and > 4.51 logs for mAb2 (Table 2). Although MLV was not detected at all for mAb2, the reason why MLV clearance from mAb2 was lower than that from mAb1 was mAb2 was toxic to indicator cells. Because of its cytotoxicity, mAb2 should be diluted adequately, so the viral titer of the mAb2 pool was slightly higher than that of mAb1. Even under high loading conditions, MLV was removed from mAbs, and a high LRV was obtained in overloaded mode.

3.4 | Effect of flow rate

It has been reported that in overloaded mode with POROS HS resin, changes in flow rate (18–36 CV/h) did not significantly affect the removal of DNA, HMWS, or HCP.[14] We analyzed the effect of flow rate on MLV removal from mAb1 in overloaded mode. The flow rate was set at 18 CV/h (RT = 3.3 min) or 30 CV/h (RT = 2 min), by taking process time into account. The flow rate affected the removal of MLV when up to 2,000 g mAb/L resin was used (Figure 3). Although MLV was completely removed when up to 2,000 g mAb/L resin was used at a flow rate of 18 CV/h, at the higher rate of 30 CV/h, MLV was detected in the eluate when 1,500 g mAb/L resin was used, and the LRV decreased to 2.89 (Table 3). According to the POROS XS manufacturer directions, the target operating flow rate is flexible, but optimal

TABLE 1 Comparison of Overloaded and Bind/Elute Modes Regarding the Removal of Impurities

mAb	Sample	Monomer (%)	HMWS (%)	LMWS (%)	HCP (ng/mg mAb)
mAb1	Load	97.54	1.60	0.85	2.42E+02
	Recovered pool in overloaded mode (2,000 g mAb/L resin)	98.56	0.69	0.75	1.87
	Recovered pool in bind/elute mode (80 g mAb/L resin)	98.56	0.70	0.74	<0.84[a]
mAb2	Load	97.13	1.83	1.05	1.67E+02
	Recovered pool in overloaded mode (2,000 g mAb/L resin)	98.87	0.37	0.76	<1.08[a]
	Recovered pool in bind/elute mode (80 g mAb/L resin)	98.79	0.44	0.76	<1.08[a]

[a]Quantitation limit.

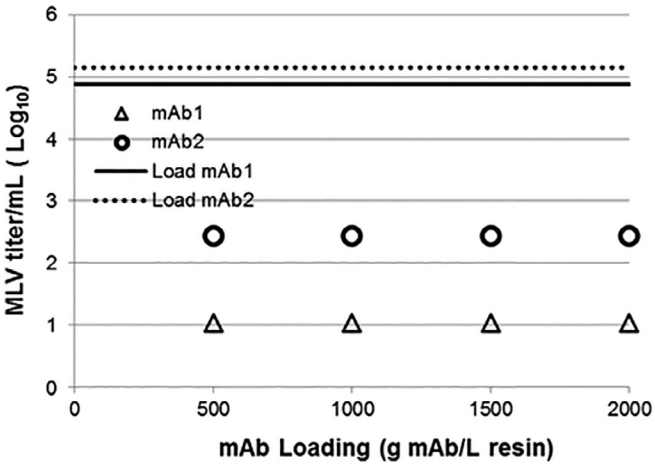

FIGURE 2 Murine leukemia viral elution profile in overloaded mode at a flow rate of 18 CV/h. (a) mAb1 (triangles) and (b) mAb2 (diamonds) were spiked with 1% (vol/vol) murine leukemia virus (MLV), loaded onto a POROS XS column, separated in overloaded mode, and the fractions were collected and assayed for MLV titer ($TCID_{50}$). Open symbols indicate that the virus level was below the detection limit of the assay

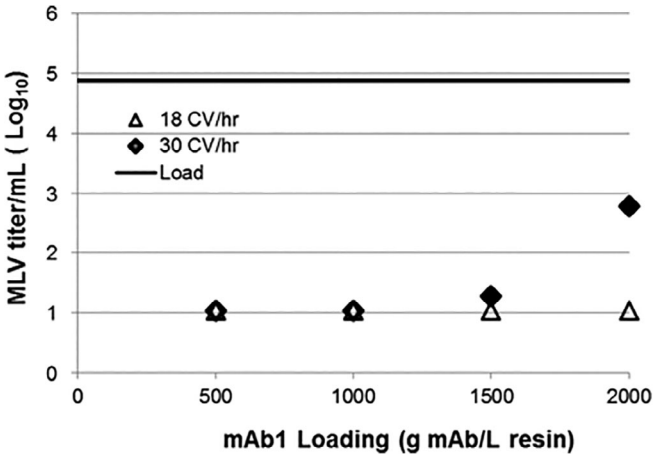

FIGURE 3 Murine leukemia viral (MLV) elution profile in overloaded mode at flow rates of 18 CV/h (triangles) and 30 CV/h (diamonds). mAb1 was spiked with 1% (vol/vol) MLV, loaded onto a POROS XS column, separated in overloaded mode, and the fractions were collected and assayed for MLV titer ($TCID_{50}$). Open symbols indicate that the virus level was below the detection limit of the assay

TABLE 2 Murine Leukemia Viral Clearance in Overloaded Mode Under Loading Conditions of 2,000 g mAb/L Resin

mAb	MLV Clearance (Log Reduction Value)[a]
mAb1	6.09 ± 0.89
mAb2	≥4.51 ± 0.25

"≥" indicates that the virus level in the product pool (up to 2,000 g mAb/L resin) was below the detection limit of the large volume titration assay.
[a]95% confidence limit.

binding should be obtained with a RT of ≥3 min. Thus, 18 CV/h (RT = 3.3 min) is considered to be efficient for mAb purification.

3.5 | Impact of CEX resin type

3.5.1 | Dynamic Binding Capacity of Each Resin

To investigate the impact of CEX resin type on MLV removal in overloaded mode, the performances of various CEX resins were evaluated. It was predicted that in the bind/elute mode, a high binding capacity resin would have an advantageous effect on the load amount. The dynamic binding capacity was compared between commercially available resins with strong cation ligands such as POROS XS, Eshmuno CPX, Capto S ImpAct, and SP Sepharose Fast Flow. Table 4 summarizes the characteristics of each resin. The dynamic binding capacity was evaluated at pH 5.0 with RT = 4 min. Figure 4 shows the breakthrough curve of each resin for mAb1. The dynamic binding capacities of each resin at 5% breakthrough are summarized in Table 5. The resins other than classical SP Sepharose Fast Flow had equivalent dynamic binding capacities. Therefore, Eshmuno CPX and Capto S ImpAct were compared to POROS XS for MLV removal, as described below.

3.5.2 | Murine Leukemia Viral Clearance in Bind/Elute Mode

Prior to comparison of three resins for MLV removal in overloaded mode, the impact of CEX resin type on MLV removal in bind/elute

TABLE 3 Murine Leukemia Viral Clearance in Overloaded Mode Under Loading Conditions of 2,000 g mAb/L Resin at Two Flow Rates for mAb1

Flow Rate (CV/h)	MLV Clearance (Log Reduction Value)[a]
18	6.09 ± 0.89
30	2.89 ± 0.33

[a]95% confidence limit.

TABLE 4 Characteristics of Each Resin Used for Dynamic Binding Capacity Study

Resin	Support Matrix	Surface Functionality	Average Particle-Size
POROS XS	Cross-linked polystyrene divinylbenzene	Sulfopropyl	50 μm
Eshmuno CPX	Surface-grafted rigid hydrophilic polyvinylether polymer	Sulfoisobutyl	50 μm
Capto S ImpAct	High-flow agarose	Sulfopropyl	50 μm
SP Sepharose Fast Flow	6% highly cross-linked agarose	Sulfopropyl	90 μm

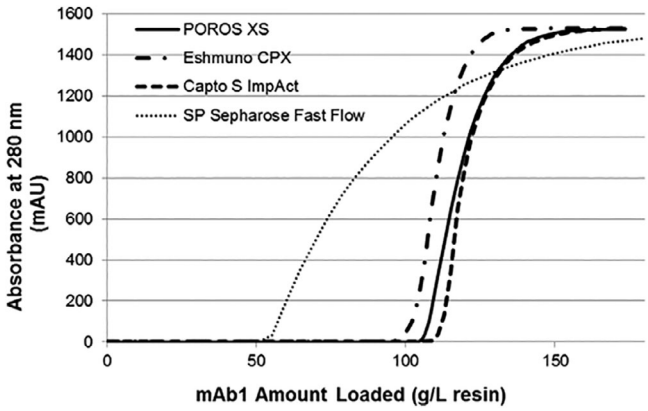

FIGURE 4 Breakthrough curve of mAb1 for each cation exchange resin: POROS XS (solid line), Eshmuno CPX (dot-dash line), Capto S ImpAct (dashed line), and SP Sepharose Fast Flow (dotted line)

mode at pH 5.0 was investigated. MLV (5% [vol/vol]) was used to spike mAb1, which was then loaded onto each column at up to 85 g mAb/L resin at a flow rate of 15 CV/h (RT = 4 min). The optimal sodium chloride conditions for elution from each resin were set based on our previous studies (data not shown). High LRVs, such as >4 logs, were obtained in all studies. In particular, >6 logs of virus was removed by POROS XS (Table 5). There were no significant differences among the three resins in the bind/elute mode.

3.5.3 | Murine Leukemia Viral Clearance in Overloaded Mode

MLV (1% [vol/vol]) was used to spike mAb1, which was then loaded onto each column at up to 2,000 g mAb/L resin at a flow rate of 30 CV/h (RT = 2 min). Because of the high flow rate, high LRVs, such as >4 logs, were not obtained (Table 5). However, it is clear that there were no significant differences among the three resins in overloaded mode, as was the case in bind/elute mode.

3.6 | Removal of other viruses in overloaded mode

In the early stages of regulatory submission (Phase I and II clinical trials), one or two viruses are sufficient for clearance studies. Later stages of clinical trials (Phase III and Product License Application) require a broad range of virus types with various physical and chemical properties, for example, DNA-based, RNA-based, enveloped, and nonenveloped.

In this study, in addition to MLV clearance, MMV, PRV, and Reo 3 clearances were evaluated in overload mode for mAb1. For all virus spiking studies, the load amount was set to 2,000 g mAb/L resin at a flow rate of 18 CV/h (RT = 3.3 min). The LRVs for all viruses are summarized in Table 6. Not only MLV but also PRV and Reo 3 were effectively removed in overloaded mode. Overloaded mode removes MMV; however, the LRV of MMV was not as high as those of other viruses.

3.7 | Viral elution profile in bind/elute mode

To investigate the mechanism of viral clearance in overloaded mode, MLV, MMV, PRV, and Reo 3 elution profiles in bind/elute mode were analyzed at pH 5.0. The results are summarized in Figure 5. For MLV, PRV, and Reo 3, viruses were not detected in the unbound and wash

TABLE 5 Dynamic Binding Capacity (5% of Breakthrough) and MLV Clearance for Each Resin

Resin	Dynamic Binding Capacity (g mAb1/L Resin)	MLV Clearance in Bind/Elute Mode (Log Reduction Value)[a]	MLV Clearance in Overloaded Mode (Log Reduction Value)[a]
POROS XS	107	≥6.06 ± 0.32	2.89 ± 0.33
Eshmuno CPX	101	5.80 ± 0.24	2.93 ± 0.31
Capto S ImpAct	112	4.98 ± 0.42	≥2.80 ± 0.40
SP Sepharose Fast Flow	57	Not tested	Not tested

"≥" indicates that the virus level in the product pool (bind/elute mode: up to 85 g mAb/L resin, overloaded mode: up to 2,000 g mAb/L resin) was below the detection limit of the large volume titration assay.
[a]95% confidence limit.

fractions (data not shown), and viruses eluted later than mAb1. The sodium chloride concentrations of the last stepwise elution containing no detectable viruses were 200 mM (MLV), 350 mM (PRV), and 200 mM (Reo 3). In contrast to these viruses, MMV was detected in all fractions, including the unbound and wash fractions (data not shown).

TABLE 6 Viral Clearance in Overloaded Mode Under Loading Conditions of 2,000 g mAb1/L POROS XS Resin

Viral Clearance (Log Reduction Value)[a]			
MLV	MMV	PRV	Reo 3
6.09 ± 0.89	2.62 ± 0.39	≥5.71 ± 0.38	8.03 ± 0.93

"≥" indicates that the virus level in the product pool (up to 2,000 g mAb/L resin) was below the detection limit of the large volume titration assay.
[a]95% confidence limit.

3.8 | Comparison between viral clearances of overloaded and bind/elute modes

For mAb1, MLV, MMV, PRV, and Reo 3 clearances were compared in overloaded and bind/elute modes. The results are summarized in Table 7. Even though the load amount in the overloaded mode was larger than that in the bind/elute mode by a factor of 20, comparable viral clearance data were obtained.

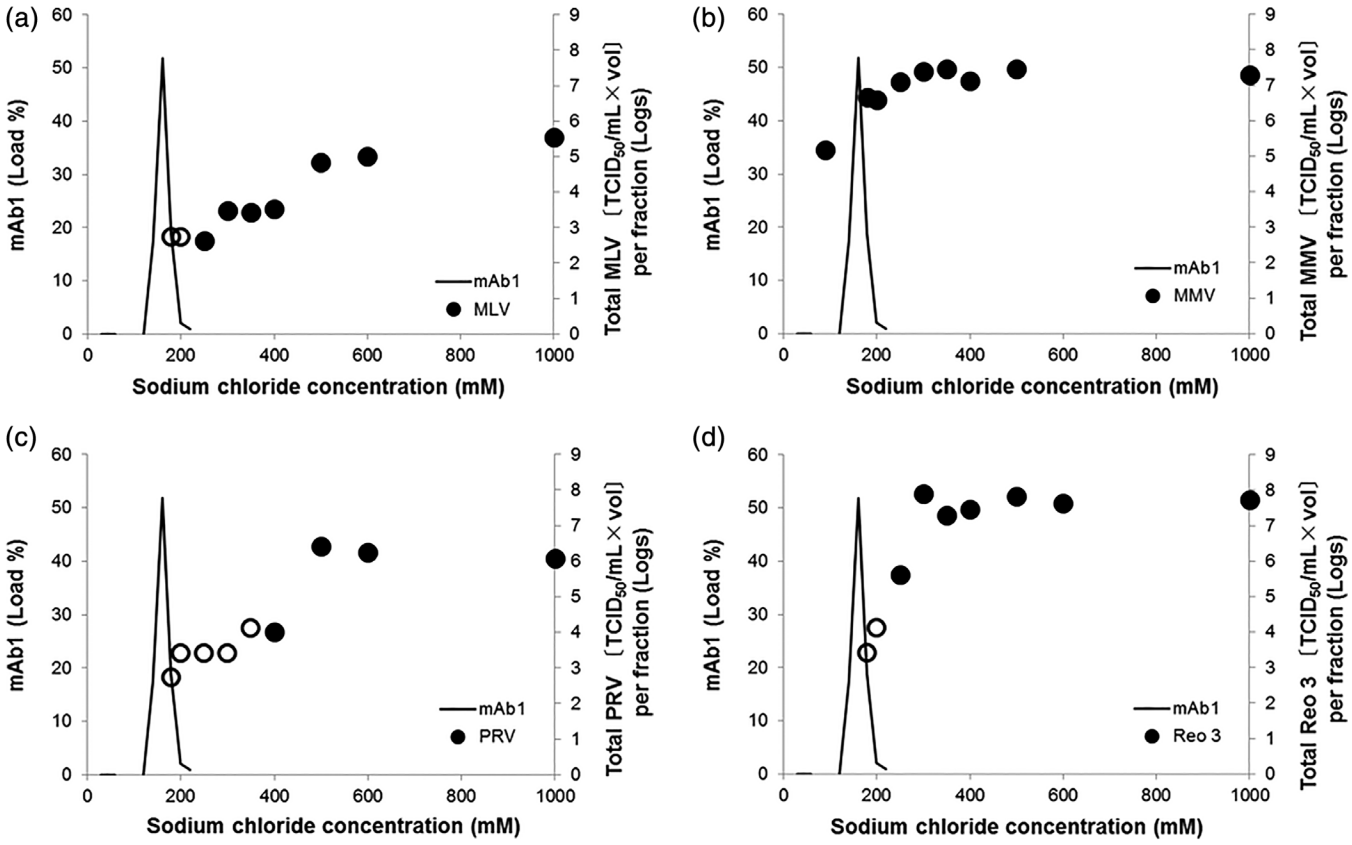

FIGURE 5 Viral elution profile in bind/elute mode for POROS XS at pH 5.0. mAb1 was spiked with 5% (vol/vol) viruses ((a) murine leukemia virus, (b) murine minute virus, (c) pseudorabies virus, and (d) Reo 3), loaded onto a POROS XS column, and eluted by a stepwise gradient of sodium chloride. The fractions were collected and assayed for viral titer ($TCID_{50}$). Open symbols indicate that the virus level was below the detection limit of the assay. Solid lines indicate the mAb1 elution profile obtained via high-performance liquid chromatography

TABLE 7 Comparison Between Overloaded Mode and Bind/Elute Mode in Terms of Viral Clearance

		Viral Clearance (Log Reduction Value)[a]			
Mode	Load Amount (g mAb1/L POROS XS Resin)	MLV	MMV	PRV	Reo 3
Overloaded	2,000	6.09 ± 0.89	2.62 ± 0.39	≥5.71 ± 0.38	8.03 ± 0.93
Bind/elute	85	6.19 ± 0.47	2.17 ± 0.51	7.43 ± 0.42	6.03 ± 0.29

"≥" indicates that the virus level in the product pool (up to 2,000 g mAb/L resin) was below the detection limit of the large volume titration assay.
[a]95% confidence limit.

4 | DISCUSSION

Clearly, CEX chromatography plays an important role in mAb purification. In fact, HMWS, HCP, leached protein A, and viruses are removed to an acceptable level via CEX chromatography in bind/elute mode. To reduce the cost of using CEX chromatography in bind/elute mode, an overloaded mode was investigated.[13,14] The authors of these studies mentioned that HMWS, HCP, and the other impurities were removed to an acceptable level in overloaded mode. However, virus removal in overloaded mode has not been reported. The present study shows the ability of CEX chromatography to remove viruses in overloaded mode for the first time.

The elution profiles of viruses in bind/elute mode will help us understand the mechanism of viral clearance in overloaded mode. For MLV, the elution profiles of Fractogel SO_3^- at pH 5.0 and pH 6.0 in bind/elute mode have been reported.[12] In the bind/elute mode, MLV was not detected in the unbound and wash fractions. In actuality, MLV was tightly bound to the resin and eluted in later fractions than the product pool.[16] In the present study, virus elution profiles in bind/elute mode using POROS XS resin at pH 5.0 were investigated. MLV was eluted in later fractions than mAb1 as in the previous report. PRV and Reo 3 elution profiles in bind/elute mode were confirmed in the present study, and it was clear that these viruses eluted in later fractions than mAb1 in bind/elute mode, as did MLV. These elution profiles in the bind/elute mode suggest that these viruses bind to CEX resins more tightly than mAb1, displace bound mAb1, and remain bound to the resin even after all mAb1 is eluted. As a result, these three viruses were effectively removed by CEX chromatography in overloaded mode.

In contrast to these three viruses, the removal of MMV via CEX chromatography in overloaded mode was poor. This observation suggests that MMV does not bind strongly to CEX resins. In fact, for the MMV elution profile in bind/elute mode in the present study, MMV was detected in all fractions, including the unbound and wash fractions, as in the previous report.[12] Because the p*I* of MLV is 5.8 whereas the p*I* of MMV is 6.2,[17] MLV binding more tightly to CEX resin than MMV is surprising. The differences in the CEX chromatography elution profiles of MLV and MMV at pH 5.0 were assumed to be due to an envelope containing charge clusters, and MLV interacts strongly with CEX resin at pH 5.0.[12] To understand the viral elution profiles in CEX chromatography, further investigation, such as determining the surface charge distribution of viruses, is required.

The mechanism of MLV clearance is considered the same as that of HMWS and HCP clearance. However, the removal of HMWS and HCP were not affected by flow rate (data not shown), although MLV clearance was slightly affected by the flow rate in this study. It is possible that the reason why a slow flow rate leads to the successful removal of MLV is related to the large size of MLV. MLV has a diameter of 100–120 nm,[18] which is close to the pore size of POROS XS resin (100–360 nm). Thus, at a high flow rate, the virus particles of MLV may not fully access the sulfopropyl ligands on the inside pores due to steric hindrance. In any case, MLV can be removed at a flow rate of 18 CV/h, which is recommended by the manufacturer.

Regarding the resin type, three strong cation ligand resins with different support matrices exhibited similar MLV clearance levels in overloaded mode (Table 5). This observation suggests that the site of MLV competitive binding to the resin is the cationic ligand and that the contribution of the support matrix can be neglected. Thus, MLV clearance is widely achieved in overloaded mode regardless of resin type, as in bind/elute mode.

Based on these results, the viral removal ability in CEX chromatography in overloaded mode can be predicted from bind/elute mode results. For MLV clearance in bind/elute mode, the effects of pH, ionic strength, resin type, level of impurities, and mAb loading are reported.[12] For setting the best conditions for viral clearance in overloaded mode, these reported data for bind/elute mode would be useful.

Once the conditions for bind/elute mode are determined, the determination of new conditions for overloaded mode is not required, in our experiences. The conditions for the bind/elute mode can be applied to overloaded mode. It is possible to predict the impurity removal performance in overloaded mode by confirming the binding affinity to the resin in bind/elute mode. Although the conditions for separating mAb monomers from MLV must be finely tuned for each mAb in bind/elute mode, the optimization in overloaded mode is less demanding because the separation depends on the difference in binding affinities between mAb monomers and MLV.

Virus particles have been commonly removed via AEX chromatography in flow-through mode.[17,19-23] Because the ability of CEX chromatography to remove virus particles in overloaded mode was demonstrated in the present study, all major impurities in mAb preparation, including HMWS, HCP, and virus particles, may be removed via a single session of CEX chromatography in overloaded mode. The data presented here suggest that overloaded mode is effective as a polishing step for therapeutic mAb.

CONFLICT OF INTEREST

The authors have no conflict of interest to declare.

ORCID

Yumiko Masuda https://orcid.org/0000-0001-5548-7520

REFERENCES

1. Reichert JM. Antibodies to watch in 2017. *MAbs*. 2017;9:167-181.
2. Vázquez-Rey M, Lang DA. Aggregates in monoclonal antibody manufacturing processes. *Biotechnol Bioeng*. 2011;108:1494-1508.
3. Shukla AA, Jiang C, Ma J, Rubacha M, Flansburg L, Lee SS. Demonstration of robust host cell protein clearance in biopharmaceutical downstream processes. *Biotechnol Prog*. 2008;24:615-622.
4. Zhou JX, Tressel T, Yang X, Seewoester T. Implementation of advanced technologies in commercial monoclonal antibody production. *Biotechnol J*. 2008;3:1185-1200.
5. Liu HF, Ma J, Winter C, Bayer R. Recovery and purification process development for monoclonal antibody production. *MAbs*. 2010;2:480-499.

6. Shukla AA, Hubbard B, Tressel T, Guhan S, Low D. Downstream processing of monoclonal antibodies—application of platform approaches. *J Chromatogr B*. 2007;848:28-39.
7. Zhang M, Lute S, Norling L, et al. A novel, Q-PCR based approach to measuring endogenous retroviral clearance by capture protein a chromatography. *Biotechnol Bioeng*. 2009;102:1438-1447.
8. Anderson KP, Low M-AL, Lie YS, Keller G-A, Dinowitz M. Endogenous origin of defective retroviruslike particles from a recombinant Chinese hamster ovary cell line. *Virology*. 1991;181:305-311.
9. International Conference on Harmonisation of Technical Requirements for Registration of Pharmaceuticals for Human Use. Viral Safety Evaluation of Biotechnology Products Derived from Cell Lines of Human or Animal Origin Q5A(RA). Web site. https://www.ich.org/fileadmin/Public_Web_Site/ICH_Products/Guidelines/Quality/Q5A_R1/Step4/Q5A_R1_Guideline.pdf. Updated September 1999.
10. U.S. Department of Health and Human Services, Food and Drug Administration, Center for Biologics Evaluation and Research. Points to Consider in the Manufacture and Testing of Monoclonal Antibody Products for Human Use. Web site. https://www.fda.gov/downloads/BiologicsBloodVaccines/GuidanceComplianceRegulatoryInformation/OtherRecommendationsforManufacturers/UCM153182.pdf. Updated February 1997.
11. European Medicines Agency. Evaluation of Medicines for Human Use. Guideline on Virus Safety Evaluation of Biotechnological Investigational Medicinal Products. Web site. https://www.ema.europa.eu/documents/scientific-guideline/guideline-virus-safety-evaluation-biotechnological-investigational-medicinal-products_en.pdf. Updated July 2008.
12. Connell-Crowley L, Nguyen T, Bach J, et al. Cation exchange chromatography provides effective retrovirus clearance for antibody purification processes. *Biotechnol Bioeng*. 2012;109:157-165.
13. Brown A, Bill J, Tully T, Radhamohan A, Dowd C. Overloading ion-exchange membranes as a purification step for monoclonal antibodies. *Biotechnol Appl Biochem*. 2010;56:59-70.
14. Liu HF, McCooey B, Duarte T, et al. Exploration of overloaded cation exchange chromatography for monoclonal antibody purification. *J Chromatogr A*. 2011;1218:6943-6952.
15. Pabst TM, Suda EJ, Thomas KE, et al. Binding and elution behavior of proteins on strong cation exchangers. *J Chromatogr A*. 2009;1216:7950-7956.
16. Miesegaes GR, Lute S, Strauss DM, et al. Monoclonal antibody capture and viral clearance by cation exchange chromatography. *Biotechnol Bioeng*. 2012;109:2048-2058.
17. Strauss DM, Lute S, Tebaykina Z, et al. Understanding the mechanism of virus removal by Q sepharose fast flow chromatography during the purification of CHO-cell derived biotherapeutics. *Biotechnol Bioeng*. 2009;104:371-380.
18. Asper M, Hanrieder T, Quellmalz A, Mihranyan A. Removal of *Xenotropic murine* leukemia virus by nanocellulose based filter paper. *Biologicals*. 2015;43:452-456.
19. Miesegaes G, Lute S, Brorson K. Analysis of viral clearance unit operations for monoclonal antibodies. *Biotechnol Bioeng*. 2010;106:238-246.
20. Miesegaes GR, Lute SC, Read EK, Brorson KA. Viral clearance by flow-through mode ion exchange columns and membrane adsorbers. *Biotechnol Prog*. 2014;30:124-131.
21. Strauss DM, Gorrell J, Plancarte M, Blank GS, Chen Q, Yang B. Anion exchange chromatography provides a robust, predictable process to ensure viral safety of biotechnology products. *Biotechnol Bioeng*. 2009;102:168-175.
22. Weaver J, Husson SM, Murphy L, Wickramasinghe SR. Anion exchange membrane adsorbers for flow-through polishing steps: part I. Clearance of minute virus of mice. *Biotechnol Bioeng*. 2013;110:491-499.
23. Weaver J, Husson SM, Murphy L, Wickramasinghe SR. Anion exchange membrane adsorbers for flow-through polishing steps: part II. Virus, host cell protein, DNA clearance, and antibody recovery. *Biotechnol Bioeng*. 2013;110:500-510.

Efficient removal of aggregates from monoclonal antibodies by hydrophobic interaction chromatography in flow-through mode

Abstract

Monoclonal antibody (mAb)–based therapeutics have been very successful in treating various diseases, including cancer. The manufacturing of these therapeutic antibodies is a complex operation since it needs to ensure quality, safety, and efficacy of the products. Low levels of aggregates are a critical quality attribute of the final product, as this will impact the biological activity. Therefore, efficient removal of aggregates from the final therapeutic product is of great importance. Hydrophobic interaction chromatography (HIC) is a versatile purification technique that can be utilized to remove aggregates in the downstream processing of mAbs. Here we illustrate an effective solution for aggregate removal in therapeutic mAb production utilizing HIC in flow-through mode, under low-conductivity conditions. Analysis of the final product revealed efficient clearance of dimers and high molecular weight (HMW) aggregates. The final process resulted in a more productive and cost-effective technique compared to the established mixed-mode bind/elute process originally designed for a challenging mAb.

Important: Thermo Scientific™ POROS™ Benzyl and Benzyl Ultra HIC Resins are designed for use with lower salt concentrations than the traditional HIC resins. With some molecules, high salt concentration can cause poor recovery due to a strong interaction between the target and the ligand.

Introduction

Since levels of aggregates impact the biological activity of a biopharmaceutical, monitoring these levels in the final mAb therapeutic is critical [1]. In general, the lowest possible concentration of aggregates is desired in the final formulation of mAbs, typically less than 1% [2].

HIC can be used as an aggregate removal tool in the downstream processing of mAbs. Because the selectivity of HIC can be affected by different factors (i.e., type of salt and concentration, buffer pH, and temperature), a well-designed process together with a robust resin are the keys to successful and highly efficient purification for aggregate removal.

Anion exchange (AEX) chromatography in flow-through mode is often utilized as the first polishing step in mAb purification after affinity chromatography. Flow-through chromatography is a mode of operation that has the benefit of increased productivity and throughput; however, it requires the resin chemistry and properties to be highly selective towards the impurities to be removed. As AEX chromatography in flow-through mode is not highly selective towards mAb aggregates, the process generally requires an additional polish step involving an orthogonal chemistry in bind/elute mode. A final polishing step in flow-through mode would be beneficial to productivity of the purification process.

Summary of the study

For the purpose of aggregate removal, the highly hydrophobic POROS Benzyl Ultra HIC Resin was optimized by high-throughput screening, for use in flow-through mode as an alternative to a generic mixed-mode bind/elute step in a customer's original purification process (Figure 1). The goal of the study was to design a more efficient and cost-effective process than the original one, but to maintain the purity at ≥99%. Introduction of an HIC flow-through (FT) step resulted in a more productive polishing process with an 8% increase in yield, greatly improved resin loading, and a reduction in residence time. Even under low-conductivity conditions and high load densities, the final product showed efficient clearance of dimers and HMW aggregates after the HIC FT step. The data show that the POROS Benzyl Ultra resin can be utilized for efficient aggregate removal in the downstream process of therapeutic monoclonal antibody production.

Goal of the study

Design a more simple and cost-effective polish step utilizing POROS Benzyl Ultra resin in flow-through (FT) mode as an alternative to the mixed-mode bind/elute (B/E) step in the original purification process (Figure 1).

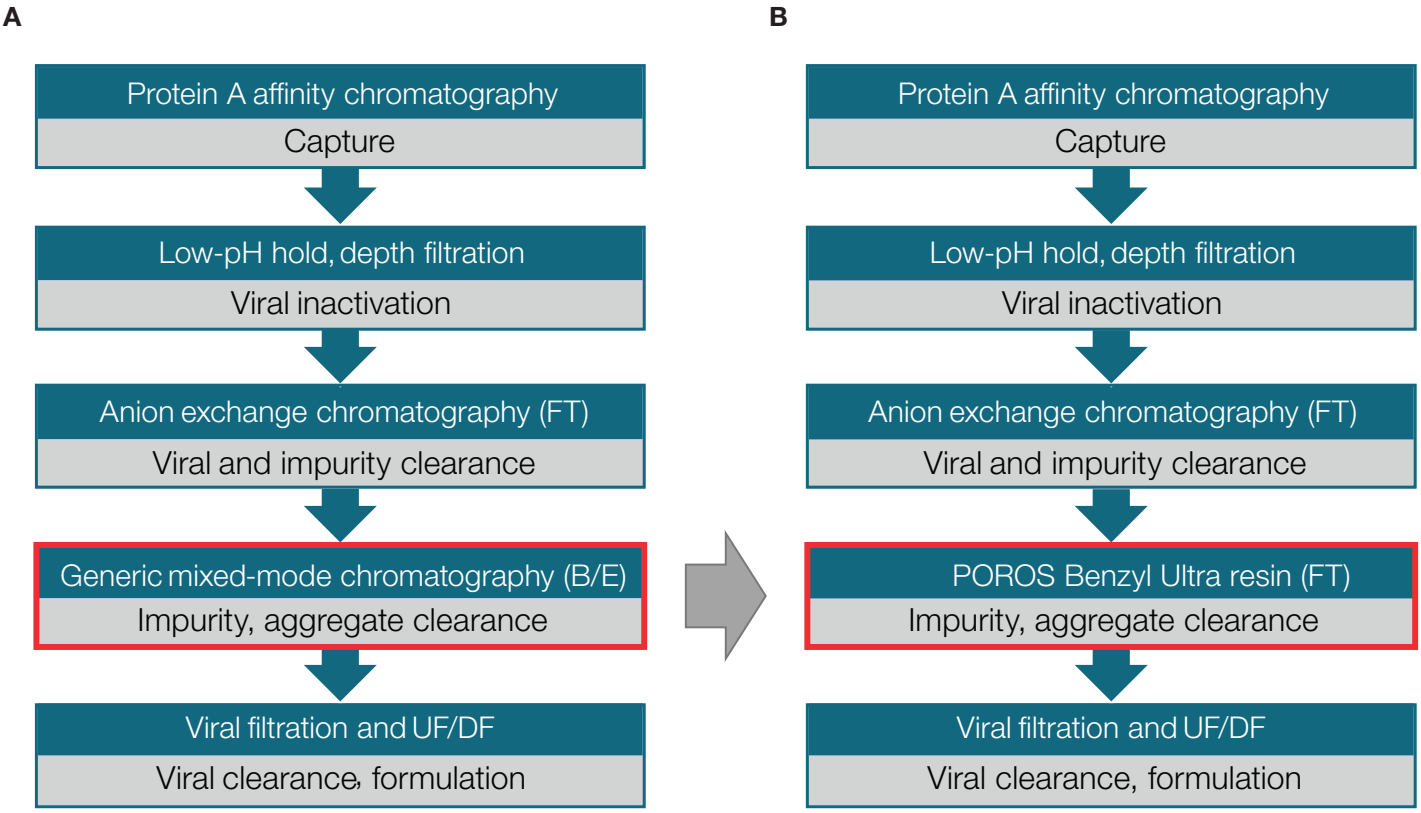

Figure 1. Comparison of (A) the original purification process with (B) the newly optimized process. The goal of this study was to design a more simple and cost-effective polish step utilizing POROS Benzyl Ultra resin in a flow-through (FT) mode as an alternative to a mixed-mode bind/elute (B/E) step in the original purification process. UF/DF = ultrafiltration/diafiltration.

Materials

Antibody

- mAb-A: a CHO-produced monoclonal antibody, purified using a protein A capture step followed by an AEX chromatography step in flow-through mode. The AEX flow-through pool contained approximately 12% aggregate.

Consumables

- POROS Benzyl HIC Resin, Thermo Fisher Scientific (Cat. No. A32558)
- POROS Benzyl Ultra HIC Resin, Thermo Fisher Scientific (Cat. No. A32565)
- Fisherbrand™ 96-Well DeepWell™ Polypropylene Microplates, Fisher Scientific (Cat. No. 12-566-121)
- Thermo Scientific™ Nunc™ MicroWell™ 96-Well Optical-Bottom Plates with Polymer Base, Thermo Fisher Scientific (Cat. No. 152028)
- Thermo Scientific™ MAbPac™ SEC-1 Size Exclusion LC Columns, Thermo Fisher Scientific (Cat. No. 088789)
- Sodium Chloride (MW 58.44), Fisher Bioreagents (Cat. No. BP358-1)
- Sodium Acetate Trihydrate (MW 136.08), Fisher Chemical (Cat. No. S209-500)
- Ammonium Sulfate (MW 132.14), Fisher Chemical (Cat. No. A702-500)
- Sodium Citrate Dihydrate (MW 294.1), Fisher Chemical (Cat. No. S279-50)

Equipment and software

- Thermo Scientific™ Versette™ Automated Liquid Handler, Thermo Fisher Scientific (Cat. No. 650-INSTR)
- Thermo Scientific™ Finnpipette™ Novus Electronic Multichannel Pipette, Thermo Fisher Scientific (Cat. No. 46300800)
- Thermo Scientific™ Varioskan™ LUX Multimode Microplate Reader, Thermo Fisher Scientific (Cat. No. VLBLATD1)
- Thermo Scientific™ Sorvall™ Legend™ XT/XF Centrifuge Series, Thermo Fisher Scientific (Cat. No. 75004521)
- Thermo Scientific™ Ultimate™ 3000 Standard Dual System, Thermo Fisher Scientific (contact our sales support team for purchase)
- Thermo Scientific™ HyperSep™ Universal Vacuum Manifold, Thermo Fisher Scientific (Cat. No. 60104-231)
- Thermo Scientific™ Pharma KingFisher™ Flex 96 Deep-Well Magnetic Particle Processor, Thermo Fisher Scientific (Cat. No. A31508)
- Applied Biosystems™ 7500 Real-Time PCR System, Thermo Fisher Scientific (Cat. No. 4351104)
- Applied Biosystems™ ProteinSEQ™ CHO HCP Quantitation Kit, Thermo Fisher Scientific (Cat. No. A27601)
- JMP™ Pro predictive analytics software, JMP Statistical Discovery
- ÄKTA™ Pure Chromatography System, GE Healthcare Life Sciences

Methods

The workflow used for process optimization can be broken down into the steps shown in Figure 2.

Defining conductivity range for mAb-A and resin interaction

The POROS HIC resins were packed into a 0.66 cm (D) x 10 cm (L) column. Each column was equilibrated with 600 mM sodium acetate in Tris buffer, pH 7.5. The mAb-A AEX pool was then loaded onto each column at 5 mg of mAb per milliliter of resin (mg/mL) at a flow rate of 300 cm/hr. To define optimal elution conductivity, a gradient elution over 10 column volumes (CV) was performed, at 300 cm/hr, starting with the high-salt equilibration buffer and gradually moving to a Tris buffer (pH 7.5) containing no salt.

Figure 2. Breakdown of steps for process optimization.

High-throughput screening for flow-through mode

To explore the critical parameters affecting resin selectivity towards aggregate removal in the flow-through mode, high-throughput screening was used (Figure 3). Yield was measured by A_{280} on the Varioskan LUX Multimode Microplate Reader. Purity was determined by high-performance liquid chromatography (HPLC)–size-exclusion chromatography (SEC) analysis (UltiMate 3000 HPLC, MAbPac SEC-1 LC column, 50 mM sodium phosphate, pH 7.0, 200 mM NaCl isocratic elution, 15 min).

To determine the optimal pH, salt type, and salt concentration of the resins, each well of a 96-well filter plate was filled with 30 µL of POROS Benzyl or POROS Benzyl Ultra resin. Then 185 µL of buffers with various salt types, salt concentrations, and pH were pipetted into the plate, followed by a 15 µL concentrated mAb spike to achieve a final phase ratio of 6.6 and load density of 6 mg/mL resin. After mixing for 30 min, the plate was centrifuged at 1,000 rpm for 3 min. The flow-through pools were collected in a 96-well UV-transparent collection plate. Protein concentration was determined by A_{280} on the Varioskan plate reader, and monomer purity was analyzed by HPLC-SEC on the UltiMate 3000 system with a MAbPac-SEC-1 column.

Conditions tested

- **Salt types:** sodium chloride, sodium acetate, ammonium sulfate, and sodium citrate
- **Salt concentrations:**
  - For POROS Benzyl resin: 10–300 mM (4–40 mS/cm)
  - For POROS Benzyl Ultra resin: 5–150 mM (1.5–25 mS/cm)
- **pH:** 5.5, 6.5, and 7.5

Contour plots for monomer recovery, aggregate removal, and selectivity factor (α) were generated using the JMP software. Monomer recovery and aggregate removal values were calculated based on a mass balance equation using the combined total concentration and HPLC-SEC purity data. The selectivity factor was calculated as the ratio of aggregate to monomer partition coefficients (K_P) as published by Kramarczyk et al. [3].

Chromatography optimization in scale-down model

POROS Benzyl Ultra resin was packed into a 0.66 cm (D) x 10 cm (L) (3.4 mL) column. Each column was equilibrated with 25 mM Tris-acetate at pH 6.8 and conductivity of 1.8 mS/cm. Each column was loaded with the Mab-A AEX pool (2.4 mg of mAb per mL of resin) at conductivity of 1.8 mS/cm and pH 6.8.

The following conditions were evaluated to further optimize the process:

- Flow rate 300 cm/hr, residence time 2 min, load density up to 350 g/L
- Flow rate 800 cm/hr, residence time 45 sec, load density up to 145 g/L

Fractions of the load (15 mL) and wash steps were collected and analyzed for monomer purity and recovery as described in Figure 3.

Chromatography process verification

After scaled-down model optimization, a verification run was executed to confirm the conditions. POROS Benzyl Ultra resin packed in a 0.66 cm (D) x 10 cm (L) (3.4 mL) column was equilibrated with 25 mM Tris-acetate at pH 6.8 and conductivity of 1.8 mS/cm. The column was loaded at 500 cm/hr (1.2 min residence time) with Mab-A AEX pool (2.4 mg/mL of resin) at conductivity of 1.8 mS/cm and pH 6.8. The final load density tested was 80 g/L resin to ensure a conservative and robust process for aggregate removal.

Figure 3. The general workflow for aggregate removal consists of filter-plate screening followed by A_{280} concentration determination and purity analysis by HPLC-SEC; statistical analysis is used to generate trends and to select process conditions.

CHO host-cell protein (HCP) of the load and flow-through pools was quantitated by an immuno-qPCR proximity ligation assay using the ProteinSEQ assay kit. Sample preparation and qPCR were performed on the KingFisher Flex 96-well automatic magnetic particle processor and the 7500 Real-Time PCR System, respectively. The lower limit of quantitation (LLOQ) for the assay is 0.2 ng/mL.

At the end of the run, the flow-through pool was collected and analyzed for monomer purity and recovery as described in Figure 3.

Results and discussion

Defining conductivity range for interaction between mAb and resin

Process optimization was started with a bind/elute experiment to define salt concentration ranges for flow-through operation. The conductivity at the maximum of the elution peak is used to determine the highest approximate salt concentration that is required to remove impurities but that also allows the target molecule to flow through. Using the POROS Benzyl Ultra resin, mAb-A elutes at the lower salt concentration range corresponding to conductivity of around 7 mS/cm (Figure 4), whereas the POROS Benzyl resin showed an elution profile at 28 mS/cm (data not shown).

The salt conductivity values of 7 mS/cm and 28 mS/cm were used to explore the flow-through parameters on POROS Benzyl Ultra and Benzyl resins, respectively.

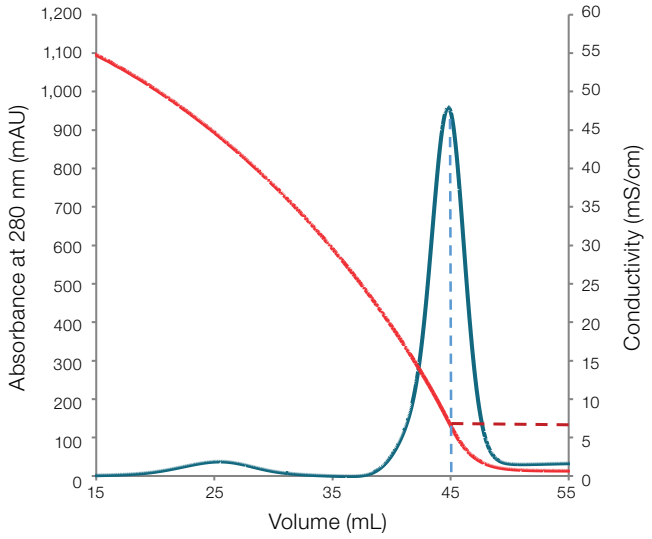

Figure 4. An example of the screening chromatogram to obtain the ideal low-salt condition for the flow-through steps. Process screening for a monoclonal antibody using the POROS Benzyl Ultra resin in flow-through mode. Gradient: high conductivity to low conductivity using sodium citrate. Based on this chromatogram, the resin was further optimized in flow-through mode under low-salt conditions starting at 7 mS/cm. Dashed lines: the maximum of the elution peak corresponds to a salt conductivity of 7 mS/cm).

High-throughput screening for flow-through mode: resin selection

High-throughput screening was conducted to determine the critical parameters affecting resin selectivity towards aggregate removal in the flow-through mode. Figure 5 shows the aggregate removal by total mass, and the selectivity factor of both resins.

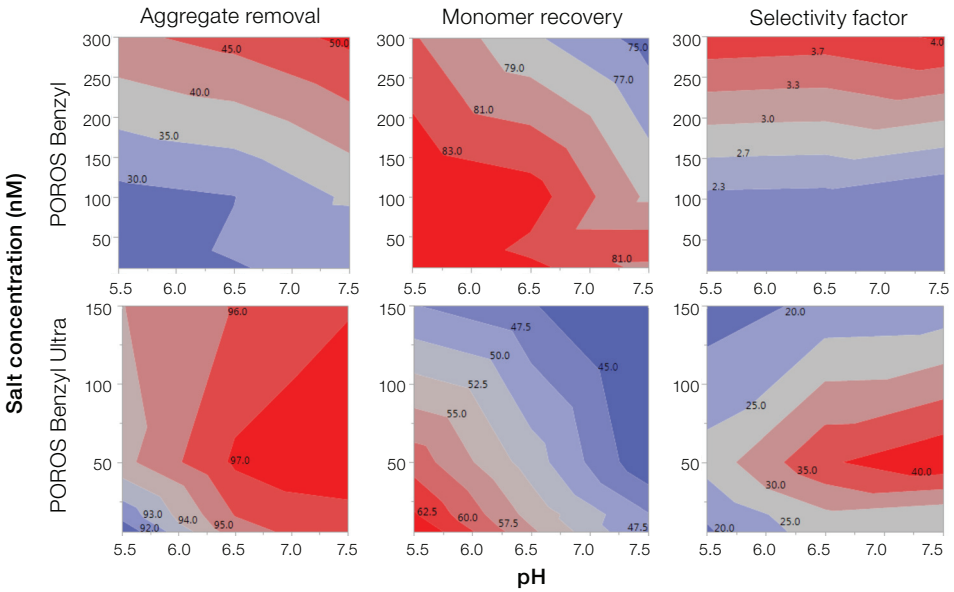

Figure 5. Contour plots showing aggregate removal, monomer recovery, and the selectivity factor for POROS Benzyl and POROS Benzyl Ultra resins, tested under a range of pH and salt concentrations. The selectivity factor is calculated as the ratio of aggregate to monomer partition coefficients (K_p) [3]. A higher selectivity factor indicates stronger aggregate binding compared to the monomers.

The POROS Benzyl Ultra resin shows strong selectivity for aggregate binding, with >90% aggregate mass removal over a broad range of conditions tested. It also exhibits a greater selectivity factor than the POROS Benzyl resin, indicating a better separation between the aggregates and monomers. Although the POROS Benzyl resin showed high monomer recovery, it did not significantly bind and remove the aggregates. The selectivity factor remained low, indicating that both the aggregates and monomers were not partitioned by the resin. In addition, the bind/elute experiments on Benzyl Ultra resin showed mAb elution at 7 mS/cm, which is compatible with the desired flow-through process step (data not shown).

While a high-throughput model for static binding of mAb at low protein load is representative of selectivity, recoveries are not indicative of a dynamic process at high protein load. Due to its high aggregate selectivity combined with bind/elute data that showed mAb elution at 7 mS/cm, the POROS Benzyl Ultra resin was selected as the optimal resin for further scale-up experiments.

High-throughput screening for flow-through mode: selection of process conditions for POROS Benzyl Ultra resin

To determine the conditions suitable for scale-up verification in column format, the raw data are visualized in an amalgamated contour plot showing aggregate removal as a function of salt type, salt concentration, and pH (Figure 6).

For scale-up to column format, the most suitable process condition chosen was pH 6.8 at conductivity of approximately 2 mS/cm. Data showed very high aggregate clearance under these conditions and also allowed for a streamlined process by directly loading onto the HIC column from the AEX flow-through step without the need for further buffer conditioning.

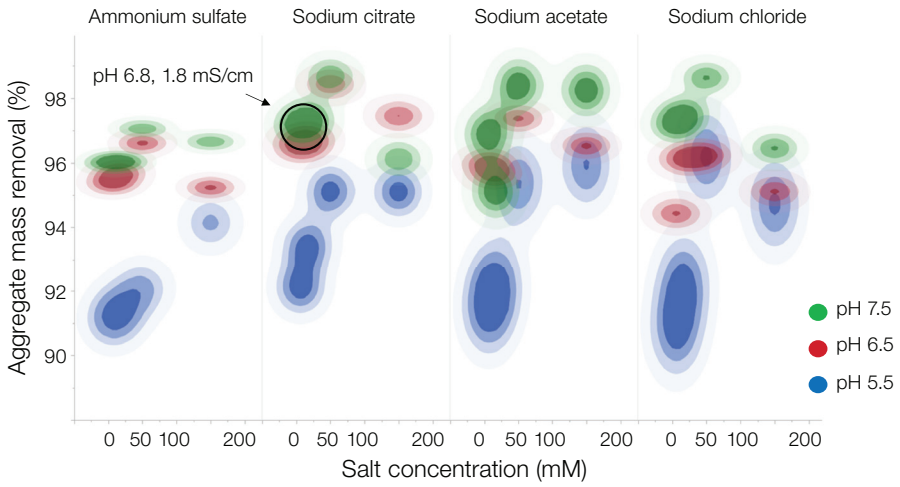

Figure 6. Amalgamated contour plot showing aggregate removal as a function of salt type, salt concentration, and pH. Sodium citrate at pH 6.8 and conductivity of 1.8 mS/cm (5 mM) was chosen for column scale-up.

Chromatography optimization in scale-down model

To simulate the manufacturing scale in a dynamic mode, a column scale-down model was tested to determine the optimal process conditions for flow-through chromatography. Breakthrough analysis demonstrated that monomer purity remained above 99% until a load density of 125 g/L resin was reached. Monomer recovery remained stable at 97% up to a load density of 200 g/L and remained above 95% for the course of the experiment (Figure 7). HPLC-SEC analysis was conducted to analyze aggregate levels in the collected fractions during the breakthrough analysis. The purity goal of 1% breakthrough of aggregates was achieved up to a load density of 125 g/L resin, showing significantly high loading capacity. This shows a critical improvement over the original aggregate removal by mixed-mode process, which was operated at a load density of 25 g/L resin with only 90% monomer recovery.

Next to high resolution and capacity, another main design goal of the POROS HIC resins was to achieve excellent linear flow rate capability. To demonstrate the ability to run at high flow rates, a similar breakthrough experiment was conducted at a flow rate of 800 cm/hr (45 sec residence time). Even at this high flow rate, a load density of 75 g/L resin was achieved without compromising monomer purity (99%) and recovery (98%) (Figure 8).

Chromatography process verification

The flow-through verification run was performed under more conservative conditions to establish a robust HIC flow-through polish step suitable for integrating with the total purification process. At a flow rate of 500 cm/hr (1.2 min residence time) and a load density of 80 g/L, the flow through pool was collected and analyzed.The final flow-through pool showed 99.3% purity, with very low levels of aggregates and high molecular weight (HMW) and low molecular weight (LMW) proteins, a significant improvement compared to the initial material with 85.5% purity (Figure 9).

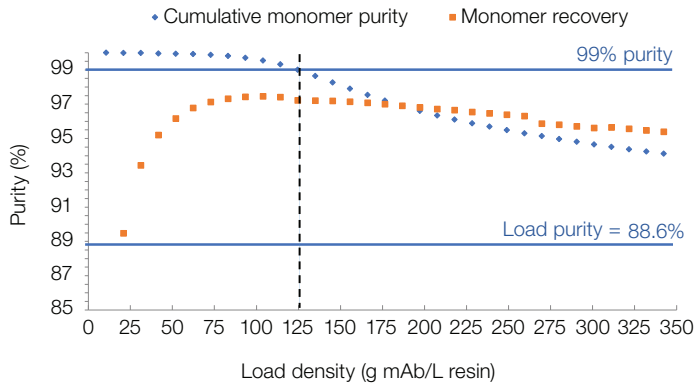

Figure 7. Breakthrough analysis of the column scale-down model, run at a flow rate of 300 cm/hr (load density up to 350 g/L resin). Monomer purity and recovery were analyzed by HLPC-SEC from 15 mL fractions. Monomer purity remained above 95% up to the maximum load density.

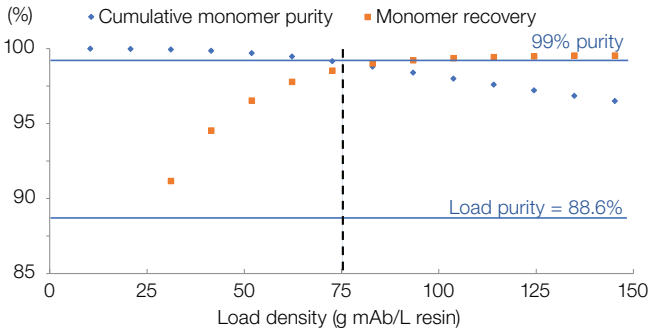

Figure 8. Breakthrough analysis of the column scale-down model, run at a flow rate of 800 cm/hr (load density up to 150 g/L). Even at the high flow rate, high aggregate clearance was obtained.

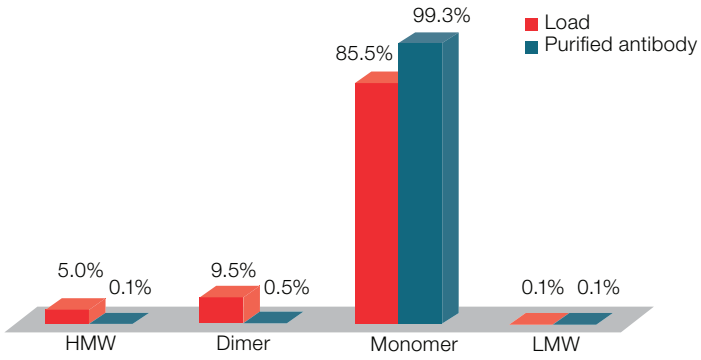

Figure 9. POROS Benzyl Ultra flow-through resin verification results. Very efficient removal of HMW aggregates and dimers was demonstrated using a load density of 80 g/L.

Conclusions

This study shows a successful and structured approach for process optimization—all the way from high-throughput screening to process scale-up and verification. The findings of this study demonstrate a more efficient and cost-effective process by performing HIC using the POROS Benzyl Ultra resin in flow-through mode, compared to the original mixed-mode bind/elute chromatography step (Table 1).

Results showed:

- Significant reduction of mAb HMW aggregate and dimer, achieved under low-conductivity conditions
- A 5-fold residence time improvement (from 6 min to 1.2 min)
- >99% purity, and 98% monomer recovery at a load density 3 times higher than the mixed-mode conditions
- Fast mass transfer and high performance at high flow rates (800 cm/hr, 45 sec residence time) without compromising efficient impurity clearance

In this study, important process parameters have been optimized, leading to a more efficient process and improved productivity. The study further demonstrates that POROS HIC resins can be utilized as a powerful tool to simplify mAb purification schemes and improve process throughput.

Supporting information to demonstrate improved process efficiency and productivity

The illustrative cost model shown in Table 2, which was developed for a 200 L harvest with a titer of 5 g/L, summarizes the cost of buffer, labor, and resin, and the total cost to process a batch of mAb-A through either the mixed-mode bind/elute step or POROS Benzyl Ultra resin in flow-through mode. By using the POROS Benzyl Ultra resin, a total time reduction of 78% could be achieved and total cost savings of >50% could be realized, demonstrating the improved process efficiency and productivity.

Table 1. Comparison between mixed-mode bind/elute and POROS Benzyl Ultra HIC Resin flow-through steps.

	Mixed-mode B/E	POROS HIC FT
Load density (g/L resin)	25	80
Monomer purity FT (%)	99	>99
Monomer recovery (%)	90	98
HCP assay* (ppm)	<LLOQ	<LLOQ
Residence time (min)	6	1.2

* ProteinSEQ Immuno-qPCR HCP quantitation assay, LLOQ <0.2 ng/mL.

Table 2. Cost model to illustrate time and cost savings from improved process efficiency and productivity.

Resin	Residence time (min)	Flow rate (cm/hr)	Loading (mg/mL)	No. of cycles required	Volume of load/cycle (L)	Total buffer volume (L)	Cumulative process time (hr)	Buffer cost (USD)	Process labor cost (USD)	Cost of resin/ batch (USD)	Total cost/ batch (USD)	Time reduction (%)	Buffer cost reduction (%)	Total cost reduction (%)
Mixed-mode (B/E)	6	200	25	3	67	794.5	5.6	$3,972.3	$1,686.8	$353.3	$6,012.3			
Benzyl Ultra (FT)	1.2	500	80	2	100	440.2	1.2	$ 2,201.1	$373.9	$335.6	$2,910.5	78	45	52

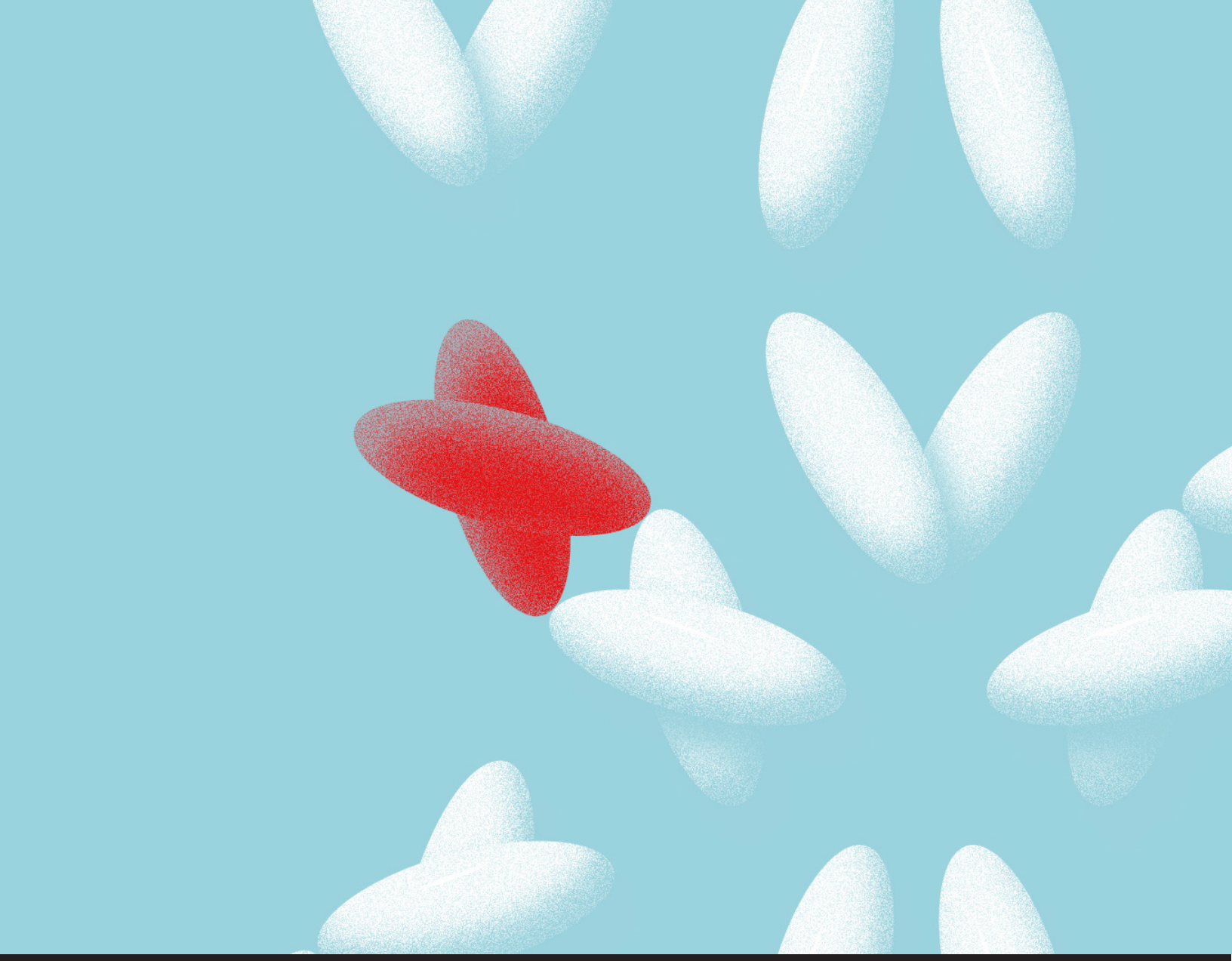

Advances in Downstream Processing of Complex Antibodies

Article Collection

Find out more at thermofisher.com/purification

POROS chromatography resins: Pharmaceutical Grade Reagent. For Manufacturing and Laboratory Use Only.

CaptureSelect ligands and chromatography resins: For Research Use or Further Manufacturing. Not for diagnostic use or direct administration in humans or animals.